CHALMERS
UNIVERSITY OF TECHNOLOGY

Feasibility study of implementing Chemical Looping Combustion with BECCS

Process modeling and techno-economic analysis of a CHP plant at Skövde Energi

Master's thesis in Innovative and Sustainable Chemical Engineering

Judit Fortet Casabella
Yunes Chehade

DEPARTMENT OF SPACE, EARTH AND ENVIRONMENT

CHALMERS UNIVERSITY OF TECHNOLOGY
Gothenburg, Sweden 2023
www.chalmers.se

MASTER'S THESIS

Feasibility study of implementing Chemical Looping Combustion with BECCS

Process modeling and techno-economic analysis of a CHP plant at Skövde Energi

Judit Fortet Casabella
Yunes Chehade

CHALMERS
UNIVERSITY OF TECHNOLOGY

Department of Space, Earth, and Environment
Division of Energy Technology
CHALMERS UNIVERSITY OF TECHNOLOGY
Gothenburg, Sweden 2023

Feasibility study of implementing Chemical Looping Combustion with BECCS
Process modeling and techno-economic analysis of a CHP plant at Skövde Energi

Judit Fortet Casabella
Yunes Chehade

Supervisor:
Gajanan Dattarao Surywanshi, Department of Chemistry and Chemical Engineering

Co-supervisor:
Mohammad Shahrivar, Department of Space, Earth, and Environment, Div. of Energy Technology

Co-supervisor:
Christer Nilsson, Skövde Energi

Examiner:
Tobias Mattisson, Department of Space, Earth, and Environment, Energy Technology

Master's Thesis
Department of Space, Earth, and Environment, Div. of Energy Technology
Division of Energy Technology
Chalmers University of Technology
SE-412 96 Gothenburg
Telephone: +46 31 772 1000

Cover: Skövde Energi's CHP plants (Block 3 and 4).
Printed by Chalmers Reproservice
Gothenburg, Sweden 2023

Feasibility study of implementing Chemical Looping Combustion with BECCS
Process modeling and techno-economic analysis of a CHP plant at Skövde Energi

Judit Fortet Casabella and Yunes Chehade
Department of Space, Earth, and Environment, Energy Technology
Chalmers University of Technology

Abstract

Climate change is an urgent worldwide issue that is mostly brought on by the accumulation of greenhouse gases, including CO_2 in the atmosphere. Carbon Capture and Storage (CCS) technologies can play an important role in the decarbonization process. Chemical Looping Combustion (CLC) using biomass as a fuel can be combined with CCS to obtain negative emissions.

This work is part of a collaboration between Chalmers University of Technology and Skövde Energi. The project includes performing a process modeling and techno-economic assessment of substituting one of the existing biomass CHP-plant boilers with a CLC-system; including the capture, compression, and liquefaction of the CO_2 obtained. The general objective is to analyze the techno-economic feasibility of the CLC technology and give some guidelines for future implementation at Skövde Energi's site. Additionally, the technology is compared with a post-combustion study using absorption with monoethanolamine (MEA), previously performed for the same combustion unit.

After an initial review of the main literature and assessment of the current boiler operation, a base case simulation of the full-chain process is performed in Aspen Plus, including gas conditioning and liquefaction of the CO_2. The process model considered heat integration of the different components together with the steam cycle for electricity production. Furthermore, a design of the fluidized bed CLC unit was conducted as well as a techno-economic analysis of the full-chain process, which was compared to the use of a post-combustion technology. Finally, through the interpretation of the obtained results, a discussion is performed on how the implementation of the technology would affect the current production and future considerations for implementation at other sites.

The work concludes that the CLC technology would lead to a total capture efficiency of 97.5 %, capturing around 101 ktonne CO_2 and obtaining a capture cost of around 800 SEK/tonne CO_2 captured, which includes the purchase and installation of equipment. This is considerably lower than what is expected in a post-combustion system, with costs of about 1,100 SEK/tonne CO_2 captured. The reason for this is due to the lower amount of energy and equipment needed for the capture process. Excluding installation costs, a capture cost of around 330 SEK/tonne CO_2 captured was obtained, which is slightly higher than the 200 SEK/tonne CO_2 of a 1000 MW_{th} design by Leckner and Lyngfelt.

Keywords: carbon capture and storage (CCS), chemical looping combustion (CLC), negative emissions, combined heat and power plant (CHP-plant)

Acknowledgments

I would like to thank our supervisor and examiner, Gajanan and Tobias, for all their help and interesting discussion throughout the thesis work. Also to Mohammad, who with his interesting ideas and positivity, taught me how to solve and approach different problems.

Furthermore, thank you to the people at Skövde Energi, especially to Christer, which has shown us the importance of believing in new technologies and pursuing his passion to become net negative.

A very special thanks to Yunes. Thank you for putting so much dedication into the work, for all the interesting discussions, and for showing me that all the details count. I wish you the best in your career.

Thanks to the department for including us in the great and interesting discussions, including the fika, and to all the friends I made throughout the master's program, and that make my life in Sweden immemorable. A very very special thanks to Hunny, for being himself with me, handling me, and helping me disconnect from all my problems. Additionally, a special thanks to all the group of people in the office for all the laughs, coffee breaks, motivational quotes, and after-works, I will always keep you in my heart.

M'agradaria agraïr als meus papes i a la meva germaneta per recolzar-me i ajudar-me a perseguir els meus somnis. Aprecio moltissim les vostres trucades i visites, que encara que no sempre ho mostro, han sigut genials. Moltissimes gràcies per sempre estar sempre amb mi. També volia donar les gràcies a les meves amigues que, per molt lluny que estiguin, sempre es senten molt aprop.

"I amb tot l'amor, ho enviaré tot a pastar fang".

Judit Fortet Casabella, Göteborg, June 2023

Endless gratitude goes towards the supervisors and examiner Gajanan, Mohammad, and Tobias, for their time and effort in helping us with the thesis. A big thanks also goes to Christer Nilsson and Skövde Energi for giving us a chance in working with the technology of the future. This work wouldn't have been possible without all of you, and I will forever be thankful.

My gratitude also goes to Judit. You have been a wonderful friend and colleague to work with. Not only are you extremely talented and smart, but you have been patient, understanding, and helpful throughout this entire work. Your future employer will be very lucky to be working with you and I wish you the best in the future.

A big thanks also go towards the department for their helpful input and time spent on helping us with some difficulties throughout the work. In particular, I would like to thank Tharun Roshan Kumar and Anders Lyngfelt for their help. And of course, I would like to thank my colleagues from the master's office who have been helpful and supportive with the presentation.

Min oändliga tacksamhet går till mina vänner Elisabeth och Nadja, som stöttat mig under åren och i min utveckling. Ni har varit där för mig under glada och jobbiga tider och kommer för evigt vara tacksam för er.

Sist men inte minst går min tacksamhet till min familj, som stöttat mig genom alla åren i min utbildning. Ni har gett mig så mycket stöd och kärlek utan villkor och jag är för evigt tacksam. Christer Wannerskog, min största tacksamhet går till dig. Inget av det jag åstadkommit hade varit möjligt utan dig. Du har varit en ovärderlig förebild, en underbar fadersfigur, och har gett mig möjligheten att bevisa mig själv. Ditt inflytande på mig har gett mig styrka att överkomma alla mina hinder i livet och ord går inte att beskriva hur mycket jag värderar allt du gjort för mig.

Yunes Chehade, Göteborg, June 2023

Table of contents

Abstract v
Acknowledgments vi
List of Tables xi
List of Figures xiii
List of abbreviations xiv
1 Introduction 1
1.1 Aim and scope 2
2 Literature review 4
2.1 Current plant layout of Skövde Energi 4
2.2 Carbon capture and storage/utilization 5
2.2.1 Post-combustion capture 6
2.2.2 Pre-combustion capture 6
2.2.3 Oxyfuel combustion and Chemical Looping Combustion 6
2.3 Chemical looping combustion technology 7
2.3.1 Biomass fuel 9
2.3.2 Choice of oxygen carrier 10
2.4 Upscaling of chemical looping combustion processes 11
2.5 Flue gas cleaning 13
2.5.1 Northern Lights 13
2.5.2 Particle cleaning 14
2.5.2.1 Cyclones 15
2.5.2.2 Electrostatic precipitators 15
2.5.3 Oxypolishing 15
2.5.4 NO_x, SO_x and HCl cleaning 16
2.5.5 Excess oxygen removal 18
2.6 Compression and liquefaction 19
2.6.1 Excess water removal 21
2.7 Literature review on the capture costs using CLC 22
2.8 Software 23
2.8.1 Aspen Plus 23
2.8.2 Aspen Energy Analyzer 24
3 Method 25
3.1 Data collection 25

3.1.1 Biomass data 25
3.1.2 Oxygen carrier 25
3.1.3 Steam cycle 26
3.2 CLC-process description 26
3.3 Modelling the existing plant 28
3.4 Setting up the simulation 28
3.5 Chemical looping combustion modelling 29
3.5.1 Fuel Reactor 29
3.5.2 Oxypolishing 30
3.5.3 Solid separation 31
3.5.4 Air Reactor 31
3.5.5 Parameter adjustment 31
3.6 Heat recovery system and steam cycle 32
3.7 CO_2 train modelling 33
3.7.1 Flue gas purification 33
3.7.2 Flue gas compression and dehydration system 34
3.7.3 CO_2 liquefaction 34
3.7.3.1 Ammonia refrigeration cycle 35
3.8 Heat integration 36
3.9 Equipment sizing 37
3.9.1 Preliminary design of FR and AR 38
3.9.2 Pressure vessels 39
3.9.3 Sizing the dehydration unit 40
3.9.4 SO_2 cleaning absorber 40
3.9.5 Intermediate CO_2 storage tank 41
3.10 Technoeconomic analysis 41
3.10.1 CAPEX 41
3.10.2 OPEX 44
3.10.3 Revenue 45
3.10.4 Economic parameters 45
3.10.5 CLC vs post-combustion 46
3.11 Sensitivity analysis 48
3.11.1 Steam temperature and pressure for electricity production 48
3.11.2 Multistage compressor 49
3.11.3 Impact of the CAPEX and OPEX on the project 49

3.11.4 Effect of the utilities price 50
4 Results 51
4.1 Chemical Looping Combustion 51
4.2 Equipment sizing 52
4.2.1 Air and fuel reactor dimensions 52
4.2.2 Downstream process unit dimensions 52
4.3 Steam cycle efficiency 53
4.4 Compression, liquefaction and carbon capture 54
4.5 Techno-economics 55
4.5.1 CAPEX 56
4.5.2 OPEX 57
4.5.3 Total plant cost 58
4.5.4 CLC vs. post-combustion 59
4.5.5 Techno-economic comparison with literature 62
4.6 Sensitivity analysis 63
4.6.1 Effect on the steam temperature 64
4.6.2 Multistage compression analysis 66
4.6.3 Impact of the CAPEX on the project 66
4.6.4 Impact on the OPEX on the project 68
4.6.5 Effect on the utility prices 69
5 Further considerations 71
6 Conclusion 73
6.1 Future work 73
Bibliography 75
A. Molecular sieve sizing i
B. Heat integration iv
C. Steam temperature sensitivity analysis GCC ix
D. Flash sizing xi

List of Tables

Table 2.1. Purity specification of CO_2 stream to be transported to receiving terminal in the scope of the Northern Lights project. 14
Table 2.2. Effect of impurities in molecular sieve and TEG dehydration system. 22
Table 2.3. Cost estimations from literature for CLC in a 1000 MW_{th} plant using coal as a fuel 23
Table 3.1. Biomass data used in the present work. 25
Table 3.2. Composition of the OC used (Ilmenite). 26
Table 3.3. Data used for the steam cycle simulation (turbines). 26
Table 3.4. Minimum allowable pressure vessel thickness for a given diameter. 39
Table 3.5. Assumed molecular sieve technology properties for this work. 40
Table 3.6. Assumptions for the techno-economic analysis. 41
Table 3.7. Equipment cost calculation equations. 41
Table 3.8. Typical factors for estimating the Project Fixed Capital Costs 43
Table 3.9. Raw material and utilities variable costs for the base case 45
Table 3.10. Implementation of MEA post-combustion capture in Block 4 from Skövde Energi. Data obtained from a past study of the company. 47
Table 3.11. Electricity and DH prices used in the sensitivity analysis. 50
Table 4.1. CLC-results from the Aspen Plus simulation performed in this work. 51
Table 4.2. Dimensions of the preliminary design proposal for the CLC-system reactors. 52
Table 4.3. Sizing of the flue gas cleaning: molecular sieve and SO_x cleaning. 53
Table 4.4. Electrical efficiency of CLC vs conventional combustion. 53
Table 4.5. CO_2 multicompression results. 54
Table 4.6. CO_2 liquefaction and ammonia refrigeration results. 54
Table 4.7. Final CO_2 purity obtained in the Aspen Plus simulation. 55
Table 4.8. Investment for each unit in the total plant. 56
Table 4.9. Fixed operational costs for the base case expressed in MSEK/year. 57
Table 4.10. Variable operational costs for the base case. 58
Table 4.11. Summary of the economic parameters for the base case. 58
Table 4.12. Utilities consumed per hour to run the plant at full load for both technologies. 62
Table 4.13. Sensitivity analysis of the calculated price per tonne of CO_2 compared with other literature studies. 62
Table 4.14. Comparison of the cost estimation per tonne of CO_2 between literature and the actual case, separated by purchased and installed cost 63
Table 4.15. Steam properties, electricity contribution, DH contribution, cooling water need and associated total cash flow of different cases of temperature and pressure modifications. 64
Table 4.16. Steam properties, electricity contribution, DH contribution, cooling water need and associated total cash flow of different cases of bleed stream modifications. 65
Table 4.17. Multicompressor economic results for the CO_2 train comparing three and four stages. 66
Table 4.18. Impact on the variation of the CAPEX on the different analyzed economic parameters. 67
Table 4.19. Impact of the utility prices on the different economic parameters 70
Table A.1. Values for B and C for equation A.2 for different particle types. i
Table A.2. Data used and calculated to size the molecular sieve equipment (adsorber). iii
Table B.1. Streams included in the heat integration. v

Table B.2. Stream descriptions. v
Table D.1. Results of flash sizing. The naming of each flash corresponds to the names in the figure above. xi

List of Figures

Figure 1.1. BECCS CO_2 cycle from sequestration to geological storage. 1
Figure 2.1. Current boiler configuration with steam generation and air preheating. 5
Figure 2.2. The general layout of a chemical looping combustion system 7
Figure 2.3. Circulating fluidized bed (CFB) principle where 1) Air Reactor, 2) Cyclone, 3) Fuel Reactor, and 4) Loop Seals. 9
Figure 2.4. Simplified process diagram including the flue gas cleaning procedure. 13
Figure 2.5. Phase diagram of pure CO_2 based on the Span and Wagner equation of state. Data obtained by approximation of the diagram stated by Deng et al. 20
Figure 3.1. CLC-process design layout 27
Figure 3.2. Simplified diagram of the CLC system. 29
Figure 3.3. Simplified diagram of the heat production system 32
Figure 3.4. Flue gas compression and purification simplified diagram 34
Figure 3.5. Simplified diagram for the CO_2 liquification system. 35
Figure 3.6. Simplified diagram of the simulated ammonia refrigeration cycle 36
Figure 3.7. Outline of the 200 MW CLC boiler performed by Lyngfelt et al. 38
Figure 4.1 Distribution of the CAPEX among the different equipment 57
Figure 4.2. Effect of the negative CO_2 incentives on the PBP as a function on the prices for the utilities 59
Figure 4.3 Comparison of the added cost per tonne of CO_2 between using CLC or MEA post-combustion technology. 60
Figure 4.4. Distribution of the added operational costs for the CLC technology 60
Figure 4.5. Comparison of the energy used per tonne of CO_2 captured for CLC and post-combustion technologies. 61
Figure 4.6. Utility pinch seen on the left figure from the orange line touching the process GCC. The same orange line has no pinch for the modified DH temperature on the right. 65
Figure 4.7. Impact on the variation of the CAPEX on the different economic parameters analyzed. 67
Figure 4.8. Impact of the Biomass (fuel) price and O_2 (oxypolishing) price on the PBP (dots) and the levelized CO_2 cost (columns). 68
Figure 4.9. Impact of the OC price on the PBP (dots) and the break-even CO_2 cost (total plant) (columns) 69
Figure B.1. Process flow diagram, numbered for stream characterization. iv
Figure B.2. GCC of the streams included in the heat integration. vi
Figure B.3. Heat exchanger network design. vii
Figure C.1. Process GCC for the high-pressure case of 150 bar. ix
Figure C.2. Process GCC for the high temperature case of 600 °C. ix
Figure C.3. Process GCC for the high temperature and pressure case of 600 °C and 150 bar. x
Figure C.4. Process GCC for the case of having no bleed stream exhaust from the turbine, focusing on electricity production. x
Figure C.5. Process GCC for the case of having a full bleed stream exhaust from the turbine, focusing on district heat production. x
Figure D.1. Process diagram naming the flashes used. xi

List of abbreviations

ACC	Annualized capital cost
AR	Air Reactor
BECCS	Bioenergy Carbon Capture & Storage
BFB	Bubbling Fluidized Bed
CAPEX	Capital expenditures
CCS	Carbon Capture & Storage
CFB	Circulating Fluidized Bed
CHP	Combined Heat and Power
CLC	Chemical Looping Combustion
CLOU	Chemical Looping and Oxygen Uncoupling
DH	District Heating
FCC	Fixed capital cost
FR	Fuel Reactor
GROT	Tops and branches (Grenar Och Toppar)
HRSG	Heat Recovery Steam Generator
IPCC	Intergovernmental Panel on Climate Change
MEA	Monoethanolamine
NET	Negative Emission Technology
NFV	Net Future Value
NL	Northern Lights
NPV	Net Present Value
NPW	Net Present Worth
OC	Oxygen Carrier
OPEX	Operating expenditures
PBP	Payback Period
PCC	Total physical plant cost
PCE	Total process plant cost
PM	Particulate Matter
POC	Post Oxidation Chamber
TRL	Technology Readiness Level

1 Introduction

The Intergovernmental Panel on Climate Change (IPCC) is flagging a need for negative emission measures to reach the Paris Agreement goal of restricting global warming to well below 2 °C [1]. Biomass is the major source of energy for about 50% of the world's population and wood biomass can be considered in the developed world as a major renewable energy source [2]. It is considered that biomass will play an important role in replacing fossil fuels and reducing greenhouse gas (GHG) emissions over the next decades [3]. Negative emission technologies (NETs), such as bioenergy with carbon capture and storage (BECCS), are an option to generate negative emissions while producing renewable energy, such as heat and/or power.

BECCS is based on the principle that plants and forests sequester CO_2 during their lifetime, which then is converted into an energy vector, for applications like heat and electricity. However, the process of biomass-to-energy can still contribute to the release of carbon dioxide previously sequestered during biomass growth [4]. These emissions can be reduced by applying carbon capture and storage (CCS) methods, such as post-combustion, pre-combustion, and oxyfuel-combustion technologies. The CO_2 captured could afterward be stored in geological reservoirs or used for other purposes in order to substitute the use of fossil fuels [4]. Different projects have already been started in order to make carbon dioxide storage possible. A clear example is the Northern Lights (NL) project, in Norway, which plans to start the injections of CO_2 captured into aquifers under the northern sea in 2024 [5]. In order to make transportation more efficient, the CO_2 captured is compressed and liquefied to be transported to the aquifer, as shown in Figure 1.1.

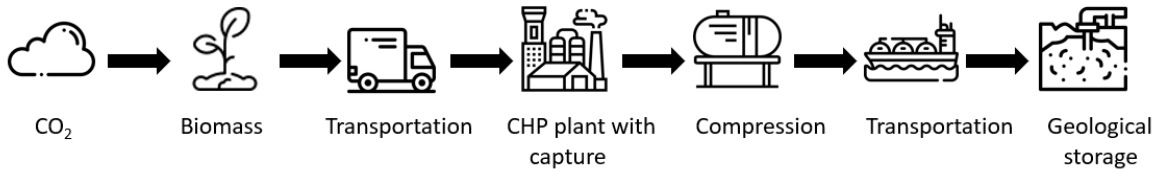

Figure 1.1. BECCS CO_2 cycle from sequestration to geological storage.

If biomass is grown sustainably, i.e. utilized biomass replaced without additional emissions, then BECCS would result in a net flow of CO_2 out of the atmosphere. The application of a CCS technology with biomass would thus achieve negative emissions and contribute to the IPCC goal [1].

Different technologies allow the capture of carbon in a combustion plant. The two more advanced technologies are post-combustion with amine absorption and hot potassium carbonate, which are mature enough to install and can be easily retrofitted in existing plants [6]. The low CO_2 content in the flue gas, however, is a significant drawback of using post-combustion techniques, as it translates to a low carbon capture efficiency [6].

Since these technologies, however, are associated with relatively high energy penalties and large costs, an additional CCS technology can be implemented, namely chemical-looping combustion (CLC) [6]. CLC is a way of combusting a fuel using an indirect transfer of oxygen from the air to the fuel by means of oxygen carriers, theoretically providing a clean flue gas of CO_2 and H_2O, which reduces the complexity of capturing the CO_2 [7]. The EU and Sweden are

currently working on policies and incentives to trade or sell negative emissions in order to compensate for other CO_2 fossil emissions. This would create an economic and environmental benefit of capturing emissions, incentivizing investors to perform CCS [8], [9].

Skövde Energi is a public company that provides heat and electricity to the municipality of Skövde. The energy is produced using different boilers situated around the region, some of them supplying district heating for the city and others only for specific buildings, like Volvo's factory or the hospital. The main heat is obtained in the location "Värmekällan" using two different blocks, Block 3 and Block 4, which together have a capacity of 58 MW. Block 3 is a CHP waste incineration plant and will not be considered in this thesis. Furthermore, Block 4 uses a biofuel cogeneration plant fired with woodchips and bark. This will be studied throughout the work with respect to the implementation of a carbon capture unit [10].

Block 4 was built in 2017, with the thought that waste incineration would not be the future for performing sustainable energy production. This CHP plant has a thermal input of around 49 MW, obtaining around 40 MW of district heating heat and 9 MW of electricity [10]. Some work has already been performed to study the possibility of using a post-combustion system, such as amine technology or chilled ammonia, to capture carbon dioxide from this block. These technologies are on a higher TRL scale and have already been commercialized, therefore they are of higher interest to the industry sector. Despite this, the electricity and utility need in the capturing process is relatively high and does not contribute to the future electrification need [11].

1.1 Aim and scope

The thesis aims to investigate what it would entail to substitute one of the biomass boilers in Skövde Energi with a CLC-system connected to a steam generation cycle. In addition, the downstream cleaning, compression, and liquefaction of the CO_2 stream are analyzed and simulated. The future goal is to eventually store the captured CO_2 underground or used it in further applications, i.e., for carbon utilization.

The thesis objective is to simulate the CHP system with a CLC technology including the compression and liquefaction of the captured CO_2 using Aspen Plus. Additionally, a heat integration, using Aspen Energy Analysis, and a techno-economic analysis are performed to conclude if the technology would be techno-economically feasible. Thereafter, sensitivity analyses of the key parameters are performed, such as raising the steam cycle temperature or varying the energy utilities market price. Moreover, a preliminary sizing and layout of a CLC fluidized bed unit will be performed.

Finally, the CLC technology is to be compared to a post-combustion amine-based process, which can be seen as the current state-of-the-art technology and for which a feasibility study has already been performed by the company. A comparison of the carbon efficiency, energy requirements, and cost is performed.

In this work, the following delimitations have been considered:

- Skövde Energi has more than one boiler which produces heat and power for the district heating system. Only Block 4, the boiler using biomass, will be studied to be substituted by a CLC-system. Nevertheless, considerations on how the other boilers would play an important role for the company, to achieve net emissions, will be described.

- The boiler is assumed to be running at full load, with approximately a 50 MW thermal input for 5,900 h/year.
- The equipment's capital cost calculation has been performed by using literature values, instead of contacting possible suppliers.
- The data for the post-combustion amine carbon capture will be extracted from the previous pre-feasibility study that has been carried out by the company.
- The sequestration of the CO_2 and biomass transportation to the plant is not considered in this report.
- The logistics of the further utilization or storage of CO_2 will not be studied in this work. The process chain will stop after the compression and liquefaction of the CO_2 stream although the conditions are provided by the NL facility in Bergen (Norway).

2 Literature review

Throughout this section, the results of the literature study will be discussed. Firstly, the current plant is analyzed together with the different carbon capture technologies existing in the market. After this, the chemical looping combustion system is explained, and the upscaling limitations are shown. Thereafter, the downstream flue gas cleaning requirements and technologies used are shown followed by an analysis of the compression and liquefaction system. Finally, a literature review on the capture costs for the CLC technology is performed.

2.1 Current plant layout of Skövde Energi

Skövde Energi is a public company that provides heat and electricity to the municipality of Skövde. Skövde is located approximately two hours from Gothenburg between Sweden's largest lakes Vänern and Vättern, which is important to note when dealing with potential carbon capture projects. A project has been started in Gothenburg, CinfraCap, to create a joint infrastructure for the transport of captured CO_2. The project is a unique collaboration between companies from the area such as Göteborg Energi, Nordion Energi, Preem, St1, Renova, and Göteborgs Hamn AB [12]. To be part of the carbon capture of NL and CinfraCap, the CO_2 would have to be transported by train or truck from Skövde to the closest harbor, to then be further transported by ship to the facility of NL in Bergen.

The main production is performed in Blocks 3 and 4, which are run by waste and biomass, respectively. The waste boiler (Block 3), situated next to Block 4, is in continuous production as waste materials are readily available and need to be processed. Therefore, the waste boiler supplies a base load for the population of Skövde, while the analyzed boiler is used as a peak load. The current boiler is used by the company in a very variable manner depending on the DH demand and volatility of the electricity prices, as both show high volatility [13].

The existing boiler at Block 4 is a bubbling fluidized bed containing sand which is fluidized by preheated and moisturized air. Looking at Figure 2.1, the flue gas exiting the boiler **(1)** goes through a series of water heating stages, starting with the superheater **(7)**, the evaporator **(2)**, the economizer **(3),** and air preheating **(4)**. The water cycle is connected to a steam drum **(5)** and steam leaves the superheater **(7)** which goes through a turbine to produce electricity and then to produce district heating [14].

Afterward, the steam is fed into the turbine, where it expands to produce work. A generator is connected to the steam turbine to utilize the work and generate electricity. The steam exits the turbine at lower pressure and temperature, and it is condensed back into liquid to be reused in the power generation cycle. In the case of Skövde Energi's plant, the turbine has two stream outputs, where a bleed stream is extracted from an intermediate pressure stage of the turbine. It is believed that turbines extracting a bleed stream will improve the plant's total efficiency, have higher flexibility during operation, and can prevent damage to the turbine blades due to high-pressure [14], [15].

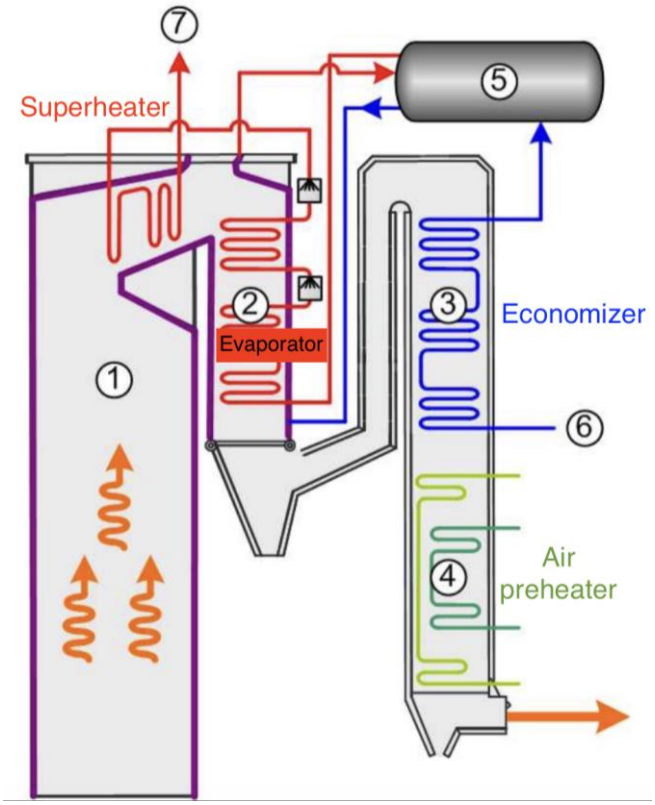

Figure 2.1. Current boiler configuration with steam generation and air preheating.

The bed material in the boiler at Block 4 operates between 700 °C and 900 °C. The boiler has a thermal input of around 49 MW and the turbine is designed to deliver 9.3 MW of electricity, already accounting for the generator efficiency, and approximately 40 MW of district heating, when the boiler is run at maximum load. Nevertheless, in Skövde Energi, the bleed stream is regulated to satisfy the needs of the population by producing more district heating or more electricity, depending on the current demand.

2.2 Carbon capture and storage/utilization

Carbon capture and storage, or CCS, is a technology that aims to reduce greenhouse gas emissions by capturing CO_2 from industrial processes such as power plants and storing it underground. CCS may be a necessary step to achieve negative emissions of CO_2 to stay within the 1.5 °C and 2 °C climate goals of the Paris Agreement [6]. This is possible by implementing CCS with biomass as an energy source in power and heat production, where the biomass has taken up CO_2 from the atmosphere during its growth. The CO_2 captured could also be utilized as feedstock in other industrial processes, such as enhanced oil recovery.

Even though CCS is considered an essential solution to reach the climate targets, the technology is not widespread, mainly due to economic reasons. Incentives can play a crucial role in accelerating CCS technology deployment. For instance, EU-ETS, which stands for European Union Emissions Trading System, is a market-based approach implemented by the EU operating on a cap-and-trade principle. It is a cap-and-trade system in which all the facilities inside the EU share a common cap on the total amount of greenhouse gas emissions allowed in the system [16]. Emissions allowances are allocated to installations such as power plants and industries, which are covered by the system. One allowance is defined to be the right of emitting

one metric tonne of CO_2 and can be traded between participants, easing flexibility in emission reduction [16]. The cap is gradually reduced over time in order to achieve emission reduction targets [9]. Although this system is at the forefront of international efforts to reduce CO_2 emissions, it does not include biogenic CO_2 emissions. For this reason, Sweden has developed a subsidy system, called reverse auctioning, to incentivize the development of CO_2 removal technologies. This system was proposed as a support system for BECCS, which plans to cover the costs of capture, transport, and storage over a period of 15 years [8].

The three main carbon capture methods described in the next Section are:

1. Post-combustion,
2. Pre-combustion,
3. Oxyfuel-combustion and Chemical Looping Combustion (CLC).

2.2.1 Post-combustion capture

In this carbon capture method, CO_2 from the flue gas is directly captured using a solvent with a high affinity for CO_2 [6]. The most studied solvent is monoethanolamine (MEA) but ammonia and potassium carbonate have also gained popularity recently [17]. The CO_2-rich flue gas and the solvent enter an absorber in which the CO_2 is absorbed by the solvent. The solvent is then regenerated in a stripper by means of heating in a reboiler and is then sent back again to the absorber. The heat required in solvent regeneration is energy intensive. This implies additional fuel consumption for a power plant and additional CO_2 that needs to be captured. Post-combustion is seen as state-of-the-art technology today as the concept is quite mature. Further, it is highly applicable for most processes in the heat and power sector as well as industrial processes as no retrofitting of the production units would be needed [6].

2.2.2 Pre-combustion capture

Pre-combustion carbon capture is a technology in which the CO_2 is captured before the fuel is burned in a facility such as a power plant. The fuel is first broken down into smaller components such as syngas, namely H_2, and CO, by means of gasification or steam reforming, followed by heat recovery for steam heating. The syngas is then led to a water-gas-shift reactor, where the CO is converted to even more H_2 and CO_2. The resulting stream, mainly consisting of H_2 and CO_2, is passed through an absorber where CO_2 is removed using the solvents named in Section 2.2.1. The flue gas would also be cleaned from potential particles and traces of sulfur containing chemicals. Finally, the remaining H_2 is combusted in a facility, producing steam and nitrogen gas [18]. Compared to post-combustion capture, solvent regeneration would be less energy intensive, as the CO_2 concentration in the flue gas would be higher as well as the pressure. These conditions are favorable for CO_2 absorption. This technology has, however, high capital costs and is complex to run [6].

2.2.3 Oxyfuel combustion and Chemical Looping Combustion

Oxyfuel combustion refers to the process of combusting a fuel using pure oxygen, as opposed to air, which eliminates the nitrogen in the flue gas, as well as the formation of NO_x gases. It is simple to separate the carbon dioxide from the resulting flue gas, which is mostly made up of steam and carbon dioxide. This can be done by condensing the steam and implementing flue

gas cleaning, again to remove traces of particles and gases, which produces a clean stream of CO_2 [19]. Normally, some of the CO_2 is recycled to the combustion unit, and hence the fuel is burned in a mixture of O_2/CO_2. The issue with oxyfuel combustion is that it requires a lot of energy to produce high-purity O_2, which in practice is primarily done through cryogenic air separation [18], [19].

CLC is a form of unmixed combustion where oxygen is provided to a fuel by means of a so-called oxygen carrier and a double reactor system, which is further explained in the next subsection.

2.3 Chemical looping combustion technology

CLC has been discussed in literature since the 1950s as an alternative to combustion [20]. It has been considered an attractive option for a NET during biomass combustion, as it inherently separates the CO_2 from the rest of the flue gas components [21]. Thus, in contrast to the technologies mentioned above, no or small energy penalties are incurred during the capture process. The process is normally carried out with a double-fluidized bed system, consisting of an air and fuel reactor. The two-reactor system contains a circulating oxygen carrier, which comes in the form of metal oxide particles. The oxygen carrier gets successively oxidized and reduced during circulation.

In the fuel reactor (FR), the fuel is oxidized by the oxygen carrier, theoretically providing a pure outlet stream of CO_2 and H_2O. The oxygen carrier is replenished in the air reactor (AR) by mixing with a stream of air, allowing it to be reused in the fuel reactor, thus completing the cycle which is also known as a CLC loop. A general illustration is shown in Figure 2.2 below [22].

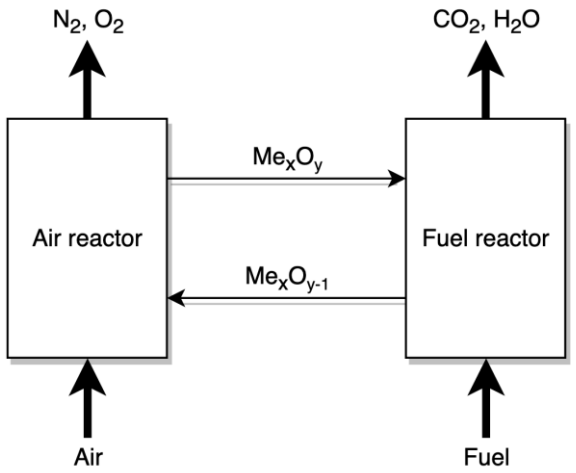

Figure 2.2. The general layout of a chemical looping combustion system [23].

During the CLC process, the combustion of the fuel will mainly take place in the FR with the heat and oxygen provided by the oxygen carrier [21].

Solid fuels are usually composed of moisture, ash, char, and volatiles. When a solid fuel is exposed to a hot-flowing gas, it undergoes three stages of mass loss, namely drying, devolatilization, and char combustion/gasification, depending on the surrounding gas. The first two stages, drying, and devolatilization, are essentially endothermic. Generally, as the solid fuel particle is gradually heated to the evaporation temperature, it releases its moisture at a

constant temperature. When all moisture is gone, the temperature again rises, at which volatiles are released, such as H_2, CO, CO_2, H_2O, and short-chained hydrocarbons at sufficiently high pyrolysis temperatures. These volatiles undergo numerous chemical reactions at high temperatures, depending on the surrounding gas. Lastly, the remaining char undergoes combustion or gasification. This step usually lasts much longer than the devolatilization and drying stages. After the complete conversion of the fuel particle, ash remains due to the presence of minerals in the fuel [24].

During CLC, the FR is usually fluidized by steam and/or CO_2 acting as gasifying agents. The volatiles and char of the solid fuel then undergo several chemical reactions, where some of which are presented in equations 2.1, 2.2, 2.3, and 2.4 [25],

$$\mathrm{C} + \mathrm{H_2O} \rightarrow \mathrm{H_2} + \mathrm{CO} \tag{2.1}$$

$$\mathrm{C} + \mathrm{CO_2} \rightarrow 2\mathrm{CO} \tag{2.2}$$

$$\mathrm{H_2O} + \mathrm{CO} \rightarrow \mathrm{H_2} + \mathrm{CO_2} \tag{2.3}$$

$$\mathrm{H_2} + \mathrm{CO} + \mathrm{volatiles} + n\mathrm{Me}_x\mathrm{O}_y \rightarrow \mathrm{CO_2} + \mathrm{H_2O} + n\mathrm{Me}_x\mathrm{O}_{y-1} \tag{2.4}$$

where reactions 2.1 and 2.2 are gasification reactions, 2.3 is the water gas shift reaction and 2.4 is the main combustion reaction in the fuel reactor [25]. Most often, the overall reactions of solid fuels in the FR are endothermic [21]. Since the conversion of char is a slow process, there is usually a small fraction unreacted which leaves the fuel reactor to the AR due to insufficient residence time. A small fraction of volatiles also leaves the fuel reactor with the flue gas. More on the unreacted volatiles is given in Section 2.5.3. As for the FR temperature, it has been shown that CO was efficiently converted to CO_2 in the temperature range of 840-900 °C. A general trend is that fuel conversion and thereby carbon capture efficiency is increased with higher temperatures, as well as low H_2 concentrations out of the FR at higher temperatures above 840 °C [26].

In the AR, the reduced oxygen carrier gets fully oxidized and regenerated by enough incoming air according to the following reaction.

$$\mathrm{Me}_x\mathrm{O}_{y-1} + 0.5\mathrm{O_2} \rightarrow \mathrm{Me}_x\mathrm{O}_y \tag{2.5}$$

Ideally, the gases leaving the AR should only contain nitrogen and small amounts of oxygen. However, the unreacted char mentioned previously that enters the air reactor is also oxidized by the oxygen in the air, forming a small amount of CO_2 that cannot be captured. Some pilot plants contain a so-called carbon stripper to avoid elutriation of unreacted char to the AR. A carbon stripper is a steam-fluidized bed, which separates unreacted char from the bed material and returns it to the fuel reactor [27]. Implementing such a unit, however, implies additional costs and process complexity, which is why it is not applied in this thesis. Rather it may be more relevant for smaller FR units where the residence time for char conversion is lower.

Furthermore, due to the presence of small quantities of nitrogen and sulfur in the char, some SO_2 and NO could be formed in the AR. This is however not considered in this study. Moreover, only a small amount of fuel ash is expected to reach the AR [21]. Similarly, this is assumed to not be the case in this study.

The overall reactions in the AR are strongly exothermic, thereby heating the oxygen carrier, which in turn provides heat for the endothermic FR [28]. It is therefore important for adequate circulation of the oxygen carrier to provide enough heat to the FR, which is mainly determined

by particle size and gas fluidization velocity. A too-high circulation is however not desired, since that implies a lowered residence time in the FR, thereby lowering carbon capture efficiency. An implication of the endothermic and exothermic nature of the FR and AR respectively, is that the FR be adiabatic to avoid heat losses and the AR be cooled to avoid overheating. Overheating of the AR may lead to issues with the oxygen carrier such as agglomeration of the bed material [21].

The CLC-system shows many similar attributes to that of a circulating fluidized bed (CFB). The AR could be set up as a CFB boiler, with some small differences such as higher solid circulation, and lower gas flow. Additionally, due to the smaller volumetric flow in the FR compared to the AR, the FR could be considerably smaller than the AR [21]. In Figure 2.3 below, a general schematic of a CLC-system provided by Leckner and Lyngfelt [21] is shown, including the AR **(1)**, cyclone **(2)**, FR **(3),** and loop seals **(4)**. The loop seals allow for only solids to pass through from one reactor to another and are preferably fluidized by CO_2 [21]. The cyclone is described in more detail in Section 2.5.2.

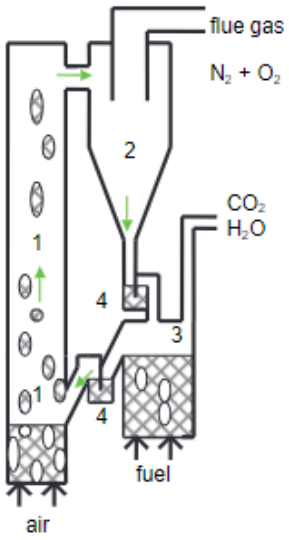

Figure 2.3. Circulating fluidized bed (CFB) principle where 1) Air Reactor, 2) Cyclone, 3) Fuel Reactor, and 4) Loop Seals [29].

In order to ensure maximum fuel conversion and a clean AR, the fuel particles need to be relatively small, therefore obtaining even smaller ash particles, leaving the process as fly ash. More on particle size in section 2.5.2. To ensure a good separation in the cyclone and not contaminate the AR, the OC must be considerably bigger than the fly ash particles [21].

2.3.1 Biomass fuel

Biomass is primarily constituted by the combination of cellulose, hemicellulose, and lignin, together with a trace quantity of extractives and minerals [30]. Normally these three components account for 40-60, 20-40, and 10-25 wt.% of biomass material on a dry basis, respectively [31].

The biomass composition is analyzed performing the proximate and ultimate analysis. In the proximate analysis, the volatiles, ash, and fixed carbon are shown, where their percentages sum up to 100 %. Additionally, in some cases, the moisture content is also included in the analysis.

For the ultimate analysis, the percentages of H, C, N, O, and S are expressed [3]. In some cases, the chlorine and ash percentage are also shown in the ultimate analysis.

In the renewable energy directive 2018/2001 of the EU, one of the extended requisites for the sustainability of criteria to perform large-scale biomass for heat and power using forest biomass is the following: the country of origin must have laws in place related to avoiding the risk of unsustainable harvesting and accounting from forest harvesting [32]. In Sweden, more than half of the land area is covered by forests, approximately 23 million hectares, which makes forest biomass an abundant source to use in order to increase renewable energy use and sustainable production. Although Sweden has only 1% of the world's commercial forest areas, it contributes to around 10 % of the global forest industry business, including sawn timber and pulp and paper products [33]. In order to produce these products, the forest generates some "residues", including chips, tops, and branches (GROT), which are mainly utilized as bioenergy. The combustion of these solid components is quite common in CHP plants [34].

The energy contained within biomass, known as its calorific value, is released as heat energy during combustion. It is one of the most crucial factors in order to determine a fuel's energy potential. The researchers can determine the heat capacity of biomass fuel by either conducting experimental investigations or calculating it using the ultimate and proximate analysis results. It is important to be aware of the ash content in biomass because it has a lower melting point than the combustion temperature due to its alkaline content, resulting in fouling and slagging [35]. High levels of chlorine and alkali in biomass can cause corrosion, therefore it is important to know their concentration [36].

The heating value of biomass can be reported using LHV or HHV and either on a dry or wet basis. Typically, biomass contains high levels of moisture (about 30-40 %), which affects its heating value in comparison to fossil-based fuels such as coal (about 6 %) [35].

2.3.2 Choice of oxygen carrier

Selecting an appropriate oxygen carrier is crucial for the success of the CLC process, which is why considerable time has been dedicated to the testing of various oxygen carriers in pilot plants over the years. By 2020, more than 8,000 hours of operational experience with manufactured oxygen carriers had been accumulated, while over 3,000 hours of experience had been gained using natural or waste materials as oxygen carriers [37].

Initially, nickel-based oxygen carriers were the most extensively tested, primarily because of their reactivity with methane as a fuel. However, this does not apply to solid fuels, and they are associated with health issues, safety, and high cost. Hence, they will not be further discussed [37].

Copper-based oxygen carriers are associated with excellent chemical looping and oxygen uncoupling (CLOU) ability. That is, the copper oxide releases its oxygen which in turn reacts with the fuel, as opposed to a conventional oxygen carrier, which directly reacts with the fuel. A clear drawback however with copper oxide is its high cost [37].

Manganese-based oxygen carriers are cheaper than nickel and iron oxides, but they have not been as extensively researched as other metal oxides. As of 2020, they have only been tested for less than 100 hours using only gaseous and liquid fuels [37].

Iron oxides, with the reduced and oxidized states of Fe_2O_3 and Fe_3O_4 respectively, demonstrate strong reactivity towards syngas, which could be advantageous for CLC processes using solid fuels that generate syngas during devolatilization. Under highly reducing conditions, however, FeO and Fe may be formed which reduces the ability of full oxidation of the gas [37].

Oxygen carriers also have the ability to be composed of combined oxides. That is, oxides composed of more than one metal, such as $CaMnO_{3-\delta}$ and Fe-Cu oxides. These types of oxygen carriers show some CLOU characteristics, along with high solid fuel conversion.

As for natural ores or waste materials, iron materials are popular due to their large availability and low cost. A particular oxygen carrier known as ilmenite is the most used low-cost material in operation with solid fuels. Ilmenite is a mineral, also known as iron titanium oxide with the chemical formula $FeTiO_3$ in its reduced form and $FeTiO_5 + TiO_2$ in its oxidized form. Ilmenite is one of the most abundant titanium minerals and it is currently mined in large quantities [38]. Ilmenite has been tested for numerous hours using a variety of fuels in many different pilot plants. Moreover, ilmenite has been tested for over 12,000 hours as a bed material in a 75 MW_{th} CFB boiler [37]. There are other natural ores and waste materials, such as manganese ores, that are associated with a higher fuel conversion, but result in a greater loss of fines, which may be expensive to replenish during continuous operation [37].

During CLC-operation, it has been shown that a layer of Fe forms around the TiO_2-particle. The layer accumulates and may make the particle brittle, eventually leading to cracks and pores in the particle causing it to break. Additionally, oxygen carriers such as ilmenite absorb alkalis found within the ash in the biomass, causing the bed to defluidize due to agglomeration. Biomass ashes generally consist of higher levels of alkali than coal, such as Na and K. However, biomass generally contains lower levels of ash than coal, which increases the lifetime of the oxygen carrier [26], [37]. The estimated lifetime of ilmenite is in the range of around 200-800 hours depending on the type of fuel [26]. According to a life cycle assessment done on natural gas-powered CLC, the lifetime of ilmenite can be assumed to be on the higher end of 700-800 hours [39]. This is considering that natural gas combustion contains no ash. However, since biomass contains a small amount of ash, the lifetime in the scope of this report is assumed to be 600 hours.

An additional factor that requires consideration during operation is the temperature of the AR which preferably needs to be kept below around 1050 °C, due to the potential defluidization of ilmenite [39]. This was also confirmed during a discussion with the examiner. Hence 1050 °C could be considered the maximum limit of operation without significant issues. In summary, ilmenite is feasible as an oxygen carrier in the scope of this report due to its low cost, availability, performance, and operational experience.

2.4 Upscaling of chemical looping combustion processes

Chemical looping combustion has its origins way back in the 1950s. A patent was filed by Lewis and Gilliland in which a carbon-containing fuel was oxidized by copper oxide to produce pure CO_2. Even back then, the term oxygen carrier was used. The term chemical looping was first introduced in the 1980s though, and since then, over 600 types of oxygen carriers have been tested for many different fuels, sizes, and products [20]. The number of pilot plants which have increased from a few in 2004 to 46 in 2018, as well as the size from barely 1 kW_{th} to the biggest pilot plant of 1 MW_{th} in Darmstadt as of 2012 [20], [40]. The number of pilot plants

utilizing solid fuels, such as coal and biomass, has also increased from being nonexistent in 2004 to accounting for 60 % of all pilot plants in 2018 [21], [40].

As explained by Leckner and Lyngfelt [21], results in small pilots are not directly translatable to the large scale [21]. Therefore, there will be uncertainties during scale-up, which need to be considered in the scope of this report. However, some experience with similar technology of CFBs facilitates full-scale development. An advantage of upscaling is the fact that the reactors will be larger, which provides an additional larger residence time for char conversion. This makes it potentially possible to use fuels of larger sizes than pilot plants, which reduces the risk of fuel elutriation with the flue gas. A direct comparison of the performance of different-sized pilot plants is difficult to make because it is affected by many different parameters. A comparison of the performance, done for different particle sizes of a 100 kW_{th} and 1 MW_{th} plant showed varying results of carbon capture, fuel conversion, and gas conversion. However, the larger 1 MW pilot plant showed generally worse performance, due to its lower operating temperature. As mentioned previously, the performance of CLC-operation is greater at higher temperatures due to the gasification reactions that favor a higher temperature in the FR [26].

Currently, Block 4 at Skövde, the facility in question in this work, has a thermal input of around 49-50 MW, which presents some issues during simulation. As mentioned, small pilots are not directly translatable to the large scale, and the largest pilot plant in operation has a thermal input of 1 MW. Therefore, there are going to be uncertainties in the validity of the simulation. During a discussion with the examiner, a feasible parameter is the CO/CO_2 ratio in the flue gas out of the FR. The conclusion was that a CO/CO_2 molar ratio of approximately 5 % was a feasible expectation for a potential 50 MW_{th} CLC unit utilizing ilmenite. It should be noted that the fuel will likely be well mixed with the oxygen carriers. Hence, fuel particles will be present on top of the bed, and inferior contact between the oxygen carrier and fuel is inevitable. Still, the use of CLOU oxygen carriers or a staged reactor design could be possibilities to improve this figure. This has however not been considered in this work and realistically, some char will inevitably be unconverted in the FR during upscaling, where 1 % from the FR to the AR was assumed to be a reasonable assumption.

The extent of oxygen carrier reduction in the FR is determined by the contact between the oxygen carrier and fuel. A higher residence time implies a higher extent of reduction and more successive endothermic reactions, thereby providing a lower outlet temperature. In pilot plants, the temperature difference between AR and FR varies between around 50 °C – 100 °C and has even exceeded 100 °C during an experiment using the 100 kW_{th} unit at Chalmers [41], [42]. The conversion of oxygen carrier is therefore uncertain and highly depends on the dynamics of the FR. During this study, the conversion of the oxygen carrier was assumed to be enough to account for the higher residence time of the potential larger unit of 50 MW_{th} as opposed to pilot plants. An 80 % conversion was thereby assumed, providing a larger temperature difference of the AR and FR of around 150 °C. Further discussion is given in section 4.1.

A potential CLC unit implemented in a plant must be built as a dual-purpose boiler. Due to the similarities of a CLC and a CFB, a CLC unit should be built as a CFB with a FR separately attached, also designed as a CFB, which may be inactivated if the CLC-operation turns out to be unfeasible and does not meet expectations. In that case, the plant may run as a CFB, and the risk of investment is lowered due to the flexibility of the system [43].

2.5 Flue gas cleaning

During combustion of solid fuels, several components are found in the flue gas apart from H_2O and CO_2. Typical solid fuel combustion products are ash and other solid particles, unconverted fuel components along with NO_x and SO_x [44]. These typical components are discussed in this section, along with the challenges they induce and conventional solutions, to ensure that standards and limits required for transportation and storage of the CO_2 are met. It follows that the removal methods are done sequentially in order to reduce the temperature to avoid heat integration complexity. A flow chart showing the layout of CLC-operation and the method of removing impurities and unwanted components in the flue gas is shown in Figure 2.4.

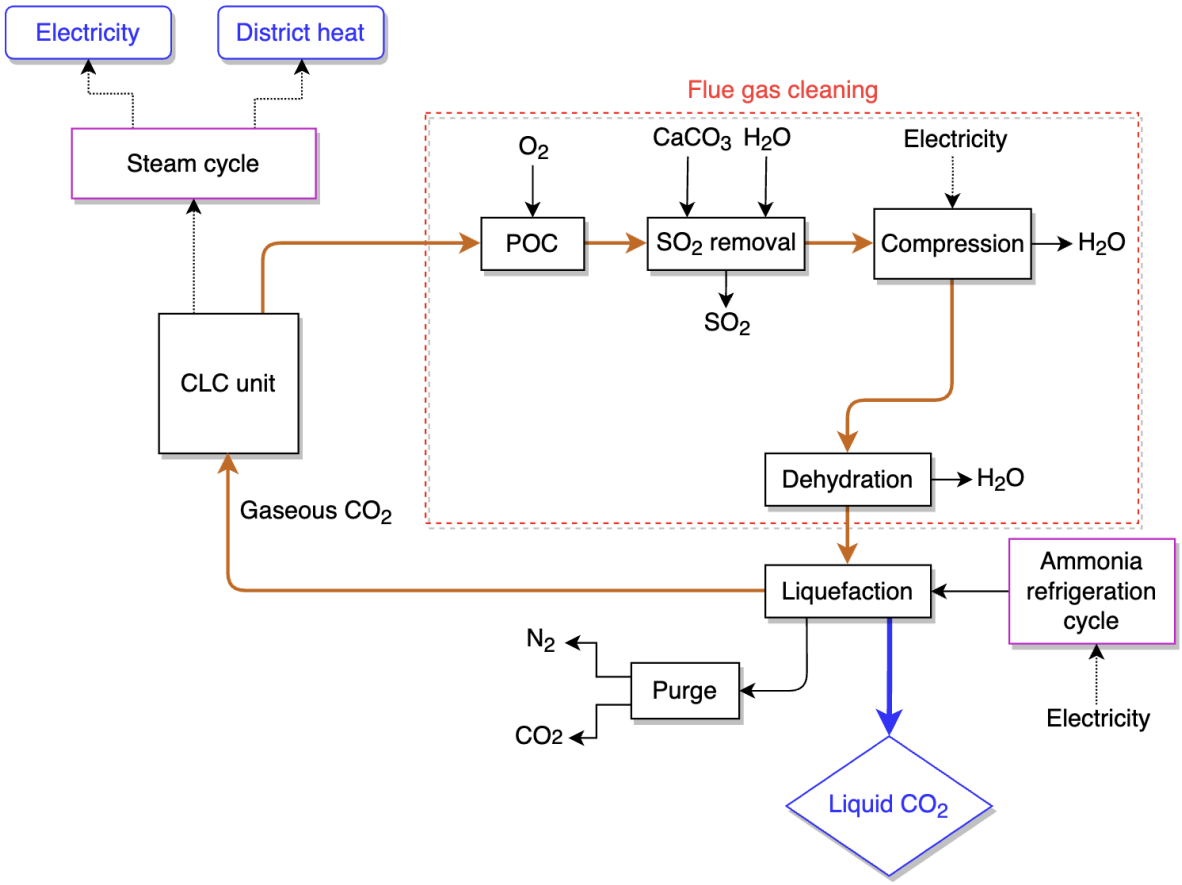

Figure 2.4. Simplified process diagram including the flue gas cleaning procedure.

As seen in Figure 2.4, the flue gas cleaning includes the post-oxidation chamber (POC) for oxidizing unconverted gases from the FR such as H_2 and CO, SO_2-removal, as well as compression and dehydration for water removal. Note that unliquefied CO_2 is recycled to the FR. More on that in section 3.7.3. During the following sections, the procedures for removing flue gas impurities following the chart in Figure 2.4 will be presented, also including particle removal in the CLC unit.

2.5.1 Northern Lights

Northern Lights (NL) is a carbon capture and storage project and a large-scale initiative that has the goal of transporting and storing the CO_2 emissions from industrial sites in Europe, shipping them to an onshore terminal on the Norwegian west coast and storing the emissions

underground at a storage site beneath the North Sea. Incorporated in March 2021 as a partnership between Equinor, Shell, and TotalEnergies, the project is a component of a larger initiative to reduce CO_2 emissions to the atmosphere and battle climate change. As earlier mentioned, NL plans on initiating the storage injections by 2024 and storing 1.5 million tonnes of CO_2 every year [45], [46].

As previously mentioned in Section 2.1, the current objective of Skövde Energi is to transport the liquefied CO_2 by train, to one of the closest habilitated harbors in order to store it in the NL facility. Considering NL as the receiving terminal, some specifications must be ensured to provide long-term safety and integrity of various infrastructure components. This is taking into consideration the safety, material selection, thermodynamics, and chemical reactions during transport and storage [46]. In the following table, the required purity of the CO_2 stream to be transported is shown.

Table 2.1. Purity specification of CO_2 stream to be transported to receiving terminal in the scope of the Northern Lights project [46].

Component	Concentration, ppm (mol)
H_2O	≤ 30
O_2	≤ 10
SO_x	≤ 10
NO_x	≤ 10
H_2S	≤ 9
CO	≤ 100
Amines	≤ 10
NH_3	≤ 10
H_2	≤ 50
Formaldehyde	≤ 20
Acetaldehyde	≤ 20
Hg	≤ 0.03
Cd, Tl	Sum ≤ 0.03

As seen in Table 2.1, numerous potential flue gas components need to be regulated before transportation can occur. In this thesis, formaldehyde, acetaldehyde, mercury, cadmium, thallium, amines, and ammonia are assumed to be negligible. Furthermore, the presence of sulfur in the fuel is assumed to be decomposed into sulfur oxides or hydrogen sulfide [47].

2.5.2 Particle cleaning

Combustion of biomass can lead to the formation and release of different particulate matter (PM) including soot, ash, condensed fumes, volatile organic compounds, and polycyclic aromatic hydrocarbons among others [48].

In CLC, even the fuel itself is susceptible to contaminate the flue gas. The size of fuel particles plays a large role in elutriation from the FR. There is the possibility for the fuel to elutriate

from the FR if the particle size is too small, along with elutriation of char and oxygen carrier. The fuel should therefore have a size large enough to avoid elutriation and to prevent it from reaching the AR. However, it should not be too large, as this increases the residence time needed for full conversion. According to Song and Shen, Lyngfelt suggested an intermediate fuel particle size of 90-300 µm, since about 35 % of introduced char was found to elutriate for particle sizes of 74-125 µm from the FR. For bigger particles around 200-300 µm, the elutriation was found to be much lower [28], [37]. It is however difficult to specify an exact number since the elutriation depends on many other different parameters. Also as mentioned in section 2.4, larger fuel sizes may possibly be used on a large scale.

Northern Lights has specifications regarding PM and solids in the CO_2 stream generated by biomass combustion [45], [46]. The CO_2 stream is to be free from solid particles and should not contain any other impurities than those specified in Table 2.1.

In the present work, the particle size distribution has not been added for the different possible PM during simulation. Therefore, particle removal unit operations will not be modeled in detail. Rather, solids in the simulation will be separated from the rest of the flue gas using a simple separation unit in Aspen Plus. However, relevant unit operations will be described in the two following subsections which should be noted during realistic implementation.

2.5.2.1 Cyclones

Cyclones are widely used gas-solid separators in many industries for cleaning waste/flue gas. They have a simple design, low capital cost, and do not require high maintenance, which makes them ideal as pre-cleaning devices before the use of more expensive equipment such as baghouse filters or electrostatic precipitators. Cyclones use centrifugal force for the separation of solid particles from gases and are effective at removing particles of relatively larger sizes of a few µm [49], [50].

In the context of CLC, cyclones are included in the design of a CFB in the FR and AR. For the FR, the cyclone recirculates the oxygen carrier and captures other solid particles such as bypassed char. The cyclone of the AR returns the oxidized OC back to FR.

2.5.2.2 Electrostatic precipitators

An electrostatic precipitator (ESP) uses an electric charge to remove impurities and solid particles from the flue gas, without significantly impeding the flue gas flow, resulting in a low-pressure drop. ESPs have the ability to capture fine particles, and should preferably be operated at above 180 °C to avoid acid condensation due to the presence of SO_2 [51], [52].

An ESP is a good complement to the cyclone of the FR to completely capture solid particles, for a solid-free flue gas to comply with the standards of NL. Additionally, an ESP is already currently used in Block 4 to remove fly ash and dust from the flue gas. Hence, it is assumed to still be in operation during CLC-operation. During this work, potential PM from the AR, such as fragmented OC and ash, was not considered.

2.5.3 Oxypolishing

Oxypolishing is an essential step in CLC since it is difficult to achieve complete combustion in the fuel reactor. The reason being that there is insufficient contact between oxygen carrier

particles and fuel gases due to bubbling effects in fluidization systems. This results in incomplete combustion gases leaving the FR, mainly CO, H_2, and CH_4. Any H_2S present in the flue gas would also be oxidized into H_2O and SO_2. Some strategies have been proposed to enhance contact between oxygen carrier and fuel gas, enhance reaction kinetics, and higher reactivity of oxygen carrier, but it is still difficult to achieve complete combustion. Therefore, a post-oxidation chamber (POC) is installed after the FR, where the flue gas is mixed with an injection of pure oxygen to fully combust these components to CO_2 and H_2O. In a POC, the amount of oxygen provided can be adjusted, allowing for the possibility to include a variety of fuels in CLC and operating conditions [53].

The oxygen needed for the oxypolishing would have to be produced by an air separation unit, using mature cryogenic technology. Therefore, there is an energy penalty associated with the utilization of pure oxygen. The energy penalty is minimal though, due to the small amount needed for complete combustion. Moreover, the heat produced by the combustion in the POC should be used to heat up steam [53]. Since Skövde Energi is a relatively small power plant, the implementation of an air separation unit for the production of a small amount of oxygen is difficult to justify, considering the high cost of equipment. It is thereby assumed that oxygen needed for the oxypolishing should be bought by a supplier. Since providing more oxygen carrier to the fuel in the FR implies additional oxygen, it is worth noting that doing so increases fuel combustion. Consequently, the need for oxygen in the POC is reduced. There may be a trade-off between the expense of utilizing more oxygen carrier or oxygen in the POC, depending on the cost of the oxygen carrier.

As can be seen from Table 2.1, there is a need to minimize CO and H_2 in the flue gas to below 100 ppm and 50 ppm respectively. Additionally, the O_2 concentration in the flue gas may not exceed 10 ppm. Hence, the POC should be constructed to fully allow the oxygen and gaseous fuels to mix and combust to reduce all of these components as much as possible. Due to limitations on oxygen concentration as well as cost considerations, additional oxygen should not be provided in great excess. However, a small excess is probably necessary to allow for nearly full oxidation [53]. In a report about the performance of an oxypolishing step using a pilot 100 kW_{th} CLC-system at Chalmers by Mei. et al, an optimal molar fraction excess of 1 % over the stoichiometric amount of oxygen needed for combustion was optimal for achieving low fractions of CO, H_2, and O_2 in the flue gas. CH_4 was burned easily, however, CO was more challenging to keep at a low level, due to the presence of char that bypasses the cyclone and oxidizes slowly. This could be improved by lowering elutriation from the FR [53]. Larger residence and mixing times might also be possible with a larger reactor.

2.5.4 NO_x, SO_x, and HCl cleaning

Solid fuel combustion can lead to emissions of NO_x and SO_x, which are harmful pollutants. Among these, the major harmful components are NO, NO_2, and SO_2. The presence of these components in the flue gas may arise due to the presence of nitrogen and sulfur in the fuel, of which SO_x may additionally be formed by the combustion of H_2S in the POC, as mentioned in the previous section. These acidic gases are considered to be the leading cause of environmental issues such as acid rain, photochemical smog, and ozone layer depletion [54]. In addition, these contaminants are toxic, and could in high concentrations lead to health issues such as respiratory diseases, such as asthma, bronchitis, etc. [54]. Sulfur-containing components also have the potential to form corrosive chemicals, such as sulfuric acid, which has been shown to

form in several oxy-fuel laboratory and pilot scale studies [55]. Due to these reasons, research into reducing NO_x and SO_x in flue gas has been conducted over the last two decades, resulting in various technologies that are used today [54], [55]. The most widely used technologies are wet flue gas desulfurization (WFGD) for the removal of SO_x and selective noncatalytic reduction (SNCR) for the removal of NO_x.

According to Lyngfelt et al, NO_x formation in the FR in a CLC-system is low [56]. With the assumption of 0.5 % O_2 and 0.5 % N_2, the equilibrium NO_x concentration will be approximately 16-60 ppm at high temperatures of 1200-1500 °C. However, a FR operates at lower temperatures of around 900 °C. Hence, thermal NO_x formation is not expected during CLC-operation [56]. Potential NO_x-formation will be simulated in this thesis, but the assumption is that NO_x-formation is negligible. Hence, SNCR will not be implemented in the simulation and will not be further analyzed.

As the amount of nitrogen present in the flue gas is proportional to the amount of nitrogen in the fuel, it is unavoidable for a fuel containing nitrogen to have a flue gas in a CLC-system that is free of any traces of nitrogen. Northern Lights does not have a required purity related to the nitrogen amount, but to acquire a highly pure liquid CO_2 stream to be captured, potential nitrogen should be removed late in the process using flash separation due to the low boiling point of nitrogen.

WFGD is the most used SO_2 removal method because of its great efficiency, stability, and its capacity to operate at a range of different temperatures. WFGD using absorption of SO_2 in a slurry of limestone in water is the most wide-spread desulfurization method worldwide. In this procedure, the limestone slurry and flue gas are both driven into a spray tower absorber where they are combined with water. Limestone, which is basic, reacts with the acidic SO_2 before being absorbed into the liquid phase to form gypsum and leaving the absorber according to the following reactions 2.6 and 2.7 [43].

$$SO_2 + CaCO_3(s) + 0.5H_2O \rightarrow CaSO_3 \cdot 0.5H_2O(s) + CO_2 \quad (2.6)$$

$$CaSO_3 \cdot 0.5H_2O(s) + 0.5O_2 + 1.5H_2O \rightarrow CaSO_4 \cdot 2H_2O(s) \quad (2.7)$$

Where the O_2 needed for gypsum production in reaction 2.7 could be supplied by air. The solid waste product could be recycled or used in the production of fertilizer or gypsum. The main disadvantages of this process are relatively high capital and operating costs and water consumption [54].

Another issue arising from combustion processes is the potential chlorine present in the fuel. HCl, which may be produced during combustion, may cause downstream corrosion and combine with the alkali released during solid fuel combustion [57]. HCl is also a highly toxic gas and exposure may lead to several health issues. Release to the environment could be dangerous as HCl in water for instance leads to the formation of hydrochloric acid [58].

Currently, to the authors' knowledge, there is no HCl concentration requirement in the Northern Lights project. However, it is safe to assume that it should be kept low due to reasons described in the previous paragraph, namely corrosion, toxicity, environmental risks, and conserving a high process efficiency. From a discussion with the examiner, it is safe to assume that the HCl concentration in the flue gas is negligible due to the low presence of chlorine in biomass. Furthermore, as discussed in section 2.3.2, potential chlorine reacts with the ash to produce alkali chlorides. The alkali chlorides produced can deposit on downstream equipment which

can lead to fouling and reduced process efficiency, which is why proper particle separation from the flue gas is important. Potential solid particles that escape with the flue gas stream are preferably captured with an ESP. Due to the formation of alkali chlorides, chlorine potentially found in the flue gas is assumed to be reacting with the ash and is thereby removed in the ash removal process. Hence, HCl presence in the flue gas is assumed to be low. Additionally, any potential HCl in the flue gas would be neutralized by WFGD along with SO_2 [43].

In a modeling study done by Yakah et al, the removal of HCl and SO_2 in the flue gas was modeled using two absorbers in series with ten stages each. The first absorber removes the HCl simply by injection and absorption of the HCl in water with over 95 % efficiency. The second absorber, also comprising ten stages, removes the SO_2 with over 99 % efficiency. For the second absorber, a slurry of 90:10 wt.% of water and $CaCO_3$ respectively was implemented [59]. In this thesis, the presence of HCl in the flue gas is assumed to be low due to the reasons mentioned in the previous paragraph. Hence, only SO_2 removal is implemented in the modeling, using similar operating conditions and equipment as done by Yakah et al [59]. Moreover, the material costs of $CaCO_3$ and gypsum are neglected due to insufficient data in the literature.

2.5.5 Excess oxygen removal

As stated previously, an ideal stoichiometric molar excess of oxygen in the oxypolishing step is roughly 1 %. This suggests that it is likely that the final flue gas will have an oxygen content higher than 10 ppm. Therefore, a relevant oxygen removal step needs to be implemented since oxygen induces corrosion and two-phase flow in the transport [60].

There are numerous methods of separating oxygen from flue gas. Some relevant ones are listed below, ranked from most to least relevant in descending order according to Abbas et al:

- Catalytic oxidation of H_2,
- Cryogenic distillation,
- Adsorption onto a copper or based adsorbent,
- Oxidation of coal and catalytic oxidation of CO.

Key factors behind the ranking of these methods are efficiency, safety, operating conditions, and energy requirement. Catalytic oxidation of H_2 is safe, has optimum operating conditions (80 °C), has low energy requirement, and is considerably safe. However, since the oxidation of H_2 leads to the formation of water, this method increases the moisture content of the flue gas. The next method in order is cryogenic distillation, with its high efficiency and safety, but has a high energy requirement and unfavorable operating conditions (-56.6 °C), leading to a high capital and operating cost. An advantage, however, is the ability to achieve a very high CO_2 purity. Adsorption on Cu has high efficiency and safety but high operating conditions, leading to high costs. Oxidation of coal and catalytic oxidation of CO is in the lowest ranking due to the toxicity of carbon monoxide [43], [60].

The implementation of a technology to remove excess O_2 is not done in this thesis. However, if done in the future, catalytic oxidation of H_2 is deemed to be a suitable method due to the reasons mentioned above. The process involves the reaction of H_2 with O_2 to form H_2O in the presence of a noble metal catalyst such as palladium or platinum at 80 °C. It has been shown to be able to reduce the O_2 content in flue gas to below 10 ppm, given that the hydrogen content

is between 500 and 1000 ppm [60]. Cryogenic distillation may also be favorable due to its high purity potential.

2.6 Compression and liquefaction

Carbon dioxide compression and liquefaction is an essential part of the CCS chain and for other industrial applications such as enhanced oil recovery, and food/beverage production. In these applications, CO_2 is compressed and liquefied in order to reduce its volume and safely facilitate its transportation and storage.

The compression process involves reducing the volume of the gas by applying pressure. In the CLC-system, the flue gas obtained is mainly CO_2 and H_2O. To separate most of the water, different intercooling and flashing steps in each stage of the compression are applied. After the compression, CO_2 can be cooled and liquified by reducing the temperature below its critical point which, as can be seen in the phase diagram shown in Figure 2.5, is at 73.77 bar and 30.98 °C. This can be achieved using a multicompressor and an ammonia refrigerator cycle.

The optimal conditions for ship transportation are being raised as CCS chains are moving closer to implementation. In CinfraCap's first preliminary study published in March 2021, it is stated which conditions the CO_2 should have to be sent to the NL facility through the CinfraCap project [12].

When handling CO_2 in the liquid phase, it is kept at a low temperature and is then called a cryogenic liquid. Those conditions involve a saturation pressure of 16 bar and approximately -26.5 °C. In order to compensate for heat loss during transport, it is advised to cool the liquid by approximately 2 °C, which corresponds to a temperature of -28.5 °C. The transportation by ship will be at 16 bar and approximately -26.5 °C, which is chosen to maintain a maximum of 19 bar upon arrival at the NL receiving facility [12]. During this project, the final liquid CO_2 was conditioned to reach 16 bar and -28.5 °C to comply with the mentioned specifications.

During the CO_2 compression and liquefaction, there are some considerations:

- When compressing, it is important to control the temperature and pressure in order to assure that the CO_2 will remain in the gas phase. If the pressure is too high or the temperature is too low, the CO_2 can condense into liquid or solid, which could end up damaging the compression system and reducing its efficiency.
- During compression and liquefaction of the CO_2 is important to not reach the critical point, which is shown in Figure 2.5.
- When liquifying the CO_2, the temperature and pressure must be monitored in order to ensure that the CO_2 is not in the supercritical state, the state where both gas and liquid phases coexist. Once the CO_2 is in the supercritical state, further compression will cause it to liquefy.
- During the storage and transportation of CO_2, it is important to control the temperature and pressure to ensure that the CO_2 stays in liquid form, not solidifying nor gasifying.

Therefore, it is important to maintain the liquid CO_2 close to the saturation line but not on the line, to ensure that there will be no vapor phase even after its transportation [12], [61].

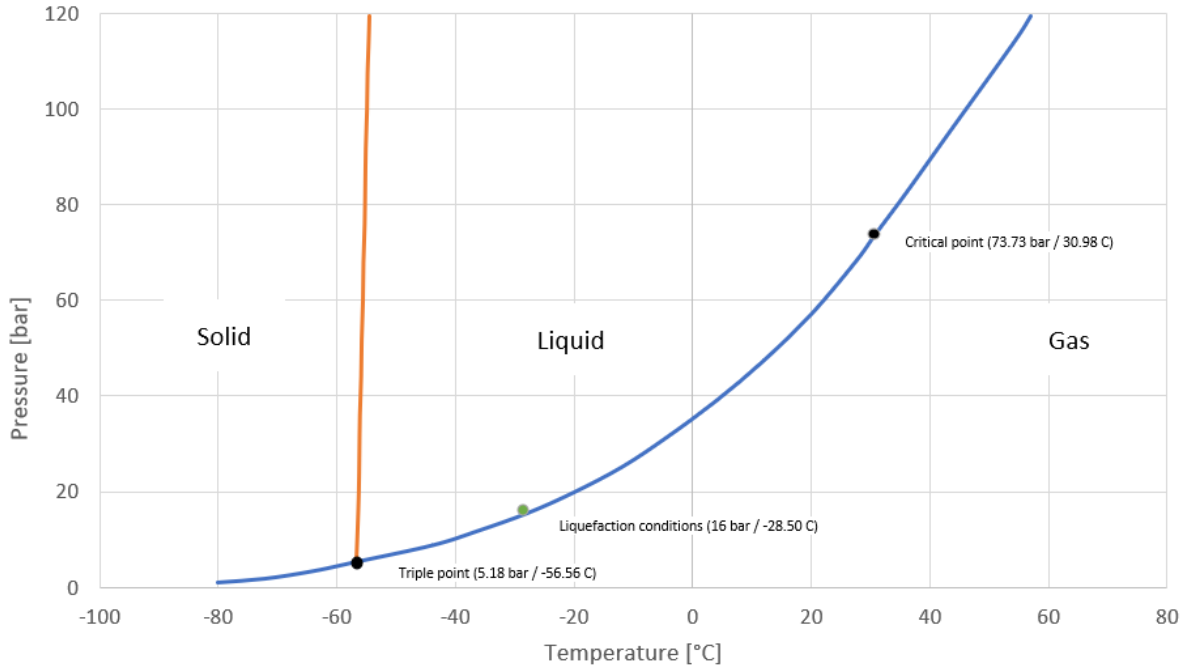

Figure 2.5. Phase diagram of pure CO_2 based on the Span and Wagner equation of state. The data was obtained by approximation of the diagram stated by Deng et al [61].

It is important to ensure that a purified CO_2, following the NL specifications shown in Table 2.1, enters the liquefaction process. For that, the study of NO_x, SO_x, HCl, O_2, and H_2O has been performed and will be conducted downstream of the CLC process. After the purification, the liquefaction process begins.

There are two main liquefaction designs, together with the compression part. The first one is named "open-cycle liquefaction" which is based on compressing the gas to a high pressure and then liquefying the CO_2 by expansion [62]. The second one, called "close-cycle liquefaction", is based on first compressing the gas and then liquefying it with a refrigeration cycle [62], [63]. It is mentioned by Gong et al, that the second option has lower energy requirements, therefore it will be used in this work [63]. Deng et al [61] suggest conducting the compression process using a multi-compressor. It is stated as a recommendation that if the final compression pressure is smaller than 25 bar, three compression stages are enough. However, when the liquefaction target pressure is above 25 bar then four stages of compression should be used [61]. A sensitivity analysis will be conducted on the appropriate amount of compression stages in the case of the studied Block 4 in section 3.11.2.

An ammonia-based two-stage vapor compression cycle with an intercooler and a main heat exchanger (condenser) is recommended to be used for cooling the CO_2-stream [61]. Therefore, all the heat exchangers in the process use water as a cooling agent except for the liquefier, where ammonia is used. The refrigerant cycle involves compressing ammonia gas with a compressor, causing it to heat up and then move into the condenser where heat is dissipated, turning it into high-pressure liquid form. It then moves through the expansion valve, where it boils and becomes significantly colder than the CO_2 that is desired to condense. This cold ammonia is used to cool the CO_2, bringing it to a liquefied state, while the ammonia is gradually warming up as it passes through the evaporator and then is pulled back into the compressor to start the cycle again [61].

After this system, the CO_2 should be fully condensed and slightly sub-cooled. When the CO_2 contains residual components, the bubble point temperature is much lower than the one for pure CO_2, and the stream, after the liquefier, might only be partially condensed. In these cases, a flash tank can be used to purge the uncondensed gas and prevent an accumulation of them in the system. The liquid obtained, which is mostly CO_2, passes through a valve in order to expand it to the desired pressure, in the CinfraCap project which corresponds to 16 bar. The obtained stream passes through a flash separator in order to store the CO_2 liquid and recirculate the uncondensed gasses to the refrigeration system [12], [61].

2.6.1 Excess water removal

During the compression process, some water is removed in the intercooling step of the multi-compressor stages. In most cases, this procedure is not enough to ensure the low concentration set for the NL project, 30 molar ppm, therefore, a water removal system must be included. There are two main technologies suggested by Leckner and Lyngfelt [21], which have been analyzed for a CLC configuration, where the water content can meet the requirement of the Northern Lights project [64], TEG and molecular sieve dehydration process [65]. It is important to note that the described technologies would play an important role in offloading the main dehydration unit, in the case of Deng et al [61] design, the compressors with inter-stage cooling and knockout, while enabling to achieve low moisture levels in the CO_2 stream [66]. The offloading could lead to smaller and less costly dehydration systems [65].

The first technology mentioned would be to use triethylene glycol (TEG) as a liquid desiccant to perform absorption. The TEG process would consist of a scrubber with a reboiler and different flash separation units which would account for the absorption of water and solvent regeneration process. A standard absorption using TEG would achieve a water content of 150 ppmv, in the best-case scenario. It is stated by Kemper et al [66], [67] that various methods currently under research could increase the drying performance of TEG absorption to achieve a water content of 30 ppm or lower.

The second technology is the molecular sieve dehydration process. It consists of a two-bed system where the spent regeneration gas is returned to the inlet of the adsorption bed. The process uses pressurized air or CO_2 for regeneration, where, if the air is used, a higher volume and therefore a bigger equipment, would be needed [64], [66]. The process could achieve a water concentration of less than 1 ppm without increasing the capital costs. If a lower water concentration is wanted, the sorbent bed cycle decreases [66].

The suggested conditions for the molecular sieve dehydration are a temperature of 30 °C and a pressure of 30 bar. For regeneration of the sorbent 175-320 °C would be needed [66].

A study was conducted by Kemper et al [66] to analyze the effect of different impurities in both proposed dehydration systems. For the molecular sieve, the following maximum tolerable amounts of components are suggested and stated in the following table.

Table 2.2. Effect of impurities in molecular sieve and TEG dehydration system [66].

Impurity	Effect on TEG system	Effect on mol. sieve system
H_2O	Formation of liquid droplets and mist can weaken absorption capacity	Formation of liquid droplets and mist can exhaust the sieve or react with the binder causing a breakdown of the structure
Inerts (N_2, H_2, CH_4…)	No effect (No limit)	No effect (No limit)
O_2	Oxidative degradation of TEG	If sulfur present: blockages (Limit 15-50 ppm)
H_2S	Limit: 3000 ppm	Acid degradation of sieve, COS can form; if O2 present: formation of SO2 and free sulfur, corrosion (limit 0-1000 ppm if O2 present)
NO_x, SO_x	Not found	Attack sieve structure reducing lifetime, acids can form during regeneration
HCl, other acids	Lower pH causes corrosion (limit 200-300 ppm for HCl)	Dealumination of zeolite framework, causing dust formation (Limit: 0-1 ppmv)
CO	Not found	No effect nor limit
NH_3	Not found	Co-adsorption if H_2O in liquid state present: ion exchange weakens sieve structure. Limit: 5-10 ppmv

Regarding the technology costs, the minimum CAPEX and OPEX for both, molecular sieve and TEG absorption, depend mainly on the operating pressure, solvent regeneration process, and other impurities. In case of high impurities, it has been calculated that the CAPEX will increase for both systems. For the molecular sieve system, the presence of impurities such as NO_x, SO_x, and H_2S would lead to a 7 % increase in CAPEX but no difference in OPEX. When the study was conducted, there was no possibility to quantify the exact effect of impurities on the TEG absorption costs [66].

There is a lot of controversy between choosing molecular sieve or TEG-modified absorption. For the TEG-modified absorption process, not enough information regarding the conditions, costs, and impurity tolerance is available. Additionally, with the available data, it is claimed that molecular sieve has a better performance and could result in lower costs. The maturity of molecular sieve over TEG absorption in the industry is what drove the implementation of molecular sieve for downstream gas purification [66], [68]–[70].

2.7 Literature review on the capture costs using CLC

One of the first estimations of the cost for CO_2 capture using CLC with solid fuels was in the project ENCAP, managed by the European Union (EU), where it was found that the price could

be as low as 10 €/tonne CO_2 captured. Later studies show other low costs of 16-26 €/tonne, 26 €/tonne, and 20-30 €/tonne using coal as fuel and 24 €/tonne when using biomass [21].

A study conducted by Leckner and Lyngfelt [21] show the following values of CAPEX and OPEX per tonne of CO_2 captured for a 1000 MW_{th} using coal as fuel.

Table 2.3. Cost estimations from literature for CLC in a 1000 MW_{th} plant using coal as a fuel [21].

Process section	Costs per tonne CO_2 captured [€/tonne CO_2]
CO_2 compression	10
Oxypolishing	6.5
Boiler cost (FR)	< 1
Oxygen carrier	2
Steam and hot CO_2	0.8
Coal grinding	0.2
Lower air ratio	-0.5
Total	**20**

Leckner and Lyngfelt [21] state that the compression of CO_2 corresponds to the highest share in the cost, which is an inevitable part of any CO_2 capture technology. The second most important cost is the oxy-polishing due to the oxygen required. It must be noted the low added cost of a CLC boiler, which consists of well-insulated reactor walls, in comparison to an extra CFB, as it is an adiabatic reactor, meaning that the walls are not used to produce steam [56]. Leckner and Lyngfelt [21] mention throughout their study that a lower air ratio is used in the designed unit, which has led to a 5 % smaller gas flow in the CLC-CFB, in comparison with a CFB. In the designed case, the air ratio is similar to a CFB unit, therefore the lower air ratio benefit is not accounted for. Additionally, in this thesis, the cost of possible grinding of OC and/or fuel is not considered. Finally, Leckner and Lyngfelt [21] conclude that the added cost relating to the boiler system could be very low and that the main focus to reduce costs is in gas conversion while maintaining a low OC cost [21].

Furthermore, Deng et al [61] explain throughout their work that a cost of 16-21 €/tonne CO_2 will be incurred in order to compress and liquefy the CO_2 to a pressure of 15 bar, depending on the amount of impurities.

The results from this work will be compared with the previously mentioned values from the literature in order to understand their differences and analyze the technology competitiveness.

2.8 Software

In this section, the two main software tools used in the current work are briefly described.

2.8.1 Aspen Plus

Aspen Plus® is the leading process simulation software in the chemical industry and is utilized for a wide range of applications. Reactors, separators, pressure changers, heat exchangers, and other unit operations are all simulated in this robust tool for chemical and process engineers.

Using a graphic interface, process flow diagrams can be constructed by connecting different unit operations. Aspen simulates processes involving the handling of solid materials, fluids, and electrolytes using a vast database of physical attributes, mathematical equations, and thermodynamic models [71].

Aspen works well for both applications involving the simulation of combustion processes and chemical looping combustion. Its ability to handle solid materials in processes like biomass combustion, oxygen carrier oxidation and reduction, and power generation by means of a Rankine cycle is an advantage.

2.8.2 Aspen Energy Analyzer

Aspen Energy Analyzer is a software tool developed by Aspen Technology for engineering and optimizing solutions regarding process energy analysis. The energy management software is used for performing optimal heat exchanger network design to minimize process energy [72]. The software provides a set of features and capabilities to perform energy analysis and identify opportunities for energy savings in the process industry.

Some of its key functionalities are data integration, energy performance indicators, energy simulation, energy optimization, energy reporting, benchmarking, and targeting. The possibility of integrating the program with other software from AspenTech is an advantage when analyzing the process systems.

In the project, Aspen Energy Analyzer is used to perform the heat exchanger network, based on the target load of utilities calculated by it. In addition, the Grand Composite Curves (GCC) and the utility curves are plotted using the software.

3 Method

The process of the project is explained in detail throughout this section. This involved getting important parameters from Skövde Energi and choosing the most pertinent presumptions to use. A simulation procedure of a CLC process was presented, together with the relevant parameters used. Steam generation cycle, downstream flue gas cleaning, CO_2 compression, and liquefaction were also simulated. Additionally, heat integration was used to quantify the heat recovery potential. The proposed process design was then the subject of a techno-economic study and sensitivity analyses were performed. The resulting process was lastly compared to a post-combustion process previously conducted by the company for the same boiler unit.

3.1 Data collection

The data for the reference plant have been taken from the data given by Skövde Energi [13]. Some data, which was not provided by the company, was assumed and taken from the literature and it is given below.

3.1.1 Biomass data

The biomass used at Skövde Energi's facility is a mixture of woodchips, GROT, and bark which depends on each "batch". As the fuel composition is constantly changing, the data used for the present work corresponds to the prerequisites specified by the manufacturer of the current CHP plant. The calorific value, proximate, and ultimate analysis data are expressed in Table 3.1 [73].

Table 3.1. Biomass data used in the present work [73].

Calorific value	Lower calorific value (moisture-free) [MJ/kg]	19.1
	Lower calorific value [MJ/kg]	10.51
Proximate analysis	Moisture content [%]	45
	Ash [% dry matter]	2.5
	Fixed carbon [% dry matter]	17.1
	Volatile matter [% dry matter]	80.4
Ultimate analysis	Carbon [% dry matter]	50.11
	Hydrogen [% dry matter]	5.9
	Oxygen [% dry matter]	40.93
	Sulfur [% dry matter]	0.04
	Nitrogen [% dry matter]	0.5
	Chlorides [% dry matter]	0.02

3.1.2 Oxygen carrier

In this work, a CLC model has been designed for ilmenite. The composition of the ilmenite ore used in this work has been extracted from Cheng et al [74], where different OCs are studied,

and the most important components of ilmenite ore are mentioned. This ilmenite ore is composed of many different components, but the major components have been used in the simulation, as mentioned in Table 3.2.

Table 3.2. Composition of the OC used (Ilmenite).

Composition (wt.%)	**Fe_2TiO_5**	**Fe_2O_3**	**SiO_2**	**TiO_2**
Ilmenite	54.7	11.2	5.5	28.6

It is important to note that in the Aspen Plus model, Fe_2TiO_5 is defined as $Fe_2O_3 + TiO_2$, where TiO_2 and SiO_2 are assumed to be inert.

3.1.3 Steam cycle

The data for the optimal operation of the turbines is given by the equipment supplier of the actual turbines installed at Skövde Energi. The present work intends to use the existing steam cycle to produce steam and electricity for the district heating.

The data used for the turbines is part of one of the performance tests that the supplier guarantees and it is expressed in Table 3.3. The load case used is case A, as it is the one currently being used at Skövde Energi's plant for the heat and production system [75].

Table 3.3. Data used for the steam cycle simulation (turbine) [75].

Load case	**A**	**B**	**C**	**D**
Steam at supply limit into the turbine				
Pressure (bar)	90	90	90	90
Temperature (°C)	480	480	480	480
h in Enthalpy (kJ/kg)	3,336.5	3,336.5	3,336.5	3,336.5
Flow (kg/s)	14.1	14.10	9.20	3.80
Extraction steam				
Pressure (bar)	7.1	7.0	7.9	-
Temperature (°C)	198.4	197.1	225.6	-
h bleed Enthalpy (kJ/kg)	2,841	2,839	2,898	-
m bleed Flow (kg/s)	1.73	1.89	1.23	0
Exhaust steam at supply limit				
Pressure (bar)	1.34	1.13	1.13	1.13
h out Enthalpy (kJ/kg)	2,622	2,588.5	2,618.8	2,645.8
m out Flow (kg/s)	12.36	12.20	7.96	3.79
District heating temperature (°C) [13]	50-120	100	100	100
Electrical output at a terminal on generator (kW_{el})	**9,294**	**9,662**	**5,959**	**1,566**

3.2 CLC-process description

A brief description of the CLC-process is given in this section, following the information given in the theory sections above, along with a full process flow chart shown in Figure 3.1.

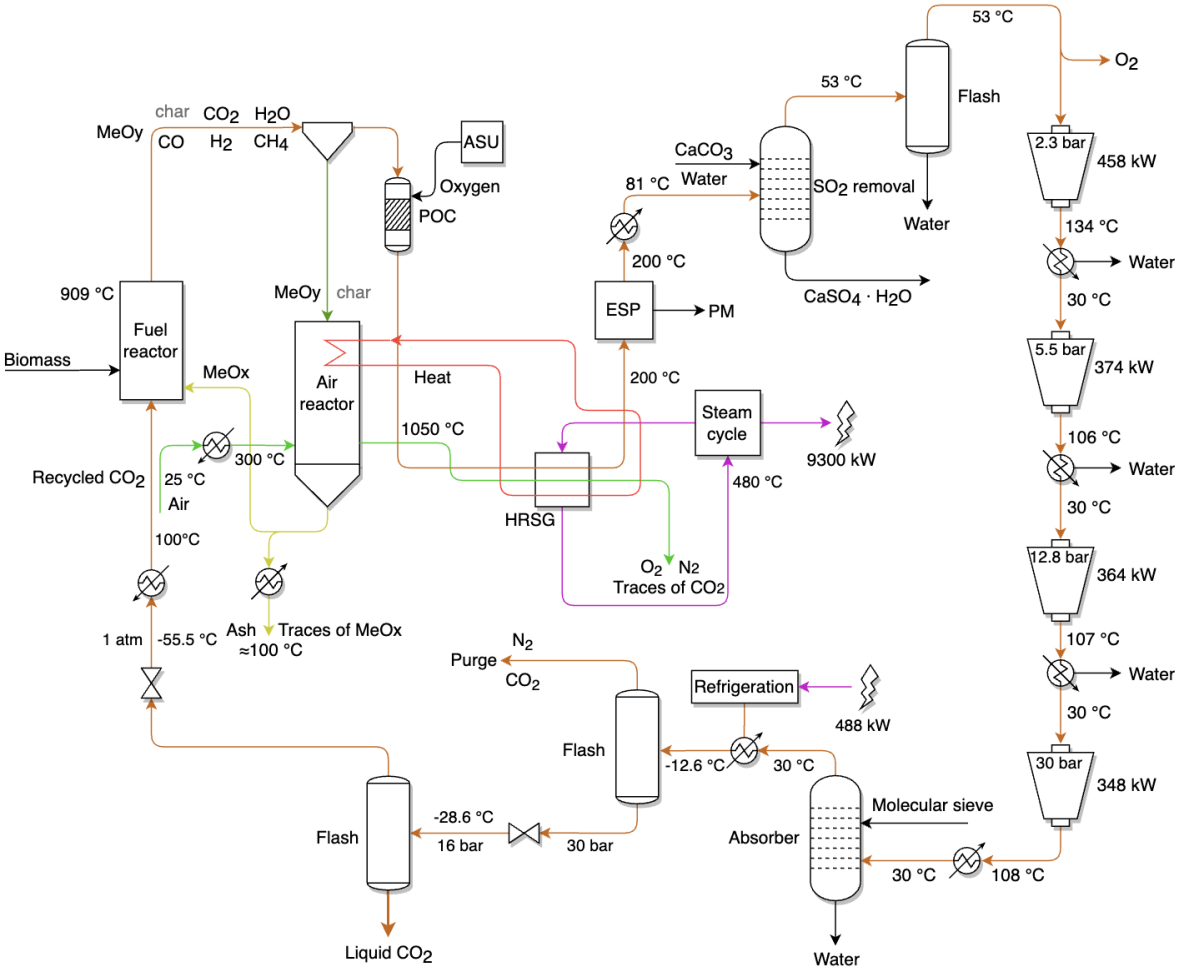

Figure 3.1. CLC-process design layout.

As shown above, the flue gas produced during CLC-operation is separated from solid components with a cyclone and then goes through a POC for complete volatile fuel conversion. The solids that were separated in the cyclone go to the air reactor and a subsequent ash handling and separation system, which was not modeled due to unknown particle size distributions. The heat of the flue gas and the air reactor was used to heat up steam in the HRSG for electricity and district heat production. A more detailed description of the steam cycle is given in section 3.6. The relatively cold flue gas enters the ESP for further small particle separation such as fly ash, which again was not modeled due to unknown particle size distribution. It follows that the ESP shown in the flow chart is theoretical and not included in the simulation. Rather, solid separation is simply separated using a simple separation block in Aspen. Complete PM separation is assumed in this thesis, which implies no solid particles in the flue gas. The flue gas was further cooled and SO_2 removed by WFGD using literature data [59], where a negligible amount of CO_2 is also assumed to be released, according to reaction 2.6. Water is then separated with a flash unit prior to the multicompression stage, and excess of O_2 in the flue gas is disregarded due to insufficient simulation data. Hence, its concentration is assumed to be negligible. The flue gas was then the subject of four-stage multicompression with intercooling and water separation. The compression was done with equal pressure ratios followed by high-pressure dehydration by means of absorption using molecular sieve. The flue gas was then cooled using an ammonia refrigeration cycle which is described more in detail in section 3.7.3.1. The resulting CO_2-stream was separated and purged using a flash column to

get rid of N_2. The liquid stream was throttled, and again separated, capturing the pure CO_2-stream and reusing the vapor as a fluidization agent in the FR after throttling and preheating. The vapor was extracted at this point due to the purity of the stream, thereby reducing the cost of the entire flue gas purification chain. Nevertheless, a comprehensive analysis of this was not done. In the following subsections, the design procedure will be explained and justified in further sections.

3.3 Modeling the existing plant

In this work, steady-state modeling of the current of a reference plant at Skövde and CLC plants is performed using Aspen Plus. The reference plant was initially modeled for biomass drying, combustion, basic ash separation, air preheating, and steam cycle power generation in a Rankine cycle to learn the basics of using Aspen Plus. The traditional combustor in Skövde Energi is then replaced by an AR and FR in order to model the CLC plant. The same input parameters were used for modeling the CLC plant to have a better understanding of different processes.

3.4 Setting up the simulation

To start an Aspen Plus simulation the steam class needed to be set. MIXCINC steam class was used in this work which allowed the mixture of three sub-streams: MIXED, Conventional Inert (CI) solid, and Non-Conventional (NC) solid. The sub-stream "MIXED" consists of all the components in the liquid and vapor phase whereas the "CI Solid" and "NC Solid" consists of all the solid compounds with and without molecular weights, respectively. Due to the unknown exact weight, Ash and Biomass are defined as "NC Solid" while Char and OC are defined as "CI Solid".

Biomass is defined in Aspen Plus as a Nonconventional component where the data, shown in Table 3.1, is used as an input for the component attributes together with the heat of combustion (HCOMB). To consider the formation of ash in the FR it needs to be defined in Aspen Plus. As well as the biomass, the ash is defined as a Nonconventional component and the component attributes proximate, ultimate, and sulfur analysis are defined. In the case of ash, the element ash in each component is defined as 100%.

The enthalpy and density of the biomass are needed and calculated through "HCOALGEN" and "DCOALIGT" models in Aspen Plus, respectively. In order to properly calculate the enthalpy using "HCOALGEN", the value of the dry heat of combustion (HCOMB) is specified in Aspen Plus, as expressed in the following equation.

$$\text{HCOMB} = \text{Heat of combustion (wet)} \cdot \frac{100}{100 - \%\text{Moisture}} \tag{3.1}$$

The property method chosen for the following simulations is the Peng-Robinson equation of state with Boston-Mathias modifications (PR-BM), as it is a commonly used method and performs well for hydrocarbons and other complex molecules. Compared to the PR-BM property method, Peng-Robinson has several limitations when it comes to CO_2 phase change simulations, as it tends to overestimate the vapor pressure of CO_2 at low temperatures and pressures, which can lead to inaccurate predictions of phase behavior and equilibrium properties [76], [77].

Additionally, STEAMNBS is used for the steam cycle unit operations to define water and steam. STEAMNBS is a property method commonly used in steam cycles because it is based on the latest scientific formulation for water and steam properties, which was developed by the International Association for the Properties of Water and Steam (IAPWS). It provides accurate and reliable thermodynamic data for the properties of water and steam over a wide range of operating conditions [78].

3.5 Chemical looping combustion modeling

In this Section, the CLC base case simulation is designed. The CLC-system consists of an interconnected FR and AR. The OC is reduced in the FR, in the presence of fuel and fluidizing agent, and then travels to the AR where it is oxidized again, in the presence of air. The oxidized OC re-enters the FR being reduced again, therefore completing a loop. A simplified simulation diagram of the CLC-system is shown in Figure 3.2. The numbers used over the chapter correspond to the ones in this image.

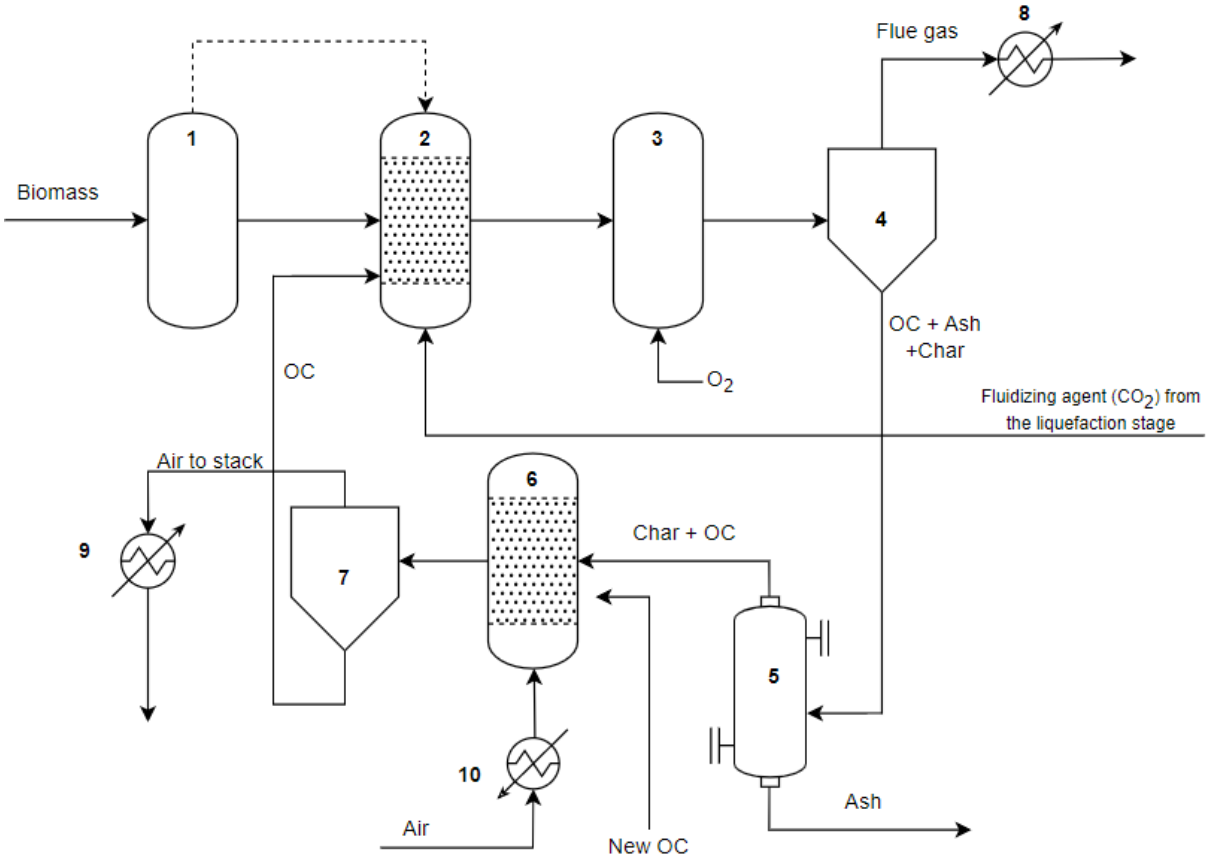

Figure 3.2. Simplified diagram of the CLC-system.

3.5.1 Fuel Reactor

The combustion of biomass in Aspen Plus is simulated using a so-called RYield reactor, to simulate decomposition of the fuel, and an RGibbs reactor, for combustion. Therefore, the FR is the combination of these two.

The decomposition of biomass, performed in an RYield reactor **(1)**, shown in Figure 3.2, is endothermic which requires heat that is provided by the RGibbs reactor **(2)**. The FR is a mixture

of highly endothermic reactions, produced by the OC, and a partially exothermic reaction, generated by the fuel combustion, which leads toward endothermicity. The modeling of the two reactors is explained in more detail in the following paragraph. Additionally, in order to follow the CLC design, the RGibbs that model the FR does not contain a stream of air to induce the combustion, instead, the combustion is induced by the OC flow, which gets reduced in the FR supplying oxygen to the reaction.

The first reactor, RYield **(1)** is used when this yield is known but it does not require reaction stoichiometry nor kinetics of the reactions. The yield defined in the reactor specifications is guessed and it is computed by a calculator block. The different components that will be obtained when performing the decomposition of biomass are added and an arbitrary yield is set. The defined components are H_2O, ash, C, H_2, N_2, Cl_2, S and O_2. It is worth mentioning that in addition to the MIXED sub-stream products, the RYield block forms carbon in the CI sub-stream and ash in the NC sub-stream.

To set the calculation block, the different mass yields are set for each variable together with the proximate and ultimate analysis of important yields. Then, the factor to convert the ultimate analysis to a wet basis is defined as the following:

$$\mathrm{FACT} = \frac{100 - \text{Moisture content}}{100} \tag{3.2}$$

The different yields are calculated by using the ultimate analysis and multiplying it by the factor FACT. After, they are automatically added as an input value in the RYield reactor. In addition, the proximate analysis is used to read the moisture content of the fuel.

Subsequently, the RGibbs reactor **(2)**, FR, is defined in order to use the heat of combustion formed in the RYield **(1)** and combust the decomposed products. RGibbs reactor models reactions calculating the chemical and phase equilibrium by minimizing the Gibbs free energy of the system. In the reactor, all the possible products of the reaction must be added to the reactor input parameters. This includes all the possible products that the ilmenite can have when reduced/oxidized. 1 % of the char (C solid) entering the reactor is set as inert in the simulation in order to be able to transport it with the OC into the cyclones and not have 100 % carbon conversion in the reactors.

The fluidization agent in the present work is part of the CO_2 not liquefied in the liquefaction stage and heated up to 100 °C. Using CO_2 as a fluidizing agent has already been studied by Leckner and Lyngfelt [21], and is proven to be preferred from an efficiency point of view. Steam will also be present in the FR due to the presence of moisture in the fuel, thereby leading to a higher char conversion.

3.5.2 Oxypolishing

An adiabatic RGibbs reactor **(3)** was utilized in the design of the POC contained in the CLC-loop to mimic post-combustion treatment for enhanced combustion yield. Pure oxygen, which could be sourced from an air separation unit, is entering the reactor at saturated vapor with -183 °C and 1 bar [53], [79]. However, in this work, the oxygen source is not studied.

The oxypolishing cost depends on the pressure drop in the post-oxidation chamber. In Aspen Plus, the pressure drop cannot be calculated, therefore, in the model, it is not considered that a

pressure drop is occurring. For the cost calculations, it is assumed that the pressure drop in the chamber will be similar to the one calculated by Farajollahi et al 2022, therefore 2 % [80].

3.5.3 Solid separation

As mentioned in Section 2.5.2, PM dynamics will not be modeled in detail, since particle size distributions of different particles in the flue gas have to be known. After the oxypolishing, the OC, ash, and char are separated using a cyclone **(4)**, as shown in Figure 3.2. In the present work, "Sep" has been used. All the previously mentioned solids go into a separation unit **(5)** where the OC is recovered. The separation unit used in this work is a "Sep" unit, but in a real design, solid separation by different particle sizes would be used. In this recovery, the ash leaves the system losing some OC with it. Potential remaining PM in the flue gas after the cyclone is assumed to be removed by an ESP. Prior to the ESP, the flue gas is cooled to around 200 °C to avoid acid condensation.

3.5.4 Air Reactor

After the solid separation **(5)**, as shown in Figure 3.2, the oxygen carrier together with the unburned char enter the AR. An isothermal RGibbs reactor **(6)** has been used to simulate the AR set to a temperature of 1050 °C. As the reaction is highly exothermic, cooling is needed to ensure the desired isothermal temperature. In the reactor, the oxygen carrier is oxidized by the addition of air, which has been preheated **(10)**, in order to increase the reactor efficiency. The amount of air added corresponds to an air ratio of approximately 5 %, as is indicated in literature for CLC, as anything higher than that value would entail flue gas losses [23]. In order to calculate the air losses, the following equation has been used in function of the molar fraction of oxygen leaving the air reactor ($x_{o_2,out}$).

$$\frac{0.21\ (1 - \ x_{o_2,out})}{0.21 - \ x_{o_2,out}} \tag{3.3}$$

Additionally, a source of clean OC is added into the AR to compensate for the loss during the ash separation unit **(5)**. The oxidation of the OC together with the combustion of char takes place in the AR producing an oxidized metal, CO_2, and air excess (N_2 and O_2).

After the oxidation of the OC, the excess air together with the OC enters a cyclone **(7)**, simulated using a Sep, in order to separate the gas/solid mixture. The OC is then re-introduced into the FR **(2)** to get reduced again, supplying oxygen and heat to the combustion, and closing the loop.

3.5.5 Parameter adjustment

After closing the CLC-loop in the simulation, some parameters were adjusted for proper simulation results. As mentioned in 2.4, an important parameter considered in the FR simulation design is the ratio of CO/CO_2 out of the FR as explained in 2.4. The simulation was performed such that this ratio was kept at around 5 mol.%, to achieve feasible simulation results for that of a hypothetical 50 MW_{th} unit. Another parameter was the temperature difference between the fuel and AR which was discussed to be around 150 °C. In order to acquire these results, the oxygen carrier reduction efficiency had to be modified, while simultaneously adjusting the oxygen carrier flow around the CLC-loop. At the same time, the air flow to the

air reactor was adjusted to allow for an air ratio of 5 %. This was done using solvers in Aspen Plus. The CO/CO_2 ratio and the AR/FR temperature difference solvers were constructed to reach their specified values with high tolerances to achieve simulation convergence and reduce the chances of errors.

3.6 Heat recovery system and steam cycle

To simulate a heat recovery steam generator (HRSG), two heat exchangers, **(8)** and **(9)**, are placed after the cyclones **(4)** and **(7)** in order to model the exchange of the heat produced and generated steam, as shown in Figure 3.2. In addition, the heat extracted from the AR **(6)** is also exchanged to produce steam.

The steam cycle is designed with the data given by Skövde Energi, which is expressed in Table 3.3. As mentioned, the data used is for Load case A, as it is the currently used case by Skövde Energi. A simplified version of the system modeled in Aspen Plus is shown in Figure 3.3.

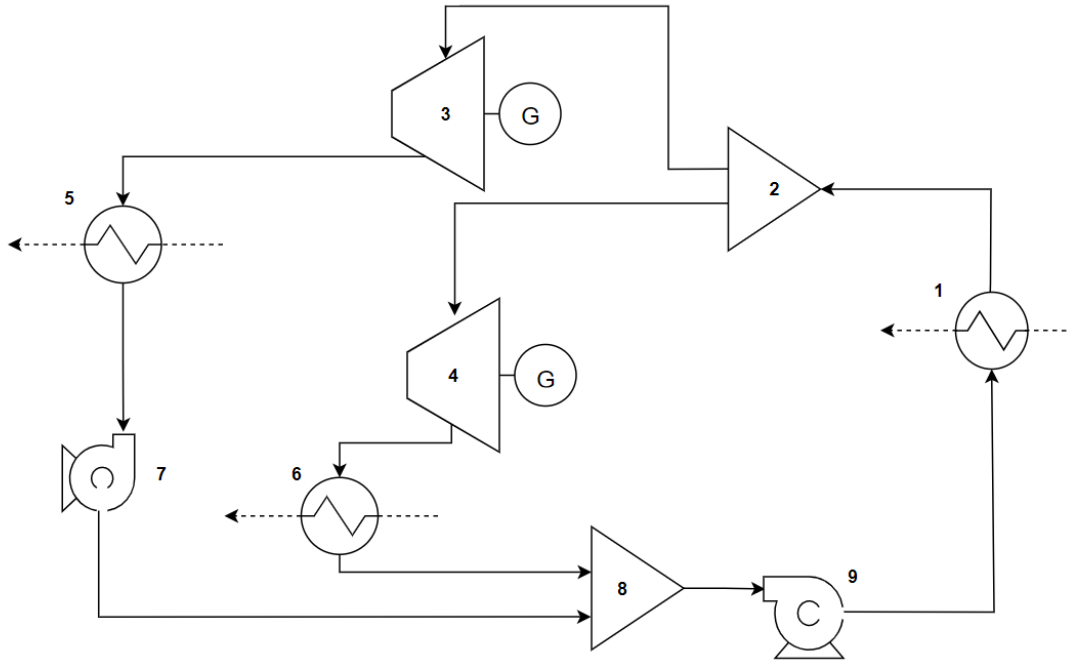

Figure 3.3. Simplified diagram of the heat production system

In the Aspen model, the addition of a bleed stream extracted from the steam turbine has been simplified by simulating two turbines operating at different pressures. In the work, this simplification has led to a definition of two turbines (ST1 and ST2), but it needs to be noted that, in the physical system, only one turbine is used with two extraction points.

It is important to state that all the steam cycle has been simulated with the property method *STEAMNBS*, as its design is suitable to handle steam and its change of phase.

In the base case simulation, the steam is produced through an HRSG **(1)**, as shown in Figure 3.3**,** using the heat provided by the flue gases, from the air and FR, and the heat extracted to maintain the AR isothermal. In Aspen Plus, the HRSG is simulated through a system of heaters and coolers in order to exchange all the heat obtained in the process. A heat integration model using Aspen Energy Analyzer is performed and shown in Section 3.8. The steam is obtained at 480 °C and 90 bar in the heater **(1)**, afterwards, a splitter **(2)** separates the stream that passes

through all the stages of the turbine **(3)**, approximately 12.3 kg/s, from the one extracted in an intermediate stage also called bleed stream **(4)**, approximately 1.8 kg/s. A generator is connected to the steam turbine in order to obtain around 9.3 MW of electricity, in those conditions. The first simulated turbine **(3)**, simulates a single large stream flow path that passes through all the stages of the turbine, extracting the stream at a lower temperature and pressure, 108 °C and 1.3 bar, producing most of the electricity, around 8.9 MW. In the second simulated turbine **(4)**, a bleed or extraction line is simulated which separates approximately 12 % of steam going into the turbines, with a discharge of 198.4 °C and 7.1 bar. Following the provided information by Skövde Energi, the isentropic efficiencies are 0.791 and 0.798, respectively.

The district heating system is warmed up using heat exchangers **(5)** and **(6)**, shown in Figure 3.3, in order to provide heat to the grid. Subsequently, the medium-pressure steam is pumped up **(7)** to the same pressure as the bleed stream in order to mix them, in the mixer **(8)**. The mixed streams are pumped up to 90 bar **(9)** closing the steam cycle.

3.7 CO_2 train modeling

In this subsection, the modeling of the CO_2 train is explained, starting with flue gas purification, compression dehydration, and liquefaction.

3.7.1 Flue gas purification

To obtain a purified CO_2 liquefied gas after the carbon capture, an analysis is performed on the concentration of the different components forming the flue gas obtained. This concentration is compared with the NL specifications, shown in Table 2.1, in order to decide if extra purification is required.

Some of the parameters such as H_2O, O_2, and SO_2 exceed the specified levels of NL. It is important to mention that NL's specifications are just a guideline as they have not started the storage of CO_2. Additionally, due to the amount of chloride in the biomass, some HCl is theoretically formed. It is important to keep in mind that 50 % of the chloride is assumed to react with the ash in order to form alkali chlorides such as KCl, while the rest, would remain as HCl. As the remaining practical HCl would be very low, it won't be considered an impurity in this work. However as mentioned, present HCl would be removed during limestone absorption in the WFGD. The same mechanism will happen with SO_x, the sulfur will react with the ash and reduce its concentration by about 50 %. As the concentration of SO_x is 20 times higher than permitted, removal would be required, which can be performed through limestone absorption. Following the absorption stage, the SO_2 and HCl levels will most likely be low enough to comply with NL's standards. The removal technology is approximated with an ideal separator block. The energy consumption and dimension parameters will be estimated from literature data [59].

The oxygen level obtained in the CO_2 gas is approximately 15 times the allowed, which is due to the excess amount of oxygen added in the oxypolishing step. This excess is required to ensure a proper ratio of $CO/CO_2 \approx 5$ %, in addition to decreasing the amount of H_2 obtained. The removal of oxygen excess is expected to be required but it will not be implemented in this study as mentioned previously, because the technologies available for it are still immature. The removal of this impurity is performed with an ideal separator block but it will not be considered in the energy nor cost calculations.

Additionally, more than 3,000 ppm of H_2O is obtained, even after the multi-compressor with intercooling and flash separation stage. A dehydration step with molecular sieve technology will be added to the simulation and explained in Section 3.7.2, in order to reach the required levels for NL (below 30 ppm of water).

Moreover, to construct a system using catalytic oxidation, proper knowledge of reaction kinetics and reactor design is needed, which is not easily found in literature. Cryogenic distillation is also an extensive process and therefore, O_2 reduction will not be further considered in this thesis.

Lastly, it is important to point out that the levels of NO_x are below 1 ppm, therefore the removal of this component will not be needed.

3.7.2 Flue gas compression and dehydration system

In Figure 3.4, a simplified diagram of the flue gas compression system and CO_2 purification is shown. To perform the flue gas compression, a first flash separation **(1)** is added to have a pure vapor fraction entering the multi-compressor. In there, approximately 60 % of the water mixed with the gas is separated. Afterward, a multi-compressor **(2)** with intercooling and flash separation is set. Following the design proposed by Deng et al [61], a three or four stages multicompressor is optimal for this specific work. In this case, four stages of compression are used but the impact of this decision will be analyzed in a sensitivity analysis [81].

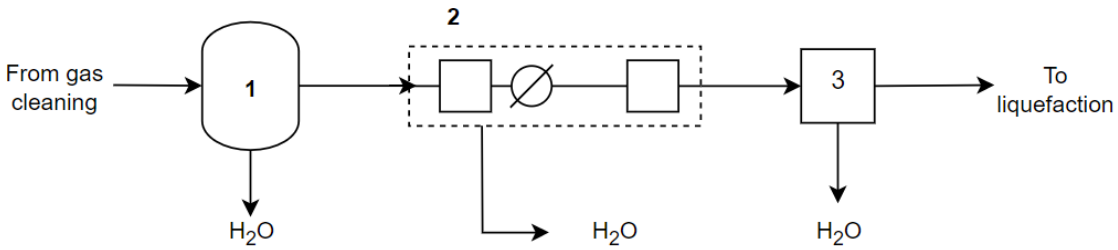

Figure 3.4. Flue gas compression and purification simplified diagram

After the multi-compressor stage, a dehydration unit **(3)** has been placed to reduce the amount of water in the CO_2 further to below the NL specifications. According to Deng et al [61], a molecular sieve adsorber system would be suitable after gas compression but before the liquefaction. The molecular sieve adsorber considered would need 30 °C and 30 bar as operating conditions and it would reduce the water concentration to less than 1 ppm [61]. As mentioned previously, the removal technology is approximated with an ideal separator. The costs and energy consumption will be estimated from literature data [66], [82].

3.7.3 CO_2 liquefaction

In Figure 3.5, a simplified version of the liquefaction system used in the present work is presented. As explained in the theoretical part, the liquefaction will be performed to obtain 16 bar and -28.5 °C. The CO_2 will be obtained at 2 °C subcooled to compensate for possible heat losses during transportation [12].

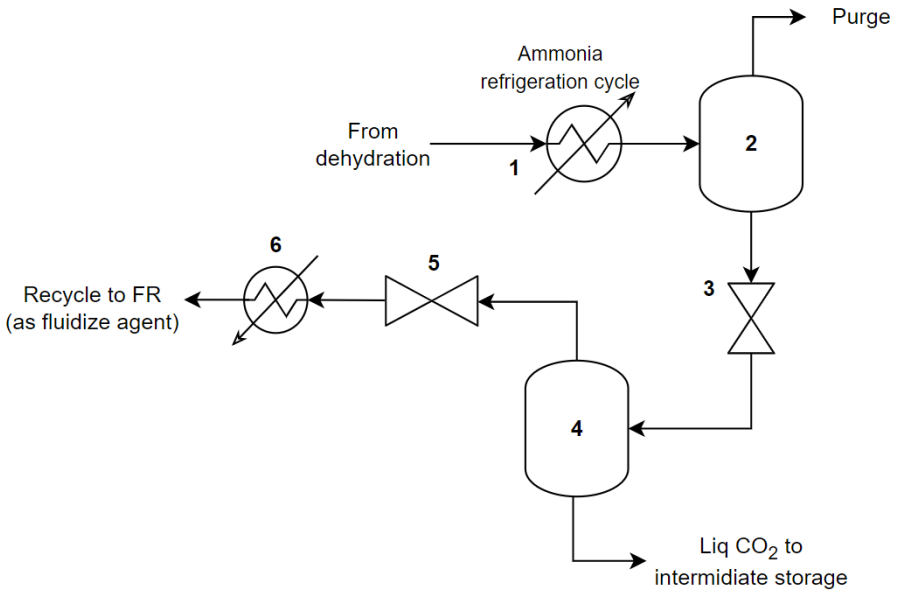

Figure 3.5. Simplified diagram for the CO_2 liquefaction system.

To perform the liquefaction, CO_2, in the gas phase, enters the ammonia refrigeration cycle. In there, ammonia at approximately -22 °C exchanges heat with the CO_2 at 30 °C, lowering the temperature of the gas, until -12.6 °C, and liquefying it. A flash separator **(2)** is added after the liquefaction to purge the non-liquefied gases, mostly N_2 and CO_2. In this flash, some CO_2 is lost, therefore lowering the liquefaction efficiency. After, valve **(3)** changes the pressure from 30 bar to the desired liquefied pressure, 16 bar. This process cools the liquefied CO_2 even more until the desired temperature of liquefaction is -28.5 °C. Finally, a flash **(4)** separated the liquefied CO_2 from the un-condensed one, which will be placed in an intermediate storage. The un-condensed CO_2 is recycled to the FR as a fluidizing agent. For that, a valve **(5)** and a heater **(6)** are placed in order to obtain a CO_2 stream at 100 °C and 1 bar.

The system has been optimized for the suggested conditions for transportation mentioned by NL [12], therefore, some CO_2 is not being liquefied after the liquefaction stage. Instead of recirculating it to the ammonia refrigeration cycle, it has been considered that it would be used to fluidize the FR. Further research could be performed to find the most efficient process for CO_2 liquefaction.

3.7.3.1 Ammonia refrigeration cycle

The ammonia refrigeration cycle is simulated in Aspen Plus to analyze the heat and power needed together with the flow of ammonia in the cycle for this specific process. A simple diagram of the process is shown in Figure 3.6.

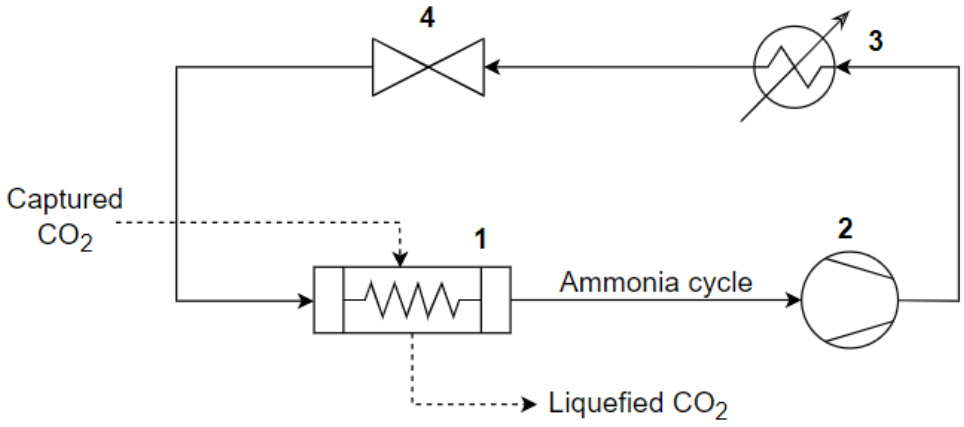

Figure 3.6. Simplified diagram of the simulated ammonia refrigeration cycle

The ammonia in the refrigeration cycle is vaporized in the heat exchanger **(1)**, shown in Figure 3.6, of the refrigeration cycle in order to exchange this heat of vaporization to liquefy the CO_2. After, a compressor **(2)** increases the pressure and a condenser **(3)** to condense the ammonia. In order to close the refrigeration loop, a valve **(4)** is installed to reduce the pressure until the ammonia reaches a lower temperature than the liquefied CO_2.

The refrigeration cycle was constructed in Aspen Plus by choosing appropriate pressures of the evaporator and condenser, as a way to decide the minimum temperature difference of the heat exchangers. The evaporator minimum temperature difference was chosen to be 10 °C between the refrigerant and CO_2-stream to be cooled. The condenser minimum temperature difference was chosen to be 15 °C to reduce the need for cooling water, which was assumed to be heated from 10 °C to 20 °C. The procedure of the refrigeration cycle was then initiated starting with the evaporator. An arbitrary vapor fraction of the refrigerant entering the evaporator was assumed. The flow of refrigerant was then determined by means of a simple energy balance of the evaporator. The compressor was inserted to compress the refrigerant up to condenser pressure, assuming an isentropic efficiency of 80 %. The condenser was inserted cooling down and condensing the refrigerant to a saturated liquid state. A valve was then used to throttle the refrigerant, thereby leading back to the evaporator. However, the vapor fractions were not similar. To get the same vapor fraction, a solver was used which modified the refrigerant flow rate to achieve the same vapor fraction, thereby closing the loop.

3.8 Heat integration

A heat exchanger network was designed for the CLC-process with the only heat source being the fuel combustion. It was also designed to maximize DH production and thereby minimizing the need for cooling water. The DH water at Skövde Energi is to be heated up from 50 °C to 120 °C at 16 bar and the income from selling DH is at 600 SEK/MWh according to Skövde Energi. Although the cost of the DH is variable throughout the year, a constant value has been used in this thesis to simplify the economic analysis. A cooling water system needs to be implemented in Skövde Energi's plant due to the need to cool some of the streams below the temperatures of that of the DH system. In this analysis, it is assumed that cooling water is available. The cooling water is assumed to be heated from 10 °C to 20 °C.

Aspen Energy Analyzer was used to construct a grand composite curve (GCC) of the streams included in the heat integration. The GCC is shown in Figure B.2 in Appendix B. Aspen Energy Analyzer calculates the minimum flow needed for the most expensive utility which in this case is cooling water, by activating a utility pinch point based on the global minimum temperature difference, which in the scope of this report is assumed to be 10 °C. The rest of the cooling needed in the process is provided by DH.

The design of the heat exchanger network was then started. The heat exchangers were all assumed to be of countercurrent configuration to allow for more effective heat transfer, and the pressure drop was assumed to be negligible. The areas of the heat exchangers were calculated using equation (3.4) below:

$$A = \frac{Q}{U\Delta T_{LM}} \tag{3.4}$$

Where Q is the heat duty, ΔT_{LM} is the log mean temperature difference and U is the overall heat transfer coefficient. The log mean temperature difference was calculated using equation (3.5) below,

$$\Delta T_{LM} = \frac{\left(T_{hot,in} - T_{cold,out}\right) - \left(T_{hot,out} - T_{cold,in}\right)}{\ln\left(\frac{T_{hot,in} - T_{cold,out}}{T_{hot,out} - T_{cold,in}}\right)} \tag{3.5}$$

And the overall heat transfer coefficient was calculated from equation (3.6) below.

$$U = \left(\frac{1}{h_{hot}} + \frac{1}{h_{cold}}\right)^{-1} \tag{3.6}$$

Where h_{hot} and h_{cold} are the individual heat transfer coefficients of the hot and cold sides of the heat exchangers. Using equation (3.5), fouling in the heat exchangers is assumed to be negligible, as well as conduction heat transfer resistance. The calculations of equations (3.4)-(3.6) are done by Aspen Energy Analyzer. The individual heat transfer coefficients are entered manually for each stream depending on the nature of the streams, i.e., if they are gases, liquids, condensing, or evaporating. The numerical values are mean values chosen based on literature [83]. The design of the heat exchanger network was done in Aspen Energy Analyzer. More details on the design procedure are given in Appendix B.

Note that the heat integration included the entire system, where the focus was to maximize DH production from available high temperature process streams and thereby minimize cooling water needs, as well as eliminate the need for any other hot utilities other than the heat acquired from burning fuel.

3.9 Equipment sizing

Some of the equipment needed in this project require sizing to calculate their costs. In this subsection, the FR, AR, and columns will be preliminarily sized. In Appendix D, flash drum sizing is also shown.

3.9.1 Preliminary design of FR and AR

In order to understand the dimensions of the CLC technology, the AR and FR were sized. To do so, the premises of the Design proposal for a 200 MW_{th} CLC-CFB boiler published by Lyngfelt et al [56] were used. The design is based on the two following premises:

- Although a lot of small CLC pilots are in operation, the proposal would be a first of a kind, therefore, unexpected difficulties may arise in the system. For this reason, the design must allow to have high flexibility in order to ensure continuous production. Thus, the design will have an AR that can be used also as a CFB boiler. This would significantly reduce the economic risk for the end-user, i.e., Skövde Energi.
- To accommodate for unexpected difficulties the unit should be designed to have good flexibility with respect to the fuel and OC, as well as other operational parameters, like load and solid inventories. This will allow us to perform research and development (R&D), including the evaluation of other fuels, operational strategies, and OC.
- In order to ensure R&D, the unit should also be equipped with detailed pressure measurements and be fitted with ports for gas and solids sampling and visual observation.

The general outline suggested by Lyngfelt et al [56] would be followed for this design and it is shown in Figure 3.7. This design is based on a 200 MW thermal input and is composed of two interconnected CFB boilers. This is a bit different than most of the pilot-scale units which have been used, normally composed of a CFB, an AR, and a bubbling fluidized bed boiler, as FR. It is expected that a dual CFB configuration would also be appropriate for the 50 MW_{th} boilers at Block 4 in Skövde.

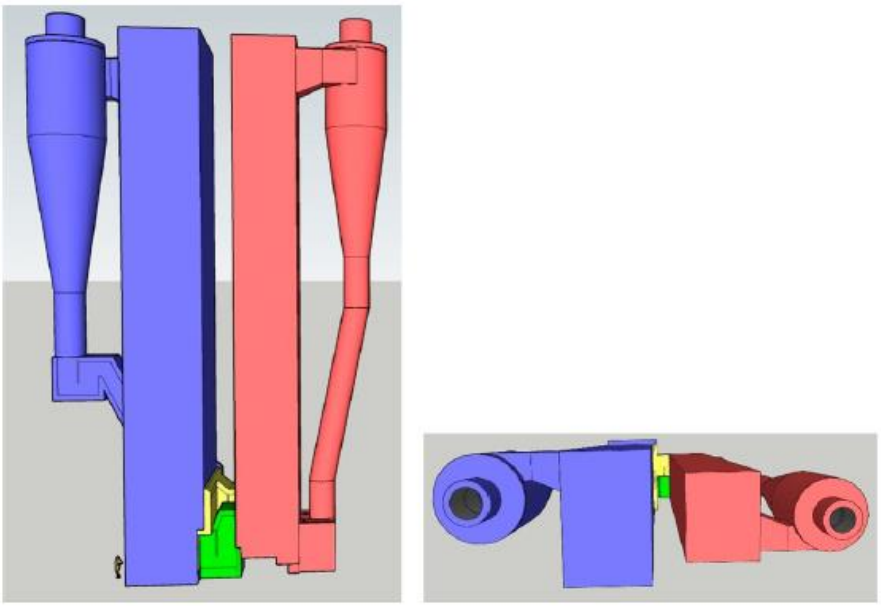

Figure 3.7. Outline of the 200 MW CLC boiler performed by Lyngfelt et al [56].

The exact dimensions of the current design are chosen in order to achieve a gas velocity of 6 m/s in the AR not considering reactions and a velocity of 5.5 m/s in the upper part of the FR assuming full gas conversion [56]. According to the volumetric flow rate of both reactors and

the mentioned velocities, the cross-sectional area of the reactors can be calculated following equation (3.7).

$$A = \dot{V}/v \tag{3.7}$$

It is important to note that with the current simulations performed, the height of the reactors cannot be estimated, therefore it is assumed the actual boiler height, 20 meters, would be enough to achieve a proper conversion and adequate residence time in the reactor. Additionally, Skövde is already constrained by the already existing building structure. A further study using, for example, a CFD tool, could be performed in order to estimate the reactors' height.

Additionally, the cyclone diameter has been designed following the equation (3.8) [84]:

$$D = 0.675 \cdot \sqrt{Q} \tag{3.8}$$

As shown in Figure 3.7, the oxygen carrier is transported from the AR to the FR by the yellow loop seal and returned to the AR by the green loop seal, which connects the two reactors. A sizeable portion of the cooling of the AR/CFB will employ configurable external fluidized heat exchangers, which are not included in the picture, to achieve great flexibility. Additionally, there will be two solid fuel feeding systems: one for the FR and one for the AR/CFB. The latter would be utilized only if the boiler was operated in "normal" CFB mode, without CO_2 capture. There will be a post-oxidation chamber after the FR's outlet where any combustibles still present in the output gas can be burned off using either oxygen or air [56].

3.9.2 Pressure vessels

Absorbers and flash drums were constructed as vertical pressure vessels made of carbon steel. In this section, the procedure for sizing the pressure vessels is shown for their final cost estimation. The dimensions were acquired using Aspen. In order to get the weight of pressure vessels, a vessel thickness needed to be estimated, due to their hollow cylindrical shape. A relevant formula for calculating the wall thickness is given by equation (3.9) below [85],

$$t = \frac{P_i d_i}{2S - 1.2P_i} \tag{3.9}$$

where S is the maximum allowable stress, which for steel is 12.9 kpsi (889 bar), P_i is the internal pressure and d_i is the internal diameter. Additionally, equation (3.9) is applicable in those cases where the calculated thickness t is larger than the minimum practical wall thickness, which depends on the vessel diameter. Table 3.4 below shows the relationship between the minimum wall thickness and vessel diameter.

Table 3.4. Minimum allowable pressure vessel thickness for a given diameter.

Vessel diameter (m)	Minimum thickness (mm)
1	5
1-2	7
2-2.5	9
2.5-3.0	10
3.0-3.5	12

Finally, given the vessel height, diameter, and thickness, its mass can be calculated through the following equation [85],

$$\text{shell mass} = \left(\frac{(d_i + t)^2}{4} h - \frac{d_i^2}{4} (h - 2t) \right) \pi \rho \tag{3.10}$$

which calculates the volume of a hollow cylinder with caps on the top and bottom, multiplied by the density ρ to get the shell mass. The density of the carbon steel was assumed to be 7,850 kg/m^3 and h is the vessel height.

3.9.3 Sizing the dehydration unit

The dehydration unit consists of two adsorber columns using molecular sieve as an adsorbent with the characteristics explained in Table 3.5. An example of a molecular sieve with those characteristics can be the one from the suppliers, a type A zeolite structure with a pore size of 3Å [86]. As the costs for the molecular sieve are not public, the assumed capacity, bulk density, and adsorbent price from CEMCAP will be considered for this work.

Table 3.5. Assumed molecular sieve technology properties for this work [86], [87].

Adsorbent capacity [kg water/100 kg of adsorbent]	16.4
Adsorbent bulk density [kg/m^3]	720
Adsorbent pore size [Å]	3
Adsorbent particle size [mm bead]	3
Cycle time (time of adsorption) [h]	4

Following the procedure established by CEMCAP, together with Kohl & Nielsen, the adsorbers are sized [87], [88]. The procedure to calculate the height and diameter of the columns is shown in detail in Appendix D.

The thickness of the column and therefore the shell mass can be calculated using equations (3.9) and (3.10), extracted from the chemical engineering design book for pressure vessels [85]. The material assumed for the adsorption columns is carbon steel. The cost equation shown in Table 3.7 for the pressure vessel is used to calculate the direct costs of the adsorbers and the total cost of the molecular sieve technology.

3.9.4 SO_2 cleaning absorber

As mentioned in Section 2.5.3, SO_2 cleaning is done by means of an absorption column with ten stages. Again, note that the number of stages and temperatures needed for SO_2-removal were chosen following the work of Yakah et al [59]. The only thing differing from the conditions in the report are the flows, which are scaled appropriately to get similar inlet and outlet temperatures. The absorption column was applied in Aspen using the PR-BM property method, even though it may be inaccurate, with the intention to get a rough estimation of its dimensions. A more appropriate property method for WFGD would be an electrolyte model, such as ELEC-NRTL, due to the ionic interactions in WFGD. Nonetheless, a rough amount of

$CaCO_3$ and H_2O required for absorption was acquired and should therefore not be used as data in the simulation. Additionally, the raw material flows and costs of these components, as well as products formed such as gypsum, were unknown. Hence, only rough dimensions were desired, which were acquired from Aspen.

3.9.5 Intermediate CO_2 storage tank

For the current analyzed site location, it is important to have intermediate storage for the liquefied CO_2. As mentioned in Section 2.5.1, the current objective for the company is to transport the liquefied CO_2 by truck, to the railways, followed by train, to the closest habilitated harbor. From the harbor, a ship would transport it to the facility of NL, in Norway.

It can be approximated that once a day a truck would be sent to the railways, therefore, it is believed that the tank would need to hold a maximum of two days of storage. In order to calculate its volume, the production of two days of capture at a high load is assumed together with a 15 % buffer.

3.10 Techno-economic analysis

The techno-economic analysis is done by means of capital cost estimations (CAPEX) and running costs (OPEX). The main assumptions of the techno-economic analysis for the base case are shown in the following table.

Table 3.6. Assumptions for the techno-economic analysis [13].

Economic lifetime of the plant (years)	20
Interest rate (%)	5
Annual operating time (h/year)	5,900
Biomass chip price (SEK/MWh)	250

3.10.1 CAPEX

The capital cost for the process includes the capital costs for FR, cyclone, AR, oxypolishing reactor, ash and waste OC handling, WFGD for SO_x removal, molecular sieve technology, heat exchanger network, pumps, compressors, and intermediate storage. The cost of each equipment was estimated through literature data. Some equipment that already exists in Block 4 of Skövde Energi has not been considered a CAPEX. These are the steam turbine, the ESP, and the biomass drying and grinding.

The capital costs for each equipment are explained in the table below, which contains the source of each equation.

Table 3.7. Equipment cost calculation equations.

Unit operation	Units for Size calculation [S]	Equation		Units of cost	Reference
FR	Surface area [m^2]	$1500 \cdot S$	(3.11)	2015 M€	[80]
Cyclone	Diameter of the cyclone [m]	$260\,000 \cdot S$	(3.12)	2014 M$	[87]
AR (CFB)	Heat extracted in the AR [MW]	$0.288 \cdot S + 5.08$	(3.13)	2014 M$	[80]
Oxypolishing	Gas flow [kg/s] (S_1), temperature out of the reactor (S_2) and the pressure out and in of the reactor [bar] (S_3 and S_4)	$\frac{48.67 \cdot 10^{-6} \cdot S_1 \cdot (1 + e^{0.018 \cdot S_2 - 26.4})}{0.995 - \frac{S_4}{S_3}}$	(3.14)	2011 M$	[80]
Ash and OC waste handling	Makeup OC (S_1) and ash cleaning (S_2) flow [kg/s]	$4.6 \cdot \left(\frac{S_1 + S_2}{6.7}\right)^{0.56}$	(3.15)	2018 M$	[80]
Column / pressure vessel	Shell mass [kg]	$-400 + 230 \cdot S^{0.6}$	(3.16)	2006 $	[89]
Sieve trays	Diameter [m]	$100 + 120 \cdot S^2$	(3.17)	2006 $	[89]
Molecular sieve	Cost of the adsorber and desorber [€ 2015] (S_1) and mass of adsorbent [tonne] (S_2)	$S_1 + 3600 \cdot S_2$	(3.18)	2015 €	[80]
HEX	Area of the HX [m^2]	$10\,000 + 88 \cdot S^1$	(3.19)	2006 $	[89]
Pumps	Flow [L/s]	$3\,300 + 48 \cdot S^{1.2}$	(3.20)	2006 $	[89]
Compressors (centrifugal)	Power [kW]	$8\,400 + 3\,100 \cdot S^{0.6}$	(3.21)	2006 $	[89]

Floating roof tank (intermediate storage)	Capacity [m^3]	$53\,000 + 2\,400 \cdot S^{0.6}$ (3.22)	2006 $	[89]
Turbine	Power [kW]	$-19\,000 + 820 \cdot S^{0.8}$ (3.23)	2006 $	[89]

It should be noted that the current CHP plant has adequate unit operations for the study, thus an investment for them, in the base case, is not needed. Additionally, Skövde Energi has an ash removal system that could be reused when shifting to a CLC technology. Nevertheless, a unit to separate not only ash but also waste solids and OC needs to be added, of which its cost is calculated in the equation for "Ash and OC waste handling", expressed in Table 3.7. Finally, a cone roof tank is used as intermediate storage for the liquefied CO_2, in order to wait to be transported to the final storage site. It is accounted to last for a maximum of 2 days, over the weekend, with a buffer of 15 %.

Table 3.7 also contains the year for which the equipment cost applies. Most equipment cost estimations apply for different monetary years and need to be adjusted for inflation to reflect the current value of money, following equation 3.24 [90]. The CEPCI index of January 2022 was found to be 797.6 according to a source, and adjusting for January 2023 using the Chemical Engineering Magazine, the CEPCI index of January 2023 is 805.6 [90].

$$\mathrm{CC}_{\mathrm{year\ 2023}} = \mathrm{CC}_{\mathrm{year}\ X} \cdot \frac{\mathrm{CEPCI}_{\mathrm{year\ 2023}}}{\mathrm{CEPCI}_{\mathrm{year}\ X}} \tag{3.24}$$

For the pressure vessels, namely absorbers and flash drums, carbon steel is chosen as the construction material. Carbon steel is the most commonly used material in engineering due to its affordability, versatility in shaping and sizing, and robustness and malleability. It is, however, susceptible to corrosion, mainly at higher temperatures. Carbon steel will rapidly oxidize rapidly at higher temperatures, which is why its use is limited to below 480 °C. In this thesis, carbon steel is assumed to be used for equipment cost since most streams in the CLC process are below 480 °C, apart from the heat exchangers which are assumed to be of type 304 stainless steel, which can handle higher temperatures [89]. The AR and FR will also be assumed to be made out of type 304 stainless steel due to their high temperatures and the corrosive environment of the FR.

The total plant cost (total PCE) is defined to be the capital cost sum of all the equipment needed for the project. In addition to it, the fixed capital and the working capital need to be considered. The typical factors for estimating the Project Fixed Capital Cost stated for a process type with solids and fluids in the Chemical Engineering Design book are used and expressed in Table 3.8 [89]. These factors are used in equations 3.25 and 3.26.

Table 3.8. Typical factors for estimating the Project Fixed Capital Costs [89]

Major equipment, total purchase cost	**PCE**
f_1 Equipment erection	0.5
f_2 Piping	0.6
f_3 Instrumentation	0.3
f_4 Electrical	0.2
f_5 Buildings, process	0.15
f_6 Utilities	0.2
f_7 Storages	0.15
f_8 Site development	0.05
f_9 Ancillary buildings	0.15
f_{10} Design and engineering	0.25
f_{11} Contractor's fee	0
f_{12} Contingency	0.1

The total physical plant cost (PPC) and the fixed capital cost (FCC) are calculated using the following equations:

$$\mathrm{PPC} = \mathrm{PCE} \cdot \left(1 + \sum_{i=1}^{9} f_i\right) \tag{3.25}$$

$$\mathrm{FCC} = \mathrm{PPC} \cdot \left(1 + \sum_{i=10}^{12} f_i\right) \tag{3.26}$$

which include the factors mentioned in Table 3.8. The working capital cost is assumed to be low, 5 % of the fixed capital cost, as it is a simple single-product process. In addition, the fixed capital cost is annualized through 20 years with an interest rate of 5 %.

The annual capital cost (ACC) is calculated by multiplying the FCC with the annuity factor (a):

$$\mathrm{ACC} = \mathrm{FCC} \cdot a \tag{3.27}$$

Where the annuity factor (a) is calculated from the interest rate (i) and an economic lifetime of the plant (n) in order to find the present value of receiving that annuity for the economic lifetime period:

$$a = \frac{i}{1 - (1+i)^{-n}} \tag{3.28}$$

3.10.2 OPEX

The OPEX costs are broken down into fixed operational costs and variable operational costs.

Regarding the fixed operating costs different categories are considered. Following the Chemical Engineering Design book together with the professional knowledge from Skövde Energi, some assumptions have been considered in order to calculate them [89]:

- Maintenance is assumed to be 1 % of the fixed capital costs as the CHP plant usually has a low maintenance requirement.

- For the labor costs, it is assumed that currently 8 operators are needed to run the plant. After implementing the change of technology together with adding the compression and liquefaction part, a total of 12 operators are assumed that would run the plant. As the plant is designed to be in Sweden, the salaries are according to the actual plant, which corresponds to 40,000 SEK per employee. It is possible that, if the technology requires further investigation from an R&D perspective, this number could increase. Therefore, an overhead cost of 45 % of the salary wages is assumed to account for these variations together with the supervision and management cost. Additionally, 5 % of the operating labor cost is taken to account for the lab cost.
- As the investment will have a high footprint impact on the actual plant, a rate of capital (rent of land and/or buildings) would be considered as 0,5 % of the fixed capital cost. Insurance and taxes to allocate environmental charges and cover superfund payments would be considered as a typical value of 0.5 % and 1 % of the fixed capital cost, respectively.

For the variable operating cost, the cost of the different raw materials and the utilities are used and shown in Table 3.9. The variation of some of these values will be studied in the sensitivity analysis.

Table 3.9. Raw material and utilities variable costs for the base case

Raw materials and utilities	Price	Unit	Year	Reference
Biomass	250	SEK/MWh	2023	[13]
OC makeup	0.42	USD/kg	2011 $	[91]
Oxygen	100	€/tonne	2016	[92]
Molecular sieve	3,600	€/tonne	2014	[87]
Cooling water	0.4	SEK/m^3	2023	[89]
Electricity	1,000	SEK/MWh	2023	[93]

The lifetime of the OC has a high impact on its variable costs. From literature, it is known that a pilot plant using ilmenite suggested a lifetime of 600-800 h [39], [77], [94]. This estimation does not consider any interactions with ash, therefore some studies state that the lifetime might decrease [21]. As the biomass used in this work is quite low in ash content, a value of 600 h is used [39]. In order to understand the effects of the lifetime of the OC on the total plant cost, a sensitivity analysis is recommended. The OC makeup flow has been calculated assuming the solid inventory needed for the two reactors together. A value of 850 + 250 kg/MW_{th} is considered for the FR and AR respectively [39], [77].

3.10.3 Revenue

From the analyzed plant situated in Skövde Energi (Block 4), DH and Electricity are produced. The pricing of the utilities is highly dependent on the market price, therefore Skövde Energi keeps a variable load depending on the demand. In this study, only the full load capacity case has been studied but two different market prices will be analyzed.

The electricity prices considered in this work are 500 SEK/MWh and 1,000 SEK/MWh, following the NordPool yearly average predictions for the area where Skövde is located [93]. For the DH prices, the analysis will be conducted at 600 SEK/MWh, as it is the 2023 price,

following Skövde Energi, together with 375 SEK/MWh, to analyze the impact of it [13]. It is important to note that the main analyses are conducted using higher utility prices.

Additionally, the negative emissions obtained by the captured and stored CO_2, obtained from a biogenic source, can be used as carbon credits to compensate for the emitted CO_2 from the waste-to-energy boilers used in the same company, or sold as CO_2 credits for other nearby companies. There is currently no CO_2 credits market, therefore the price of them is assumed [95]. In January 2023, the value of the EU-ETS was around 90 €/tonne CO_2 [96]. For most of the CCS studies, a price of 100 €/tonne CO_2 is assumed, as the trend shows that prices are going to rise in the future [95], [96].

3.10.4 Economic parameters

The techno-economic analysis for different configurations and conditions has been discussed and compared based on the following economic parameters.

The levelized price of CO_2 ($LCCO_2$) (capture) is the minimum price that the CO_2 should be sold at for the investment to break-even, expressed in SEK per tonne of CO_2 captured. If the product is sold at a higher price, the project would become profitable. This is the value that is comparable with the different literature findings.

$$\mathrm{LCCO_2(capture)} = \frac{(\mathrm{ACC} + \mathrm{OPEX})_{\mathrm{capture}}}{\mathrm{tons\ CO_2\ captured}} \tag{3.29}$$

The levelized cost of CO_2 ($LCCO_2$) (total plant) is the minimum price at which the CO_2 has to be sold to break-even, considering the total plant cost and the revenue produced by selling the utilities.

$$\mathrm{LCCO_2(total\ plant)} = \frac{\mathrm{ACC} + \mathrm{OPEX} - \mathrm{Utilities\ revenue}}{\mathrm{tons\ CO_2\ captured}} \tag{3.30}$$

The simple payback period (PBP) is an estimate of the number of years it would take to recover the investment:

$$\mathrm{PBP} = \frac{\mathrm{Total\ FCC}}{\mathrm{Average\ annual\ profit}} \tag{3.31}$$

The net present value (NPV) is the current value of a future stream of payments over the lifetime of the project, in this case, 20 years:

$$\mathrm{NPV} = \sum_{n=0}^{20} \mathrm{Net\ cash\ flow} = \sum_{n=0}^{20} \frac{\mathrm{Revenue}_n - \mathrm{Costs}_n}{(1+i)^n} \tag{3.32}$$

Additionally, the net future value (NFV) is the value of a future stream of payments in the last year of the project, therefore in year 20.

$$\mathrm{NFV} = \sum_{n=0}^{20} \frac{\mathrm{Net\ cash\ flow}}{(1+i)^n} \tag{3.33}$$

When calculating the NPV, NFV, and payback period, a price per tonne of CO_2 of 1000 SEK is assumed, as mentioned in 3.10.3 [95].

3.10.5 CLC vs post-combustion

Skövde Energi performed a pre-feasibility study to analyze the economic impact of building a post-combustion technology in the studied plant [13]. The technology selected is absorption with monoethanolamine (MEA) together with a compression and liquefaction plant.

The data obtained by Skövde Energi is used in order to compare it with the technology studied, CLC. For that, the same assumptions as the report using post-combustion are used to compare the two different capture technologies. The data reported on the study of implementing MEA post-combustion capture in Block 4 is summarized in the following table.

Table 3.10. Implementation of MEA post-combustion capture in Block 4 from Skövde Energi. Data obtained from a past study of the company [13].

Parameters	Values
Flue gas flow [Nm^3/h]	67,587
CO_2 content in the flue gas [vol. %]	13.6
Evaluated scenario (Block 4) [Tonnes captured CO_2 per year]	73,000
Capture rate [%]	90
Losses in liquefaction stage [%]	5
Net electricity production [MW]	4.8
Net DH production [MW]	36.3
Cooling water requirements [MW]	10
Electricity price [€/tonne CO_2]	50
DH price [€/tonne CO_2]	37.5
Depreciation [years]	20
Interest rate [%]	5
Operating hours [h/year]	5,900
Added CAPEX [M€/tonne CO_2]	61
Total added cost [M€/tonne CO_2]	110

In the previous work performed by Skövde Energi, it was found that the MEA post-combustion technology requires low-pressure (LP) steam in order to operate the reboiler at 4-5 bar (140-150ºC). In addition, the cooling requirement need is quite high, this could be solved by implementing a heat pump, which could be studied and compared in future work [13].

Moreover, the amines studied consist of using a "proprietary mixture" which is bound to the selected supplier. As the data is extracted from a preliminary study, it is assumed that the amine needs to be replaced with 0.1-0.5 kg/tonne of CO_2, which would depend on the NO_x and SO_x content in the flue gas. Additionally, in the study, the waste volumes are assumed to be based on a compilation of supplier information. The amines are reactive against NO_x and SO_x and form by-products, thus the amount of waste products is strictly correlated to the flue gas composition. In the report, 0.3 kg/tonne of CO_2 is assumed as the amount of waste, which is extrapolated to be 22 tonnes of waste amine/year. [13]

In terms of liquefaction, a high-pressure expansion (Joule-Thompson process) is assumed to be used in the post-combustion project [13]. All the economic calculations there are performed based on the heat and mass balances [13].

In the case of this study, comparing CLC with post-combustion based CCS, the assumed electricity and DH prices considered are in the lower range, 500 SEK/MWh and 375 SEK/MWh respectively. For this reason, when comparing the two technologies, only these utility prices will be analyzed [13]. For all other purposes, the electricity price and DH price are 1,000 SEK/MWh and 600 SEK/MWh respectively.

The efficiency of the post-combustion technology is lower than the modeled efficiency for the CLC technology, therefore, although the same initial conditions in the plant are used, the amount of CO_2 captured per year will not match. For this reason, the comparison is performed per tonne of CO_2. The sensitivity analysis includes the study of energy utilized and price per tonne of CO_2 capture, separated by CAPEX and OPEX.

3.11 Sensitivity analysis

In this subsection, the methodologies to perform the sensitivity analyses are presented.

3.11.1 Steam temperature and pressure for electricity production

A major benefit of CLC lies in its capacity to increase the steam temperature within a power plant to increase electricity production. Traditional combustion power plants often experience substantial fouling, primarily due to the presence of ash, where alkali components accumulate on heat transfer equipment, consequently diminishing the boiler's heat transfer capabilities. The primary heat extraction in a CLC process occurs in the cooled AR, consisting mainly of nitrogen, oxygen, and oxygen carrier. This composition significantly reduces fouling and corrosion on heat transfer equipment, theoretically allowing for elevated steam temperatures.

In this sensitivity analysis, the steam temperature and pressure of the steam cycle are increased separately and combined, where the DH- and electricity production potential are compared using relevant prices according to Skövde Energi and electricity market prices. Different bleed stream scenarios of the turbine exhaust are also considered, as well as DH temperatures. A DH selling price of 600 SEK/MWh is assumed according to Skövde Energi and an electricity price of 1,000 SEK/MWh. The operating time of the plant is 5,900 h/year and the DH acts as a cold utility with a temperature range from 50 °C to 120 °C at 16 bar as previously mentioned in the heat integration. The current steam data is presented in case A of Table 3.3, as 480 °C and 90 bar. Different scenarios are considered for the sensitivity analysis:

- Steam temperature of 600 °C at the same pressure (90 bar),
- Steam pressure of 150 bar at the same temperature,
- Both higher temperature and pressure at 600 °C and 150 bar,
- Steam temperature of 600 °C at the same pressure, but with DH temperature 50 °C to 100 °C,
- No bleed stream (complete expansion to 1.34 bar with a focus on electricity production),

- Complete bleed stream (complete expansion to 7.1 bar with a focus on DH production).

As in the heat integration, a global minimum temperature difference of 10 °C was assumed. The district heating and electricity production revenue potential was then compared for these different cases in the total cash flow. The total cash flow also included the cost of cooling water, which was assumed to be 0.4 SEK/m^3, for those streams that cannot be cooled by DH water. Heat exchanger networks were not designed for the different cases and capital costs were deemed negligible as opposed to the revenue of district heating and electricity. The isentropic efficiency of the base case was assumed to be constant for all cases. In the cases of raising steam temperature and/or pressure, the cost of a new turbine was included in the total cash flow. The capital cost of a new turbine was determined using equation 3.23, adjusted using CEPCI, and annualized using equations 3.27 and 3.28. The contributing electricity costs included in the total cash flow were those that are directly affected by altering the steam properties, which is the work done by the turbine and the pump. This is denoted by net electricity production in the results in Section 4.6.1. It is worth noting that this analysis is only done using one value of electricity and DH price, namely those values mentioned in the previous paragraph.

For every case, the utility grand composite curve was used as a guideline for utility needs. These graphs are presented in Appendix C.

3.11.2 Multistage compressor

During the plant design, compressors were used to raise the pressure of some gaseous streams, namely the CO_2-stream for subsequent liquefaction and in the ammonia refrigeration cycle. A sensitivity analysis was made for those streams during the process design, by examining the effect of the number of compressors in series with interstage cooling needed, for minimizing the annual cost. Having more compressors with interstage cooling generally reduces the total power needed to achieve the desired pressure elevation, which could save money, given a certain electricity price. In this analysis, the cost of a compressor was calculated using equation 3.21, adjusted using CEPCI, and annualized as previously done using equations 3.27 and 3.28. The cost of electricity was again assumed to be 1,000 SEK/MWh and the operating time of the process was 5,900 h/year. The cost of adding an additional heat exchanger and flash in the case of additional stages was included. The cost of an additional flash was assumed to add another 100,000 SEK which was also annualized. The cost of an additional heat exchanger was added using equation 3.19, where it was assumed that additional heat exchangers are small and therefore cost approximately 10,000 USD as of 2006. As done with the compressors, the cost of the heat exchanger was adjusted using CEPCI and annualized. The final saved amount of money was calculated as the difference between saved electricity, and the difference in the annual cost of additional units.

For the CO_2-stream, the saved amount was compared using three and four compressors. As for the refrigeration cycle, one compressor was deemed to be enough, and no further analysis was conducted given its already low power requirement. An additional compressor with intercooling would not save a significant amount of power.

3.11.3 Impact of the CAPEX and OPEX on the project

The methods to calculate the total capital and operational cost are approximated using literature values although they are highly dependent on the different suppliers and construction companies. For this reason, a sensitivity analysis is performed in order to analyze the impact of a misestimation when calculating the CAPEX and OPEX.

As it has been mentioned, the source of the oxygen is not taken into account in this work, therefore the variability of the price is high. The assumed value throughout the work is 100 €/tonne CO_2 [92], but other sources suggest that this price could vary by ±50 % depending on the location and production of it [92], [97], [98]. Additionally, the OC price reported in literature is very variable, as CLC has not been scaled up, therefore, there is no market for it. Estimations are made by different papers where the price range from 1,000 SEK/tonne to 6,000 SEK/tonne of ilmenite, therefore an analysis of different values within the stated range is performed [21], [91], [99]. Finally, the CAPEX and fuel price are varied in order to understand the impact on the techno-economic results.

3.11.4 Effect of the utility price

A major benefit of the implementation of CLC is the minimization of energy needed to obtain pure CO_2, due to the fact that two reactors are used, easing the capture process. The price of utilities has a high contribution to the total cost of the plant, and therefore it will be studied as a sensitivity case.

It is important to note that the price of electricity is extremely variable, as it is highly dependent on the demand. Due to the variable and unstable estimations of the future prices and the impact on those, a sensitivity analysis is performed on the effect that changing the utility prices has on the economical parameters, explained in Section 3.10.4.

In order to simplify the analysis, only two cases are analyzed, and they are shown in Table 3.11, maintaining the value constant over the different years. The analysis is performed in Sections 4.6.3 and 4.6.5.

Table 3.11. Electricity and DH prices were used in the sensitivity analysis.

Case	Electricity price [SEK/MWh]	DH price [SEK/MWh]
High utilities prices	1,000	600
Low utilities prices	500	375

4 Results

This chapter includes the results from the simulation given the assumptions and parameters chosen in the literature review and method. The results include the CLC, compression and liquefaction, equipment sizing, techno-economics, and various sensitivity analyses.

4.1 Chemical Looping Combustion

After performing the simulation of the CLC technology with Aspen Plus, some general CLC-operational results are presented in Table 4.1.

Table 4.1. CLC-results from the Aspen Plus simulation performed in this work.

Fuel input [MW]	51.2
AR temperature [°C]	1050
AR inlet temperature [°C]	938
FR temperature [°C]	909
Outlet CO/CO_2 [mol.%]	4.70
Air flow to AR [kg/s]	17.6
Oxygen carrier flow [kg/s]	91.5
O_2 outlet fraction AR [wt.%]	4.25
H_2 fraction flue gas [mol.%]	2.15
CO fraction flue gas [mol.%]	1.72
C bypassed the FR to AR [%]	1
CO_2 capture efficiency [wt.%]	97.5
CO_2 capture rate [ktonne/year]	101.8

Included in the simulations is thermal input to the FR, AR, and FR temperature, air flow to the AR, oxygen carrier circulation rate, and the CO/CO_2-ratio in the flue gas from the FR. Also shown are the CO and H_2 molar fractions in the flue gas and the O_2 weight fraction out of the AR. The carbon capture efficiency of the plant and the CO_2 capture rate is also presented.

As seen from Table 4.1, the FR and AR temperatures were 909 °C and 1050 °C respectively, which were tried to be kept as high as possible for efficient fuel conversion. The AR temperature was cooled so as to not exceed 1050 °C to limit defluidization and agglomeration of the bed. This issue is not present in the simulation but rather a methodology applied to emulate realistic conditions. The temperature difference between the fuel and AR was 141 °C, which was assumed to be reasonable for a large 50 MW_{th} unit with a larger residence time compared to pilot plants.

The methodology of acquiring these results was done by also complying with the parameters explained in section 3.5.5. As explained, the CO/CO_2 ratio and the temperature difference between the AR and FR were kept at around 5 % and 150 °C using a solver, by modifying the amount of oxygen carrier, given an assumed oxygen carrier reduction efficiency (conversion)

of 80 %. This corresponded to a mass-based conversion of 3.8 %. Further thoughts are not given into this value and its realistic implications.

Also presented in the table above is the carbon (char) that was not converted and therefore went on to the AR to be combusted. This was part reason why the CO_2 capture efficiency was not 100 %. To avoid this, a carbon stripper could be considered, but it would add additional costs and process complexity.

The amount of thermal energy into the system was increased from around 50 MW to 51.2 MW due to initial thoughts that energy would be significantly lost due to the loss of heat-containing oxygen carrier in the ash removal. That hypothesis turned out to be less significant than assumed.

4.2 Equipment sizing

In this subsection, the sizes of some equipment used in the CLC plant are presented. In Appendix B the design and sizing of heat exchangers and flash units are shown.

4.2.1 Air and fuel reactor dimensions

The dimensions of the fuel and AR are presented in Table 4.2, as well as the exiting volumetric flows, calculated following the methodology in Section 3.9.1.

Table 4.2. Dimensions of the preliminary design proposal for the CLC-system reactors.

Unit	FR	AR	Source
Volumetric flow rate [m^3/s]	31.7	54.56	Aspen simulation
Cross-Sectional area [m^2]	5.76	9.10	Eq. (3.7)
Reactor height [m]	20	20	Boiler height in Block 4

As mentioned in section 3.9.1, the reactor is assumed to be designed following the configuration done by Lyngfelt et al [56], which is shown in Figure 3.7. The configuration includes a system with loop seals that are placed in order to transfer the OC between the two coupled CFB reactors, allowing them to fulfill the O_2 demand.

Due to a lack of information on the particle distribution inside the reactors, their height had to be assumed, therefore it is assumed the actual boiler height, 20 meters, would be enough to achieve a proper conversion and adequate residence time in the reactor, as mentioned in Section 3.9.1. Additionally, it needs to be considered that Skövde is constrained by the already existing building structure.

4.2.2 Downstream process unit dimensions

As mentioned in the Methodology section 3.9, the flash units, dehydration unit, and SO_x cleaning absorber have been sized. In this subchapter, the results of the sizing for the SO_x

cleaning, molecular sieve, and intermediate storage tank will be presented. The flash sizes are stated in Appendix D.

The molecular sieve adsorption column has been sized using the method from CEMCAP shown in Appendix A. The dimensions are presented in Table 4.3. To calculate their costs, it has been designed so that only the adsorber sizing is calculated, and assumed that the desorber will have the same size.

Furthermore, the SO_x cleaning technology (WFGD) has been sized by using the calculated values from Aspen Process Economic Analyzer and the method explained in Section 3.9.4. The dimensions are presented in Table 4.3.

Table 4.3. Sizing of the flue gas cleaning: molecular sieve and SO_x cleaning.

Unit operation	**Molecular sieve columns**	**WFGD column**
	Adsorber/Desorber	**Absorption**
Column diameter [m]	0.86	2.74
Total height of the column [m]	2.25	12.80
Adsorbent mass to fill the column [kg]	104.7	-
Number of trays	-	10
Thickness of the column [m]	$1.48 \cdot 10^{-3}$	$1.233 \cdot 10^{-3}$

Finally, the design of an intermediate storage tank has been calculated with the assumptions previously stated in Section 3.9.5 and a volume of 870 m^3 would be needed.

4.3 Steam cycle efficiency

In Table 4.4, the electrical efficiency and power-to-heat ratio of the CLC-thoperation are compared to the conventional block 4 processes. For the conventional process, assumed is a thermal input of 49 MW, a net electricity output of 9 MW, and district heat production of 40 MW, as stated in Section 2.1.

Table 4.4. Electrical efficiency of CLC vs conventional combustion.

Process	**Electrical efficiency (η_{el}) [%]**	**Power to heat ratio (α) [%]**
Block 4 conventional	18.4	22.5
CLC	13.5	16.3

Due to the carbon capture process, the net electricity produced in the CLC process is reduced, and the district heat production in the CLC process is slightly higher. The lower electricity is in Table 4.4, where the electrical efficiency is lower with a net electricity production of 6.9 MW, mainly due to the multicompression and liquefaction stage, which is further discussed in the next subsection. Since district heat production is slightly higher in CLC, the power-to-heat

ratio is also reduced during carbon capture. Note that the district heat production for the CLC-process is 42.4 MW with a thermal input of 51.2 MW as mentioned in subsection 4.1.

4.4 Compression, liquefaction, and carbon capture

In this subsection, results related to the compression and liquefaction of the CO_2-stream are presented. Table 4.5 below includes relevant CO_2-multicompression and intercooler data.

Table 4.5. CO_2 multicompression results.

Number of stages	4
CO_2 multicompressor power [MW]	1.54
Intercooler outlet temperature [°C]	30
CO_2-stream outlet pressure [bar]	30
Water removed [mol.%]	97.8
Water content after multicompression [ppm]	3,269

As illustrated in Table 4.5 above, four stages were the economic choice, given the choice between three or four stages of compression, which is further presented in the sensitivity analysis in section 4.6.2. This result held under the presumption of an electricity price of 1 SEK/kWh, for which the cost of an additional heat exchanger and intercooler was justifiable due to the electricity saved, even though that amount was only 5.1 %. As mentioned, compressing the CO_2-stream to 30 bar with intercooling will allow to separate the water in the CO_2-stream and further liquefy it through the use of a refrigeration cycle and throttling. Also noted from the table above is the high H_2O-content that needs to be lowered to below 30 ppm to comply with the standard of NL. It was not justifiable to add additional stages in the multicompressor unit to lower the water content further due to economic reasons, which is why a dehydration unit was applied after this process. The intercooler temperature was chosen to be 30 °C which is also presented in the table above, because that temperature was low enough to significantly reduce power consumption, but also minimized the water content after multicompression. This, however, was not strictly examined during the process design. Following the work performed by Kempera et al [66], the mentioned pressure was also necessary to properly operate the dehydration unit.

Table 4.6. CO_2 liquefaction and ammonia refrigeration results.

Ammonia compression work [MW]	0.49
Cooling duty [MW]	1.67
COP	3.42
Ammonia circulation rate [kg/s]	1.47

As seen in the table above, the compression work enabling the liquefaction process is relatively low at 0.49 MW. Hence, only one compression stage was implemented since the electricity savings of having multiple compressors in series with intercooling would not be economically justifiable. This refrigeration cycle setup was constructed with the intention of fully cooling the CO_2-stream from 30 °C to -12.6 °C, without intermediate cooling using cooling water. The

reason being to avoid the necessity of an additional heat exchanger and minimize cooling water needs. This analysis, however, was not thoroughly done. After cooling the CO_2-stream, a small fraction of vapor was purged consisting of mainly CO_2 and N_2. This was a contributing factor to the CO_2 capture efficiency of 97.5 % presented in Table 4.1. An advantage of the purge is a reduction of N_2 in the captured CO_2-stream, which makes it possible to store a slightly greater amount of the captured CO_2. The final purity of the liquid CO_2 to be transported and stored is presented in Table 4.7, which meets NL's standards.

Table 4.7. Final CO_2 purity obtained in the Aspen Plus simulation.

Component	Concentration, ppm (mol)
H_2O	19
O_2	-
SO_x	1.5
NO_x	0
H_2S	0
CO	0.5
NH_3	0
H_2	0.3

The concentration of O_2 in the pure flue gas is in reality unknown because an O_2 removal process was not simulated. However, as mentioned in 2.5.5, it is realistically possible to achieve an O_2 concentration of below 10 ppm using catalytic oxidation using H_2. It may be interesting to consider the implementation of an electrolyzer to produce the H_2, as well as the production of O_2 needed for the oxypolishing. However, the amount of H_2 needed is in the order of ppm as discussed in section 2.5.5. The oxygen need for oxypolishing is significantly higher at around 0.2 kg/s and producing that amount of O_2 using electricity may lead to significant energy penalties, as opposed to an air separation unit, which is more relevant for large scale. Hence, it is probably not justifiable to implement an electrolyzer, at least not for O_2 production.

The concentration of H_2 would probably increase in the flue gas, with the potential implementation of a catalytic oxidation process, potentially leading to a circular issue with H_2 and O_2 concentration in the flue gas. H_2 is needed for O_2 removal and O_2 is needed for H_2 removal during oxypolishing. The exact dynamics of this implementation are however unknown. This makes cryogenic distillation potentially favorable, while also providing an extremely pure CO_2-stream. Nonetheless, the process is highly complex and not the subject of this study.

4.5 Techno-economics

In the following section, the techno-economic results for the CLC base case plant will be discussed. The overall economic assessment will depend on the utilities and levelized cost of CO_2, therefore a sensitivity analysis of those is discussed in this subsection.

4.5.1 CAPEX

The capital expenditure of this project is defined to be estimated from the total equipment cost, also called total plant cost, which includes each piece of equipment that needs to be added to the new plant. The total cost of each piece of equipment, together with the fixed capital cost and working capital are shown in Table 4.8.

Table 4.8. Investment for each unit in the total plant.

Unit	Investment (MSEK 2023)
FR walls	5.96
FR cyclone	14.43
Oxypolishing reactor	4.57
AR (including cooled walls and cyclone)	145.9
Ash and OC waste handling equipment	21.49
Compressors	10.73
Flash units	0.99
HX units	6.41
Intermediate storage	3.38
Molecular sieve	0.33
SOx cleaning equipment	0.72
Total plant cost	215.11
Fixed capital cost	958.29
Working capital	47.91

The different equipment shown in Table 4.8 is separated by unit operation. All the compressors used in the plant, compressing the CO_2 and in the ammonia refrigeration cycle, are considered under the compression unit. In the same way, the flash units used throughout the compression and liquefaction state are expressed under flash units in Table 4.8.

The cost of purchasing the AR is the highest, which corresponds to more than 68 % of the TPC, followed by the ash and OC waste handling equipment (10 %) and FR equipment (including the walls and the cyclone). The investment cost for the AR cyclone has been calculated and it is equal to 37.86 MSEK. It should be noted that the cost of the endothermic FR is 7 times smaller than the cost of the AR. This is because only endothermic walls are considered for the calculation of the FR, while, for the AR, a CFB boiler with steam generation is assumed.

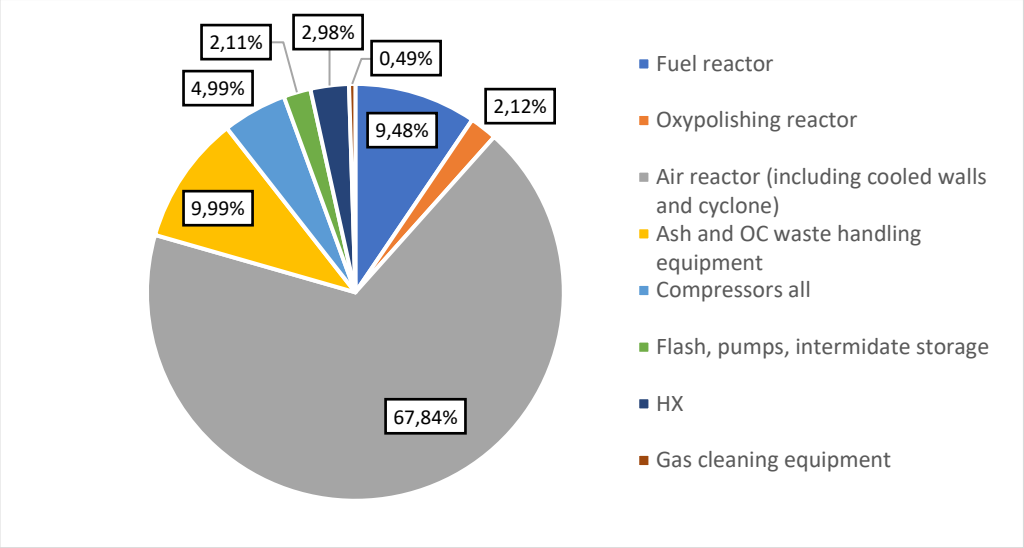

Figure 4.1 Distribution of the CAPEX among the different equipment

Throughout this work, the calculations to size the gas cleaning equipment, for SO_x and H_2O cleaning, have been performed. In Figure 4.1 the impact of those in the TPC, as predicted by Deng et al [61], is negligible. It should be noted that more small equipment, such as pumps, will be needed to run the plant. Hence, such a small contribution to the total plant cost has not been considered.

4.5.2 OPEX

The total fixed operational costs for the total plant in the base case are shown in the following table:

Table 4.9. Fixed operational costs for the base case expressed in MSEK/year.

Parameters	Cost [MSEK/year]
Maintenance	9.50
Labor	8.35
Lab cost	0.42
Rate on Capital	4.75
Insurance	4.75
Taxes	9.50
Total Fixed costs	**37.27**

The labor cost calculated assumes that the current operation is performed with 8 operators and that 4 extra operators would be added for the capture process. In the base case, a total of 12 operators and a 1.45 overhead factor are considered.

The highest contribution to the OPEX costs are taxes and maintenance, which are assumed to be 1 % of the total fixed capital. Furthermore, the variable operational costs in the base case are shown in the following table:

Table 4.10. Variable operational costs for the base case.

Type		Price	Unit	Year	MSEK/Year 2023
Raw materials	**Biomass**	250	SEK/MWh	2023	73.52
	OC makeup	0.42	USD/kg	2011	3.34
	Oxygen	100	€/tonne	2016	7.32
	Molecular sieve	3600	€/tonne	2015	0.89
Utilities	**Cooling water**	0.4	SEK/m^3	2023	0.63
	Electricity	1000	SEK/MWh	2023	13.94

In Table 4.10 the highest contribution to the variable operational costs is the fuel, i.e. biomass. The fuel is only considered when calculating the costs of the total plant, but not when analyzing the added costs for the CO_2 capture, as is mentioned in Section 3.10.

4.5.3 Total plant cost

To have an overview of the total plant cost, all the equipment necessary to run the plant, which has not previously been installed, together with the operating costs of fuel, OC, and utilities are considered in this part. As previously mentioned, the lifetime of the plant is considered to be 20 years with a 5 % interest rate. The economic results of the base case are summarized in Table 4.11.

Table 4.11. Summary of the economic parameters for the base case.

Total capital cost annualized [MSEK/year]	76.90
Variable operational cost [MSEK/year]	100.84
Fixed operational cost [MSEK/year]	37.52
Revenue from selling the utilities [MSEK/year]	190.91
LCCO$_2$ (total plant) [SEK/tonne CO$_2$]	102
LCCO$_2$ (capture) [SEK/tonne CO$_2$]	793
PBP [years]	3.35
NPV [MSEK]	4352.71
NFV [MSEK]	1530.71

The values shown in Table 4.11 are performed assuming a CO_2 credit for producing negative emissions of 1,000 SEK/tonne CO_2. This value will change over the years as it is highly dependent on the CO_2 market value, together with the policy chosen by the EU to incentivize negative emissions. Currently, in 2023, the policies to incentivize BECCS in Sweden and the EU are still under development, therefore, the value of the given subsidy is unknown [8], [9]. In Figure 4.2 the effect of the CO_2 credit income for producing negative emissions on the PBP is analyzed.

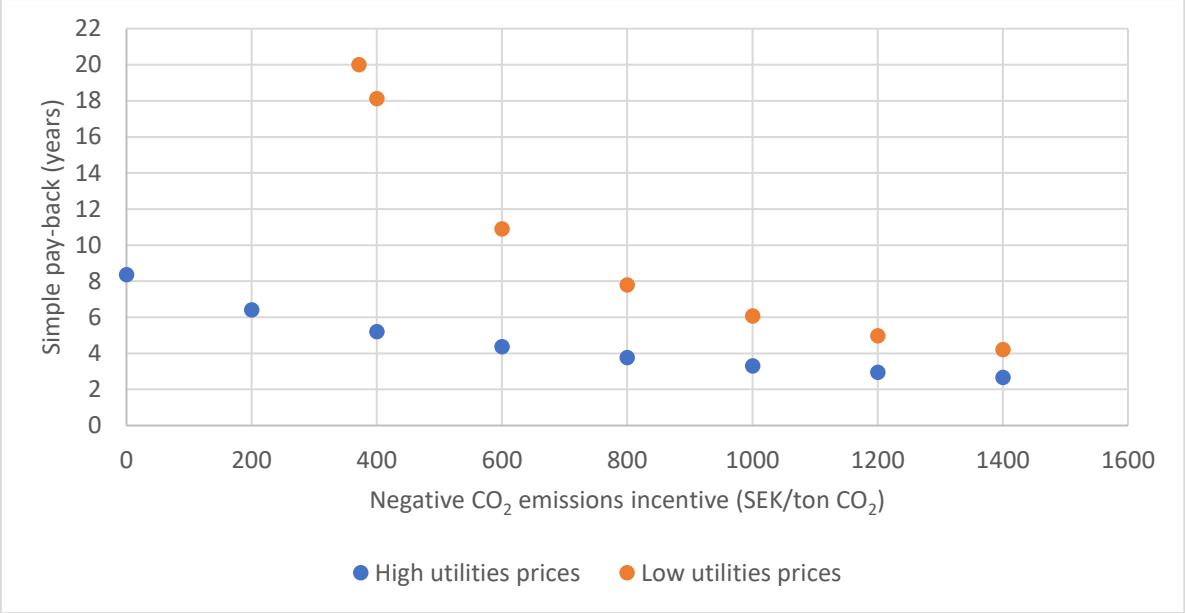

Figure 4.2. Effect of the negative CO_2 incentives on the PBP as a function of the prices for the utilities.

It is observable that, when the utility prices are at their lowest, a subsidy of more than 370 SEK/tonne CO_2 will be required to obtain profit during the lifetime of the plant. On the other hand, when the utility prices are at their highest, even without getting a subsidy, the PBP is below 10 years.

4.5.4 CLC vs. post-combustion

From the previous post-combustion capture study performed at Skövde Energi, the added costs of installing CLC in comparison of installing a post-combustion capture with MEA can be compared. The CO_2 capture efficiency is highly dependent on the technology used. In this work, the MEA-based PCC technology captures less CO_2 (73 kt/year) compared to CLC technology (101.92 kt/year). Therefore, the CO_2 capture efficiency for MEA and CLC technology are 90 wt.% and 97.5 wt.%, respectively.

In Figure 4.3, the difference between the added cost per tonne of CO_2 of implementing CLC and post-combustion with MEA is shown. The CLC added cost is 718 SEK/tonne of CO_2 while for MEA is 1,100 SEK/tonne of CO_2. Even though all the extra equipment which needs to be acquired for running a CLC plant, the CAPEX per tonne of CO_2 is 40 % lower than the post-combustion technology. It must be stated that as fixed added capital costs for the capture, the whole plant equipment is considered with the exception of the AR itself, but a cyclone needed for the CLC is added. It is observed that the MEA has a higher CAPEX per tonne of CO_2, which is believed to be due to the tall and expensive absorption/desorption columns needed.

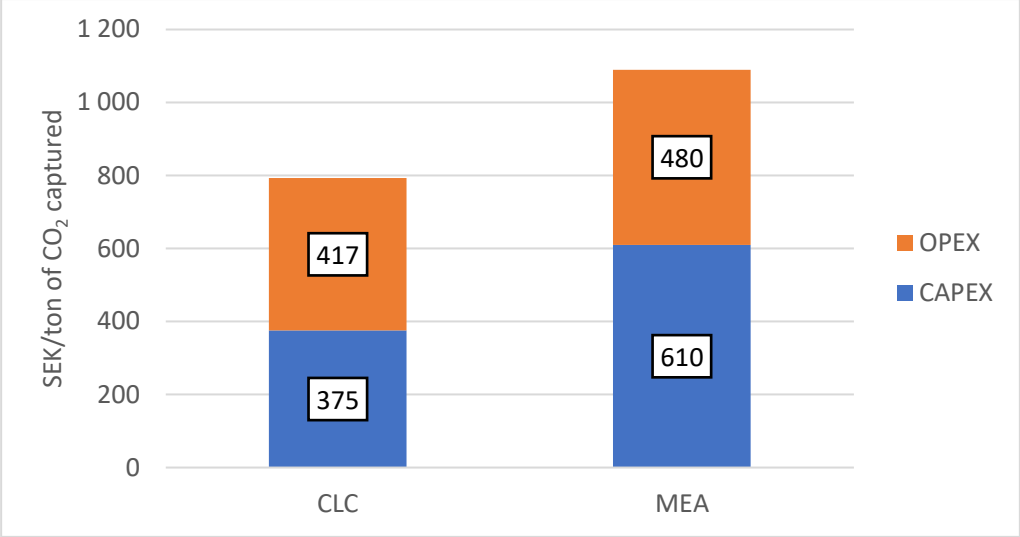

Figure 4.3 Comparison of the added cost per tonne of CO_2 between using CLC or MEA post-combustion technology.

In order to be comparable, the same assumptions for utility prices are assumed, as shown in Section 4.5.3. It is important to note that for the fixed operational costs, which include maintenance, labor, taxes, and others; the calculations have not been performed the same way. The contribution in the added OPEX costs for the CLC technology is shown in the diagram in Figure 4.4. This diagram could not be made with the post-combustion MEA technology as not enough information is provided [13].

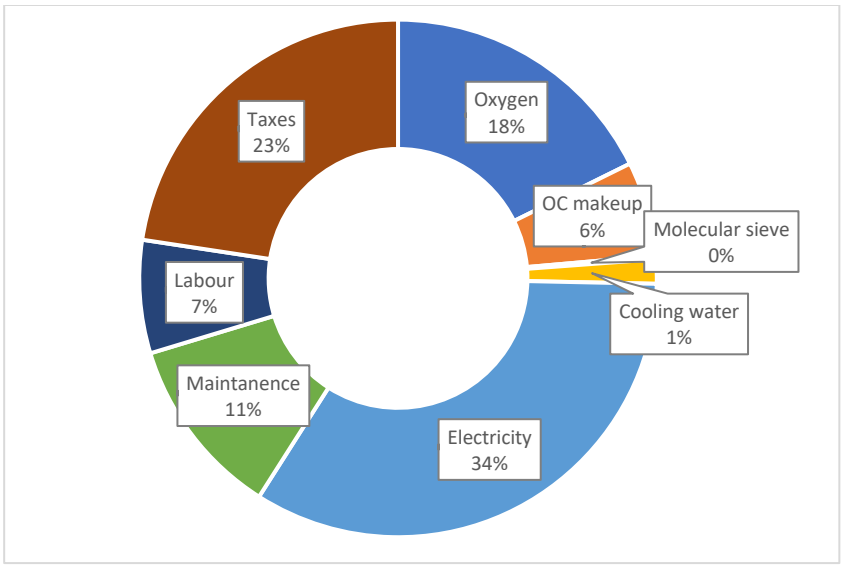

Figure 4.4. Distribution of the added operational costs for the CLC technology

It can be seen from Figure 4.5 that the main contribution to the costs is electricity, oxygen, and taxes. The molecular sieve, cooling water, and OC makeup have a very small contribution in the base case scenario. The price of OC and pure oxygen has a very unstable value in the market which depends on a lot of different factors such as vendor, location, technology of production, and others. Additionally, the cooling water price is directly related to the source of it and an extensive detailed exercise should be done to conclude its actual price. Different sensitivity analyses are performed with those prices in order to see the impact of the assumptions made.

Furthermore, as it is very well known, the main revenue for the company is currently from the production of DH and electricity utilities, therefore, the amount of energy consumed with the two technologies will have a high impact on the PBP and NPV. The difference between utilities used by the two technologies is shown in Figure 4.5.

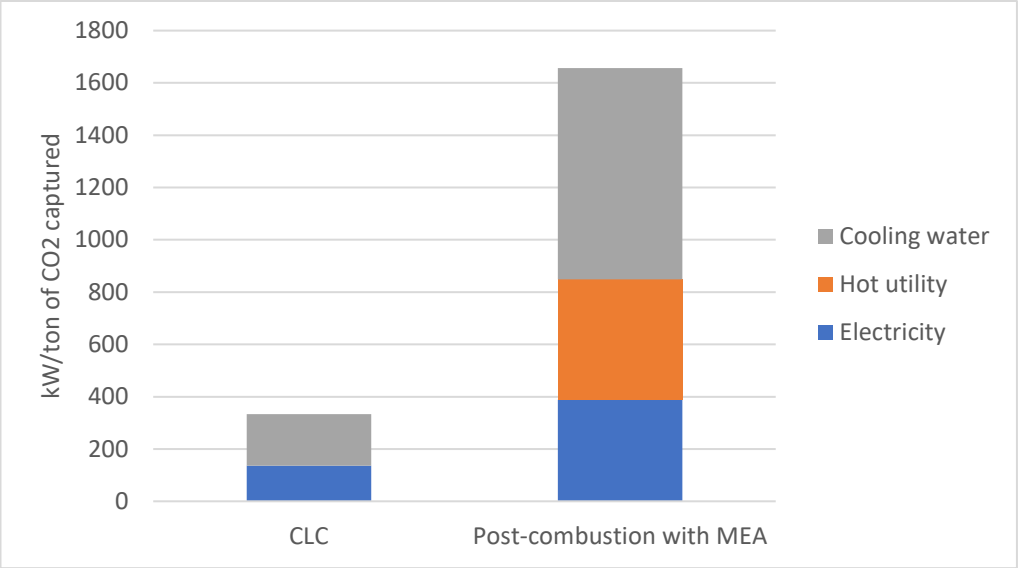

Figure 4.5. Comparison of the energy used per tonne of CO_2 captured for CLC and post-combustion technologies.

To capture one tonne of CO_2 using post-combustion, more than 1.2 MW/tonne CO_2 of extra utilities is needed. It has to be noticed that the CLC technology does not require external hot utilities as the process is self-sufficient in heat. Nevertheless, the post-combustion technology will require an external hot utility to operate the column reboiler. Additionally, more than 70 % more cooling water is needed to run the MEA post-combustion technology in comparison with CLC, per tonne of CO_2. Finally, the electricity usage per tonne of CO_2 is 60 % higher in the amine case.

The capture efficiency for the MEA process has been assumed, by Skövde Energi, to be 90 % capture rate and 5 % losses in the liquefaction. On the other hand, it has been calculated that having a CLC technology would reach a 99 % capture rate and 1.5 % liquefaction losses. The technology used to perform the liquefaction is different for the two studied technologies. As stated, the simulated system liquefies by cooling with an ammonia refrigeration cycle while the post-combustion with MEA study has been assumed to be using a liquefaction system by expansion. In the MEA case, the stream needs to be compressed at a higher pressure, hence consuming more electricity. Due to the different principles used for conditioning the CO_2, the liquefaction losses are not comparable.

The total amount of utilities needed to run the plant at full load is explained in the following table.

Table 4.12. Utilities consumed per hour to run the plant at full load for both technologies.

Parameter	CLC	Post-combustion with MEA
Electricity consumed (MW)	2.4	4.8
Hot utility consumed (MW)	0	5.7
Cooling water consumed (MW)	3.1	10
Total tonnes of CO_2 captured per year	101,921	73,000
CO_2 total capture efficiency (%)	97.5	85.5

In Table 4.12 it can be seen how the consumption of the different utilities is much higher in the post-combustion case. Furthermore, the amount of CO_2 captured in the CLC case is much higher 29 ktonne CO_2/year, hence the overall efficiency of the post-combustion process is significantly lower.

4.5.5 Techno-economic comparison with literature

A sensitivity analysis of the technology is performed by comparing it with other literature studies where the cost per tonne of CO_2 captured is calculated. In this section, only the costs related to the capture process are included. An overall comparison is shown in Table 4.13, where the estimated values from Lyngfelt et al [56] for biomass and coal, together with the values from Deng et al [61], for compression and liquefaction of CO_2. In this section, the prices from the literature, which were stated in euros, have been converted to Swedish crowns using a conversion rate of January 2023 (1 € = 10.4438 SEK).

Table 4.13. Sensitivity analysis of the calculated price per tonne of CO_2 compared with other literature studies [SEK/tonne CO_2].

Parameter	Base case	Lyngfelt et al [56] **(biomass)**	Lyngfelt et al [56] **(coal)**	Deng et al [61]
Total purchased cost	331.12	251	166-270	-
Total installed cost	783.37	-	-	-
Compression liquefaction and flue gas cleaning installed cost	155.17	-	-	167-209

As can be seen in Table 4.13, the base case corresponds to a higher price per tonne of CO_2 capture compared to the literature values, which might be related to the assumptions of OC, electricity, and O_2 price together with the lifetime of OC. Additionally, the comparison with Deng et al [61] shows that the predicted costs for conditioning the CO_2 are close to the calculated range.

To perform a more accurate comparison, the sectioned costs estimated by Leckner and Lyngfelt [21] are used as a comparison point, as it is believed to be the most relevant basis for comparison. It is important to keep in mind that the cost estimations are predictions made for different varieties of solid fuels. The values stated in Table 4.14 compare the costs per tonne of CO_2 in each part of the technology chain between the approximation made by Leckner and

Lyngfelt [21], and the current case, it is assumed that the estimations are performed for purchased cost.

Table 4.14. Comparison of the cost estimation per tonne of CO_2 between literature and the actual case, separated by purchased and installed cost [SEK/tonne of CO_2] [21]

Process section	Cost estimation by Leckner and Lyngfelt [21] (solid fuel)	Purchased CAPEX and OPEX	Installed CAPEX and OPEX
CO_2 compression	104	115.43	139.13
Oxypolishing	42-94	75.42	87.85
Oxygen carrier	14-42	32.78	32.78
Liquefaction	-	30.60	38.83
AR cyclone	-	29.81	132.80
CC Waste handling	-	16.92	75.38
Boiler cost (FR)	1-24	16.05	71.51
Cooling water	-	6.15	6.15
CC Heat exchangers (all)	-	5.05	22.49
Flue gas cleaning	-	1.71	4.57
CC Tank	-	1.19	5.28
Fixed operational	-	-	166.59

It is important to note the difference in size between the two cases; the case analyzed by Leckner and Lyngfelt [21], is 20 times bigger than the one studied in this work; therefore, it is expected that the capital price would be lower. However, although the difference in thermal load, it can be seen in Table 4.14, that the prices per tonne of CO_2 are extremely similar when talking about purchased cost. Nevertheless, the similarity in the values, it must be noted that the electricity, OC, and oxygen price play an important role in the costs, but Leckner and Lyngfelt [21] do not report the values used for the predictions.

Moreover, an extra cost is assumed for the AR cyclone, which is needed to transition from a CFB boiler system to a CLC-CFB technology. It is believed that the waste handling equipment must be included in the base case due to the need of separating the OC from the ash to recirculate it. Other sections that have not been included in the work are the flue gas cleaning and CO_2 intermediate storage which can be concluded to be negligible.

Additionally, it is confirmed that, as predicted by Deng et al [61] together with Leckner and Lyngfelt [21], the flue gas cleaning has an insignificant impact on the costs and could be assumed negligible in future cost estimations.

4.6 Sensitivity analysis

In this section, the results of the sensitivity analysis on the effect of varying the steam production temperature, and multistage compression, together with the impact of the CAPEX and OPEX in the techno-economics will be presented and discussed.

4.6.1 Effect on the steam temperature

Table 4.15 below illustrates steam properties, net electrical production, district heating potential, and corresponding revenue, for different temperatures and pressures of the steam.

Table 4.15. Steam properties, electricity contribution, DH contribution, cooling water need, and associated total cash flow of different cases of temperature and pressure modifications.

Parameters	Base case	Higher temperature	Higher pressure	Higher pressure/temperature
Steam temp [°C]	480	600	480	600
Steam pressure [bar]	90	90	150	150
Electrical output [kW]	9,263	10,912	9,694	11,536
Pump duty [kW]	205	205	345	345
Net elec. [kW]	9,058	10,707	9,349	11,191
District heating potential [kW]	42,428	34,534	41,943	32,944
Cooling water duty [kW]	3,131	9,389	3,344	10,417
New turbine [SEK/year]	-	1,856,638	1,686,590	1,942,268
Total cash flow [MSEK/year]	203.0	181.7	201.3	178.6

By examining Table 4.15, it is clear that the optimal configuration is the base case at the steam temperature and pressure currently used in Skövde Energi. If the steam temperature is increased, it will result in higher electricity production but lowers DH production, which ultimately leads to a decrease in profit. Increasing the steam pressure leads to a slight increase in net electricity production, but a decrease in DH production, which necessitates the use of more cooling water and results in waste of heat and loss of profit.

Although raising both steam pressure and temperature leads to the highest net electricity production, it still cannot compensate for the significant decrease in district heating production, which results in a loss of cash flow. The reason why the DH production is significantly reduced when increasing the steam temperature has to do with utility pinch limitations since the DH temperature is raised from 50 °C to 120 °C. In Table 4.16 below, the same results are shown for different bleed stream ratios of the turbine exhaust. An additional case using high temperature steam but modifying the DH temperature to be going from 50 °C to 100 °C is shown. Note that the base case, currently in use in the installed plant, has an 87.7/12.3 bleed ratio.

Table 4.16. Steam properties, electricity contribution, DH contribution, cooling water need, and associated total cash flow of different cases of bleed stream modifications.

Parameters	No bleed stream (100/0)	Only bleed stream (0/100)	50/50	Higher temperature (50 °C-100 °C)
Steam temp [°C]	480	480	480	600
Steam pressure [bar]	90	90	90	90
Electrical output [kW]	9,626	6,675	8,150	10,912
Pump duty [kW]	206	201	205	205
Net elec. [kW]	9,420	6,474	7,945	10,707
District heating potential [kW]	29,492	44,959	43,417	40,529
Cooling water duty [kW]	15,728	3,344	3,344	3,394
New turbine [SEK/year]	-	-	-	1,856,638
Total cash flow [MSEK/y]	156.8	196.7	199.9	204.1

From Table 4.15 and Table 4.16, it is also evident that the base case bleed ratio results in the largest cash flow, which is motivated by the same arguments as before. Having no bleed stream results in the largest expansion throughout the turbine which maximizes electricity production, at the large expense of district heating production due to utility pinch limitations and thereby resulting in a large profit loss. At the same time, focusing on total bleed stream exhaust limits the electricity production significantly compared to the base case, thereby leading to a slight decrease in cash flow as opposed to the base case. A 50/50 bleed ratio also leads to a slight decrease in profit as opposed to the base case. Looking at the higher temperature case with modified DH temperature change, the electricity production is higher than the base case, but the DH production potential is lower. However, DH production is not severely limited due to utility pinch, and therefore cash flow is higher than the base case. The presence of a utility pinch point is illustrated in Figure 4.6 below, showing part of the process GCCs, where the left figure is the modified DH temperature change, and the right figure is the standard DH temperature change.

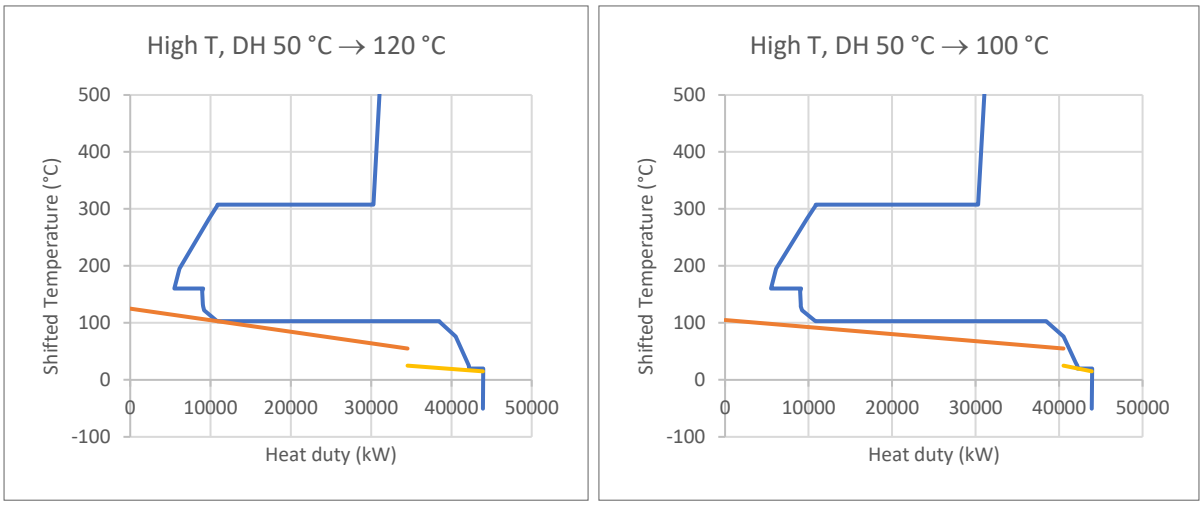

Figure 4.6. Utility pinch is seen on the left figure from the orange line touching the process GCC. The same orange line has no pinch for the modified DH temperature on the right.

Since this analysis was done using only one DH and electricity price, it is difficult to draw a clear conclusion, as the prices will be affected by market conditions and will vary over time. It was therefore not deemed relevant to try to find an optimal ratio of a bleed stream maximizing its profit. A higher electricity price would shift the favor towards maximizing electricity production at the expense of district heating, but it would have to increase approximately threefold to be more profitable, in the case of increasing temperature/pressure. Still, the electricity market can be very volatile, and the possibility to increase electricity production may be of value in future energy scenarios and may be an additional advantage of the CLC technology.

4.6.2 Multistage compression analysis

In this section, results regarding the number of compressors in the CO_2 compression train are presented. Table 4.17 below shows the power consumption, annual cost of equipment, and power.

Table 4.17. Multicompressor economic results for the CO_2 train comparing three and four stages.

Parameters	**3 stages**	**4 stages**
Power [kW]	1,628	1,544
Annual cost of compressors [SEK/year]	582,383	641,567
Annual additional heat exchanger cost [SEK/year]	-	13,507
Annual additional flash unit cost [SEK/year]	-	8,024
Annual power cost [MSEK/year]	9.60	9.11
Total annual cost [MSEK/year]	10.19	9.77

As seen above, using four stages has a lower power requirement by 84 kW, which is expected due to intercooling and excess steam removal between stages. Also seen are the higher equipment costs when using four stages, but the lower power cost which altogether sum up to the total annual costs. The total annual cost shows that using four stages is cheaper, saving 411,533 SEK/year. Hence, four compressors were used in the plant design. Note that this analysis and the entire thesis were done considering full load. At part load, the electricity savings will not be as significant, and the possibility may exist that a three-stage compressor would be more suitable.

4.6.3 Impact of the CAPEX on the project

In this section, the study of varying the fixed capital cost to analyze the sensitivity of the economic analysis is performed. As shown in Figure 4.7, a change of ±50 % in the CAPEX is evaluated to check the impact on the different economical parameters which are explained in Section 3.10.4.

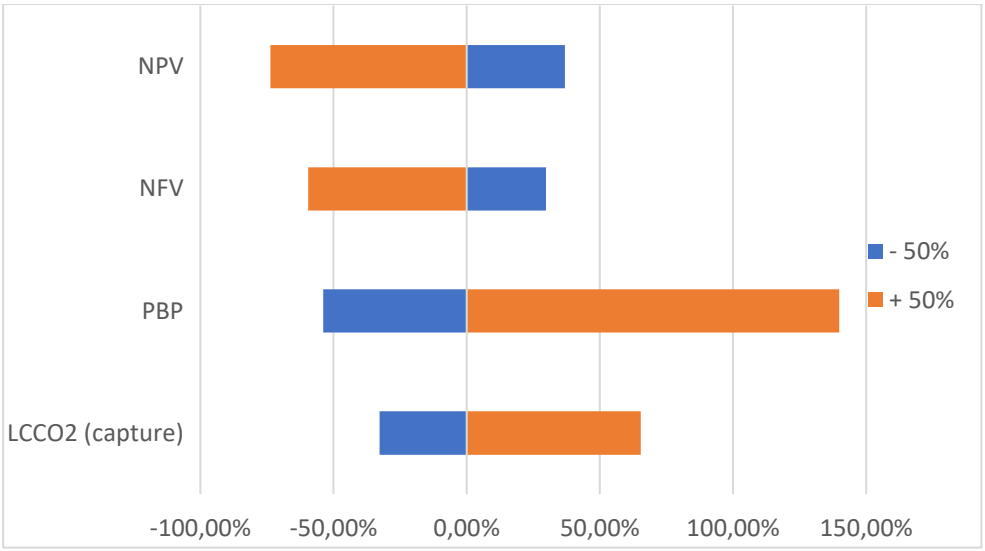

Figure 4.7. Impact on the variation of the CAPEX on the different economic parameters analyzed.

It can be seen that the PBP is highly affected by the change, while the $LCCO_2$ (capture), NPV, and NFV vary approximately in the same order of magnitude. The PBP would increase more than 2.4 times if the CAPEX is underestimated by 50 %, having a high impact on the base case analysis. Moreover, the effect on NPV and NFV varies inversely than the other parameters, as a higher CAPEX is translated to a lower profit at the end of the plant's lifetime. It is shown that if the CAPEX has been underestimated, it will lead to a higher impact on the predicted results than if it is overestimated. The numerical values of the variation are shown in the following table.

Table 4.18. Impact on the variation of the CAPEX on the different analyzed economic parameters.

Parameters	**-50 %**	**Base case (0 %)**	**+50%**
$(LCCO_2)_{total\ plant}$ [SEK/ tonne CO_2]	-447.2	102.1	1,093
$(LCCO_2)_{capture}$ [SEK/ tonne CO_2]	521.4	792.9	1,280
PBP [years]	1.50	3.35	7.81
NFV [MSEK]	5,810	4,352	1,810
NPV [MSEK]	2,160	1,530	4,150

The $LCCO_2$ of the total plant and the capture, for the case with 50 % more CAPEX, are around the values predicted for other technologies, such as post-combustion with MEA (1100 SEK/tonne CO_2) [95]. Therefore, even if the effect of varying the CAPEX estimation on the $LCCO_2$ is high, the technology will still be competitive with the different CO_2 capture techniques currently in the market. Additionally, as previously mentioned, although the CLC unit can be seen as uncertain, due to the lack of experimental work in high-load units, it could still be used as a normal CFB boiler, which would reduce the economic risk of the total project.

It is important to notice that, even if the error percentage is high, in the worst-case scenario (having underestimated the CAPEX value by 50 %) the solution would still be profitable. As this analysis is highly preliminary, additional studies will need to be performed in order to obtain a more accurate approximation.

4.6.4 Impact on the OPEX on the project

The results on the impact of the cost with high contribution to the OPEX are analyzed in this section. It is important to note that this sensitivity analysis has been performed with the highest electricity and DH prices (1000 and 600 SEK/MW respectively). However, the results follow the same tendency independently of the utility prices. In Table 4.10, it can be seen that the highest impact on the variable operational costs are the biomass, oxygen, and electricity prices. The OC has also a higher considerable impact in comparison to the molecular sieve adsorbent and the cooling water. Furthermore, the utilities prices have a high impact on the profitability of the project, but as the utilities are mainly considered as a form of revenue, and not a cost, the analysis will be performed in Section 4.6.5.

In Figure 4.8, the impact of the biomass and O_2 cost on the PBP, represented by dots, and the levelized cost of CO_2 (total plant), shown by columns, are analyzed.

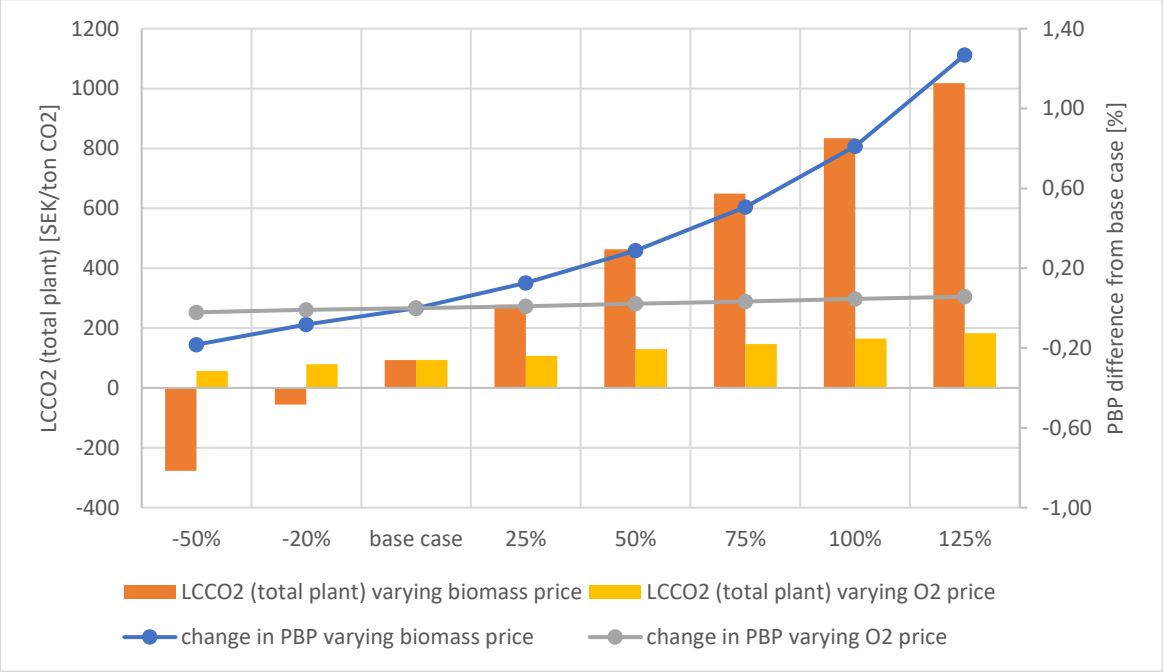

Figure 4.8. Impact of the Biomass (fuel) price and O_2 (oxypolishing) price on the PBP (dots) and the levelized CO_2 cost (columns).

The figure shows that the fuel price has a high effect on the PBP and the $LCCO_2$ (total plant). Both variables follow an exponential trend when increasing the fuel price. Considering all the base case assumptions, if the biomass price decreases to 225 SEK/MWh, the $LCCO_2$ of the total plant would be 0 SEK/tonne CO_2, meaning that Skövde Energi would not need to have revenue from the captured CO_2 in order to have a break-even price before the lifetime of the project is over. Over the years, the price of biomass is expected to be higher, due to the increase in demand to obtain net negative emissions. For this reason, future analysis of this technology requires utmost caution regarding this variable.

In Figure 4.8, it is shown that the O_2 price has a low impact on the PBP of the project, not varying the result by more than ±2 %. Although the influence on the levelized cost of CO_2 is slightly higher, it can be considered insignificant.

The impact of the OC in the OPEX is nearly insignificant, 6 %, as seen in Table 4.4, the analysis of its price has been performed as the price of the OC has a very variable cost, which has been explained in Section 3.11.3. In Figure 4.9 the same analysis as for the oxygen price has been done for the OC cost.

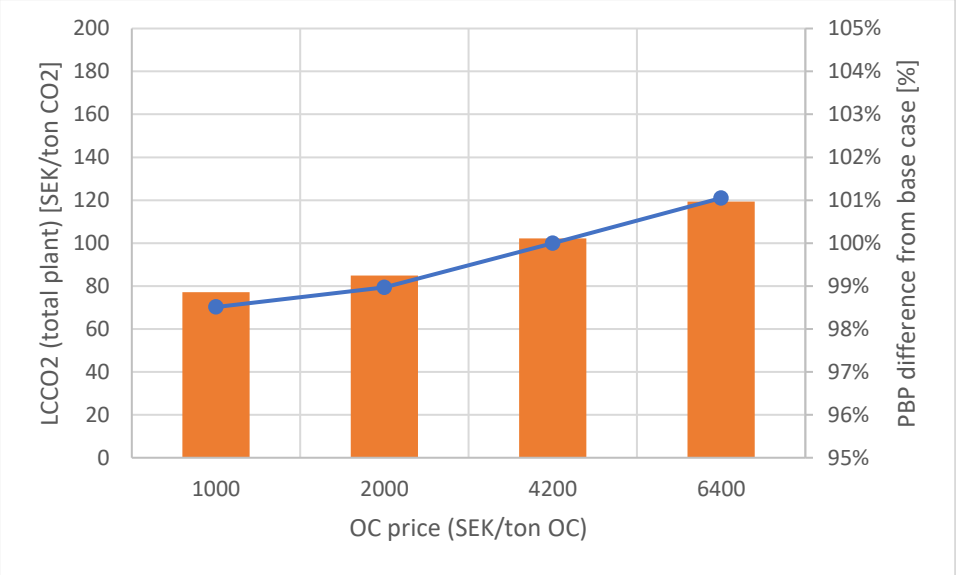

Figure 4.9. Impact of the OC price on the PBP (dots) and the break-even CO_2 cost (total plant) (columns)

As predicted, the effect of the OC price on the PBP and levelized CO_2 cost is relatively minor than to the O_2 case. In the base case, a value of 4,200 SEK/tonne OC has been assumed. A difference of ±1 % is seen in the PBP while in the break-even CO_2 price, ±30 % is observed. Both variables vary exponentially with respect to the OC price. However, even with the highest price per tonne of OC found in literature, the levelized cost of CO_2 (total plant) is below 150 SEK/tonne.

Even though there is some variation in the results when analyzing the O_2 and OC price, they have a low impact on the total plant cost, therefore, it can be concluded that the effect is rather low, which gives confidence in the results.

4.6.5 Effect on the utility prices

For the electricity and district heating utilities two different prices are analyzed, which are explained in Section 3.11.4. As previously mentioned, utility prices are highly dependent on the world's market and, therefore, they are not constant over time. To simplify this analysis, it has been considered that they are. The analysis has been done for two different levelized costs of CO_2, one considering the total plant cost, including the revenue, and the other only considering the capture costs, together with the PBP, NFV, and NPV, as shown in Section 3.10.4.

When considering $LCCO_2$ (total plant), the utility prices have a high impact as they are directly correlated to the $LCCO_2$ and they are the only source of income. Moreover, when only the costs of capture are analyzed, the electricity consumption is low and no district heating is used,

therefore the impact of the utilities cost is lower. The obtained results are shown in the following table.

Table 4.19. Impact of the utility prices on the different economic parameters

Variables	Higher utilities prices	Lower utilities prices
$LCCO_2$ (total plant) [SEK/tonne CO_2]	102.12	854.44
$LCCO_2$ (capture) [SEK/tonne CO_2]	792.92	724.52
PBP [year]	3.35	6.14
NFV [MSEK]	4352.71	1613.84
NPV [MSEK]	1530.71	478.87

As explained in Section 3.10.3, most of the capture projects are assumed to have a price of 1,000 SEK/tonne CO_2, therefore, using both utility prices the $LCCO_2$ is approximately equal to or below that. It is important to note that, even when the utility prices are lower, which translates to lower revenue, the PBP is less than half of the project's lifetime, which means that the project will be profitable.

5 Further considerations

There have been a couple of CLC upscaling designs done in literature, such as the designs published by Lyngfelt et al [21], [56] of a 1000 MW_{th} and 200 MW_{th} unit. The question remains if larger CLC-units could be successfully implemented, even larger than the one studied in this thesis. A larger unit would result in bigger and more expensive equipment. Considering that the highest expense in this work is the AR, a bigger size would result in a higher total capital cost, but potentially a lower specific cost. Additionally, it would also lead to more uncertainties during simulation, as pilot plants have only been designed up to 1 MW_{th}. However, there are some large CFB boilers which have a similar behavior, simplifying the prediction for a CLC-CFB plant. But as many of the normal CFB plants for CHP in operation today are in the size range of 50-150 MW, the currently studied CLC-CFB unit could in many ways be a first-of-a-kind commercial unit. The mentioned risks will be minimized by the fact that the unit could likely be very flexible in operation, i.e. run as a normal plant in case conditions are not favorable. But, when running the system as a CFB, the CO_2 would not be captured, reducing the amount of negative emissions.

Moreover, the feasibility assumption for the current design (50 MW_{th} unit) is based on previous experience, using pilot plants and fluidized beds, coupled with the necessary heat and mass balances. Similar methods have been performed by Lyngfelt et al [21], [56] to analyze designs for 200 and 1000 MW_{th} and conclude the feasibility of them. Furthermore, the assumption of having a feasible technology could still be applied to larger plant sizes, as the residence time would be higher, increasing the particle interactions. Moreover, the designed unit would be equipped with measurement equipment in order to evaluate performance and provide in-data for future larger units. It should be noted that a size upgrade would be required to optimize the district heating and electrical production network.

The results obtained from this work show that, in the analyzed cases, a CLC unit would have a higher cost-efficiency, nevertheless, it is estimated that the CLC technology will need additional years to be installed on such a large scale. The currently investigated and installed technologies are mostly post-combustion, such as absorption with amines or hot-potassium carbonate, due to the easiness of retrofitting an additional unit. Furthermore, those capture units are high in the Technology Readiness Level (TRL) scale with a level of 9 [100], while CLC is still at a level of 6 [4], [21], [100], [101].

In the case of Skövde, the production system is mainly driven by the DH demand of the population. For this reason, the hourly prices are studied every day to understand the possible revenue and vary the load and heat production accordingly. Moreover, it needs to be mentioned that in the future, there will be increased volatility, due to the increase in usage of renewable energy sources. For this reason, it is important to own a system that allows to have high variability. It has been mentioned by different experts in the CLC field, that the technology would be capable of handling this fuel variance, acting like a peak load for the system [21], [56], [64]. Another aspect to take into account would be safety, which will increase with technological uncertainties. Potential safety issues related to the pilot plants would have to be analyzed, as well as additional ones that may arise during upscaling, to design the plant layout.

From another perspective, as Skövde is known to have high industrial activity, following the same idea as CinfraCap in Göteborg, a shared conditioning plant could be installed. This could

reduce the installed and operational cost calculated, but a deeper analysis must be done regarding the positioning of the conditioning plant and the participants involved.

As previously mentioned, this report is presented for a specific case; a biomass boiler of about 50 MW_{th} situated in Skövde Energi and operating at full load for 5,900 h/year. Although these assumptions, most of the results could be extrapolated to other industries with similar characteristics, such as similar fuel composition and load. Nevertheless, the prices assumed for utilities and fuel would need to be adjusted to the location of the boiler, to understand which utility drives the production and optimize it. As mentioned, CLC allows to raise in the steam temperature due to the low corrosion in the AR. Increasing the steam temperature enables a higher electricity output but significantly reduces the amount of district heating generated. In other countries, where the main production is not driven by district heating, electricity production can be increased while increasing the revenue obtained.

6 Conclusion

This thesis evaluates the possibility of substituting a BFB biomass boiler of 50 MW_{th}, situated in Skövde Energi, with a CFB-CLC system which would allow an easier capture of the generated CO_2 emissions to store it achieving negative emissions. The downstream flue gas cleaning, together with the compression and liquefaction of it, has been included in the simulations. Although the logistics of how the CO_2 would be transported to the storage site have not been analyzed, it is considered that the long-term storage site would be the NL facility (Bergen, Norway). The CLC technology would be integrated into the combined heat and power plant (CHP), producing DH and electricity. This work shows that the integration of a CLC technology and CO_2 capture would be techno-economically feasible.

The simulation and heat integration process was performed and applied for the specific input given by Skövde Energi. A literature study was conducted to understand the technical limitations and include the necessary downstream sections to simulate a realistic system. Thereafter, a techno-economical study was performed to calculate the feasibility of the technology and compare it to previous literature studies. Additionally, sensitivity analyses were conducted to assess the impact of certain parameters such as the rise of the steam cycle conditions, stages in the multicompressor, and the sensitivity of the techno-economic analysis to the variation of the market prices. Finally, the results for the CLC technology were compared to the previous study conducted in Skövde Energi for the installation of a post-combustion system with MEA.

The study shows that the CLC capturing technology would be more cost-efficient than a post-combustion system with MEA absorption, as the capture efficiency is increased by more than 10%, the energy consumption is decreased by 75 % and the costs are reduced by around 30 %. The results show that the highest contribution to the costs are the CO_2 compression train and the oxypolishing, while the FR and downstream flue gas cleaning have an insignificant impact. Additionally, the study highlights that the economic viability of installing this technology has a high dependence on fuel and utility prices, which are regulated by the market.

This case study helps to have an understanding of the upscaling of the CLC technology and the high competitiveness that CLC has as a carbon capture technology. Other CHP-plants would be able to use this work to understand the basic considerations of shifting from a BFB boiler to a CFB-CLC system.

6.1 Future work

The process scheme investigated in this thesis provides various prospects for future development in order to lead to a total understanding of this technology. One area of focus should be the particle behavior, together with the combustion and oxidation/reduction reactions for the CLC loop, which could be done using CFD software. In the current work, the analysis of gas velocity, particle interaction, and distribution for both reactors have not been performed and the optimization of those parameters would have a high impact on the plant results, heat integration, and reactor dimensions. Another area could be the obtention of fluidizing agent for the FR can be analyzed further to understand the behavior and efficiency of using CO_2 and/or steam.

As mentioned throughout this project, it is important to build and operate a CLC plant with the proposed design configuration in order to understand the behavior of the technology. It is considered that, as most of the plants range from 50-150 MW_{th}, the current thermal input designed (50 MW_{th}) would be appropriate to start.

Finally, a logistic analysis on how to transport the CO_2 to the permanent storage site should be performed for Skövde Energi, as it is important to validate the feasibility of storing the captured emissions. If the analysis ends up not being economically feasible, the possibility of utilizing the emission, for example, to produce fuel, should be studied.

Bibliography

[1] "IPCC — Intergovernmental Panel on Climate Change." https://www.ipcc.ch/ (accessed Jan. 18, 2023).

[2] S. Ladanai and J. Vinterbäck, "Global Potential of Sustainable Biomass for Energy," *SLU, Institutionen för energi och teknik*, 2009.

[3] A. d'Espiney, I. Paula Marques, and H. Maria Pinheiro, "Case Study: Pathways from Forest to Energy in a Circular Economy at Lafões," *Forest Biomass - From Trees to Energy*, Feb. 2021, doi: 10.5772/INTECHOPEN.93070.

[4] A. Almena, P. Thornley, K. Chong, and M. Röder, "Carbon dioxide removal potential from decentralised bioenergy with carbon capture and storage (BECCS) and the relevance of operational choices," *Biomass Bioenergy*, vol. 159, p. 106406, Apr. 2022, doi: 10.1016/J.BIOMBIOE.2022.106406.

[5] Equinor ASA, "Northern Lights - Equinor," 2023. https://www.equinor.com/energy/northern-lights (accessed Jan. 27, 2023).

[6] K. W. Bandilla, "Carbon Capture and Storage," *Future Energy: Improved, Sustainable and Clean Options for Our Planet*, pp. 669–692, Jan. 2020, doi: 10.1016/B978-0-08-102886-5.00031-1.

[7] J. C. Abanades *et al.*, "Emerging CO2 capture systems," *International Journal of Greenhouse Gas Control*, vol. 40, pp. 126–166, Sep. 2015, doi: 10.1016/J.IJGGC.2015.04.018.

[8] Regeringen och Regeringskansliet, "Stor satsning görs på infångning av biogen koldioxid," 2022, Accessed: May 29, 2023. [Online]. Available: https://www.regeringen.se/pressmeddelanden/2022/11/stor-satsning-gors-pa-infangning-av-biogen-koldioxid/

[9] European Commission, "Emissions cap and allowances," 2021. https://climate.ec.europa.eu/eu-action/eu-emissions-trading-system-eu-ets/emissions-cap-and-allowances_en (accessed May 29, 2023).

[10] "Block 4 - Skövde Energy." https://skovdeenergi.se/fjarrvarme/natet-i-skovde/block-4/ (accessed Jan. 18, 2023).

[11] Z. Kapetaki and Miranda-Barbosa, "Technology Development CCUS," *European Comission*, Dec. 2019. https://www.researchgate.net/publication/337874020_Technology_Development_CCUS (accessed Jan. 30, 2023).

[12] CinfraCap, "CinfraCap - Gemensam infrastruktur för transport av koldioxid," Mar. 2021. Accessed: Mar. 20, 2023. [Online]. Available: https://cowi.sharepoint.com/sites/

[13] C. Nilsson, "Personal communication with Skövde Energi." 2023.

[14] S. Oji and M. Al-Owaidh, "Build a Combined Heat and Power Model from Scratch," *AIChE The Global Home of Chemical Engineers*, Apr. 2019. https://www.aiche.org/resources/publications/cep/2019/april/build-combined-heat-and-power-model-scratch (accessed Apr. 05, 2023).

[15] Y. A. Çengel, M. A. Boles, and M. Kangoglu, *Thermodynamics: an Engineering Approach*, 9th ed. 2008.

[16] European Commission, "EU Emissions trading system (EU ETS)," 2021. https://climate.ec.europa.eu/eu-action/eu-emissions-trading-system-eu-ets_en (accessed May 29, 2023).

[17] J. Salazar, U. Diwekar, K. Joback, A. H. Berger, and A. S. Bhown, "Solvent Selection for Post-Combustion CO2 Capture," *Energy Procedia*, vol. 37, pp. 257–264, Jan. 2013, doi: 10.1016/J.EGYPRO.2013.05.110.

[18] Z. Chen, "A Review of Pre-combustion Carbon Capture Technology," in *Proceedings of the 2022 7th International Conference on Social Sciences and Economic Development (ICSSED 2022)*, Atlantis Press, 2022, pp. 524–528. doi: 10.2991/aebmr.k.220405.086.

[19] R. Stanger *et al.*, "Oxyfuel combustion for CO2 capture in power plants," *International Journal of Greenhouse Gas Control*, vol. 40, pp. 55–125, Sep. 2015, doi: 10.1016/J.IJGGC.2015.06.010.

[20] Y. De Vos, M. Jacobs, P. Van Der Voort, I. Van Driessche, F. Snijkers, and A. Verberckmoes, "Development of Stable Oxygen Carrier Materials for Chemical Looping Processes—A Review," *Catalysts*, vol. 10, no. 8, 2020, doi: 10.3390/catal10080926.

[21] A. Lyngfelt and B. Leckner, "A 1000 MWth boiler for chemical-looping combustion of solid fuels – Discussion of design and costs," *Appl Energy*, vol. 157, pp. 475–487, 2015, doi: 10.1016/j.apenergy.2015.04.057.

[22] A. Lyngfelt, K. Andersson, and L. R. Pettersson, "Design of circulation system and downstream gas treatment of a full-scale boiler for Chemical-Looping Combustion," *SSRN Electronic Journal*, Nov. 2022, doi: 10.2139/SSRN.4286370.

[23] A. Lyngfelt, B. Leckner, and T. Mattisson, "A fluidized-bed combustion process with inherent CO2 separation; Application of chemical-looping combustion," *Chem Eng Sci*, vol. 56, no. 10, pp. 3101–3113, Jun. 2001, doi: 10.1016/S0009-2509(01)00007-0.

[24] S. Andersson, P.-E. Bengtsson, B. Leckner, and D. Pallarés, *Combustion Engineering*. 2016.

[25] A. Nandy, C. Loha, S. Gu, P. Sarkar, M. K. Karmakar, and P. K. Chatterjee, "Present status and overview of Chemical Looping Combustion technology," *Renewable and Sustainable Energy Reviews*, vol. 59, pp. 597–619, Jun. 2016, doi: 10.1016/J.RSER.2016.01.003.

[26] A. Coppola and F. Scala, "Chemical Looping for Combustion of Solid Biomass: A Review," *Energy & Fuels*, vol. 35, no. 23, pp. 19248–19265, Dec. 2021, doi: 10.1021/acs.energyfuels.1c02600.

[27] M. Cheng, H. Sun, Z. Li, and N. Cai, "Annular Carbon Stripper for Chemical-Looping Combustion of Coal," *Ind Eng Chem Res*, vol. 56, no. 6, pp. 1580–1593, Feb. 2017, doi: 10.1021/acs.iecr.6b03168.

[28] T. Song and L. Shen, “Review of reactor for chemical looping combustion of solid fuels,” *International Journal of Greenhouse Gas Control*, vol. 76, pp. 92–110, Sep. 2018, doi: 10.1016/J.IJGGC.2018.06.004.

[29] A. Lyngfelt and C. Linderholm, “Chemical-Looping Combustion of Solid Fuels - Status and Recent Progress,” in *Energy Procedia*, Elsevier Ltd, 2017, pp. 371–386. doi: 10.1016/j.egypro.2017.03.1179.

[30] H. Akinosho, K. Yee, D. Close, and A. Ragauskas, “The emergence of Clostridium thermocellum as a high utility candidate for consolidated bioprocessing applications,” *Front Chem*, vol. 2, no. AUG, 2014, doi: 10.3389/FCHEM.2014.00066.

[31] H. Yang, R. Yan, H. Chen, C. Zheng, D. H. Lee, and D. T. Liang, “In-Depth Investigation of Biomass Pyrolysis Based on Three Major Components: Hemicellulose, Cellulose and Lignin,” 2006, doi: 10.1021/ef0580117.

[32] “Biomass,” *European comission*, 2021. https://energy.ec.europa.eu/topics/renewable-energy/bioenergy/biomass_en (accessed Feb. 15, 2023).

[33] A. Kumar, S. Adamopoulos, D. Jones, and S. O. Amiandamhen, “Forest Biomass Availability and Utilization Potential in Sweden: A Review,” *Waste Biomass Valorization*, vol. 12, no. 1, pp. 65–80, Jan. 2021, doi: 10.1007/S12649-020-00947-0/TABLES/4.

[34] IVL Swedish Environmental Research Institute, “Sweden’s largest biofuel heat and power plant is fossil-free energy hot spot,” *Smart City Sweden*, 2023. https://smartcitysweden.com/best-practice/399/swedens-largest-biofuel-heat-and-power-plant/ (accessed Feb. 15, 2023).

[35] C. Sheng and J. L. T. Azevedo, “Estimating the higher heating value of biomass fuels from basic analysis data,” *Biomass Bioenergy*, vol. 28, no. 5, pp. 499–507, May 2005, doi: 10.1016/J.BIOMBIOE.2004.11.008.

[36] H. P. Nielsen, F. J. Frandsen, K. Dam-Johansen, and L. L. Baxter, “The implications of chlorine-associated corrosion on the operation of biomass-fired boilers,” *Prog Energy Combust Sci*, vol. 26, no. 3, pp. 283–298, Jun. 2000, doi: 10.1016/S0360-1285(00)00003-4.

[37] A. Lyngfelt, “Chemical Looping Combustion: Status and Development Challenges,” *Energy and Fuels*, vol. 34, no. 8, pp. 9077–9093, Aug. 2020, doi: 10.1021/ACS.ENERGYFUELS.0C01454/ASSET/IMAGES/LARGE/EF0C01454_0006.JPEG.

[38] H. Leion, A. Lyngfelt, M. Johansson, E. Jerndal, and T. Mattisson, “The use of ilmenite as an oxygen carrier in chemical-looping combustion,” *Chemical Engineering Research and Design*, vol. 86, no. 9, pp. 1017–1026, Sep. 2008, doi: 10.1016/j.cherd.2008.03.019.

[39] A. Navajas *et al.*, “Life cycle assessment of natural gas fuelled power plants based on chemical looping combustion technology,” *Energy Convers Manag*, vol. 198, p. 111856, Oct. 2019, doi: 10.1016/J.ENCONMAN.2019.111856.

[40] A. Lyngfelt, A. Brink, Ø. Langørgen, T. Mattisson, M. Rydén, and C. Linderholm, “11,000 h of chemical-looping combustion operation—Where are we and where do we

want to go?," *International Journal of Greenhouse Gas Control*, vol. 88, pp. 38–56, Sep. 2019, doi: 10.1016/J.IJGGC.2019.05.023.

[41] J. Ströhle, M. Orth, and B. Epple, "Design and operation of a 1 MWth chemical looping plant," *Appl Energy*, vol. 113, pp. 1490–1495, Jan. 2014, doi: 10.1016/J.APENERGY.2013.09.008.

[42] P. Markström, "Design, modelling and operation of a 100 kW chemical-looping combustor for solid fuels," CHALMERS UNIVERSITY OF TECHNOLOGY, 2012.

[43] L. R. Pettersson, "Negative CO2 Emissions from Chemical Looping Combustion: Gas Cleaning for CO2 Storage," KTH, 2022.

[44] V. D. Shmakov, "Unconventional gas," *Vestnik Sankt-Peterburgskogo Universiteta, Seriya Geologiya i Geografiya*, vol. 2010, no. 1, pp. 59–98, Jan. 2019, doi: 10.1016/B978-0-12-809570-6.00003-5.

[45] Northen Lights, "Who we are," *Northern Lights*, 2023. https://norlights.com/who-we-are/ (accessed Feb. 28, 2023).

[46] Northen Lights, "How to store CO2 with Northern Lights," *Northern Lights*, 2023. https://norlights.com/how-to-store-co2-with-northern-lights/ (accessed Feb. 28, 2023).

[47] I. Staničić, J. Brorsson, A. Hellman, T. Mattisson, and R. Backman, "Thermodynamic Analysis on the Fate of Ash Elements in Chemical Looping Combustion of Solid Fuels─Iron-Based Oxygen Carriers," *Energy and Fuels*, vol. 36, no. 17, pp. 9648–9659, Sep. 2022, doi: 10.1021/ACS.ENERGYFUELS.2C01578/ASSET/IMAGES/LARGE/EF2C01578_0010.JPEG.

[48] B. M. Jenkins, L. L. Baxter, and J. Koppejan, "Biomass Combustion," in *Thermochemical Processing of Biomass*, 2019, pp. 49–83. doi: https://doi.org/10.1002/9781119417637.ch3.

[49] R. Singh and A. Shukla, "A review on methods of flue gas cleaning from combustion of biomass," *Renewable and Sustainable Energy Reviews*, vol. 29, pp. 854–864, Jan. 2014, doi: 10.1016/J.RSER.2013.09.005.

[50] J. Gimbun, T. G. Chuah, A. Fakhru'l-Razi, and T. S. Y. Choong, "The influence of temperature and inlet velocity on cyclone pressure drop: a CFD study," *Chemical Engineering and Processing: Process Intensification*, vol. 44, no. 1, pp. 7–12, Jan. 2005, doi: 10.1016/J.CEP.2004.03.005.

[51] O. Vekemans, M. Yazdanpanah, F. Guillou, S. Bertholin, and B. Haut, "Modeling and Simulation of an Industrial-Scale 525 MWth Petcoke Chemical Looping Combustion Power Plant," *Processes*, vol. 11, no. 1, 2023, doi: 10.3390/pr11010211.

[52] David Hosansky, "Electrostatic precipitator," *Encyclopedia Britannica*, 2021. https://www.britannica.com/technology/electrostatic-precipitator (accessed Mar. 05, 2023).

[53] D. Mei, C. Linderholm, and A. Lyngfelt, "Performance of an oxy-polishing step in the 100 kWth chemical looping combustion prototype," *Chemical Engineering Journal*, vol. 409, p. 128202, 2021, doi: https://doi.org/10.1016/j.cej.2020.128202.

[54] F. Rezaei, A. A. Rownaghi, S. Monjezi, R. P. Lively, and C. W. Jones, “SOx/NOx Removal from Flue Gas Streams by Solid Adsorbents: A Review of Current Challenges and Future Directions,” *Energy & Fuels*, vol. 29, no. 9, pp. 5467–5486, Sep. 2015, doi: 10.1021/acs.energyfuels.5b01286.

[55] S. Ajdari, “Chemistry and process design of integrated removal of nitrogen and sulfur oxides in pressurized flue gas systems,” 2019.

[56] A. Lyngfelt, D. Pallarès, C. Linderholm, F. Lind, H. Thunman, and B. Leckner, “Achieving Adequate Circulation in Chemical Looping Combustion─Design Proposal for a 200 MWth Chemical Looping Combustion Circulating Fluidized Bed Boiler,” *Energy & Fuels*, vol. 36, no. 17, pp. 9588–9615, Sep. 2022, doi: 10.1021/acs.energyfuels.1c03615.

[57] X. Ren, R. Sun, H.-H. Chi, X. Meng, Y. Li, and Y. Levendis, “Hydrogen chloride emissions from combustion of raw and torrefied biomass,” *Fuel*, vol. 200, pp. 37–46, Jul. 2017, doi: 10.1016/j.fuel.2017.03.040.

[58] “Emergency and Continuous Exposure Guidance Levels for Selected Submarine Contaminants: Volume 3. Hydrogen Chloride,” *National Research Council (US) Committee on Emergency and Continuous Exposure Guidance Levels for Selected Submarine Contaminants.*, 2009. https://www.ncbi.nlm.nih.gov/books/NBK219917/ (accessed Mar. 10, 2023).

[59] N. Yakah, I.- Noor, A. Martin, A. Simons, and M. Samavati, “Wet Flue Gas Desulphurization (FGD) Wastewater Treatment Using Membrane Distillation,” *Energies (Basel)*, vol. 15, no. 24, p. 9439, Dec. 2022, doi: 10.3390/en15249439.

[60] Z. Abbas, T. Mezher, and M. R. M. Abu-Zahr, “Evaluation of CO2 purification requirements and the selection of processes for impurities deep removal from the CO2 product stream,” *Energy Procedia*, vol. 37, pp. 2389–2396, Jan. 2013, doi: 10.1016/J.EGYPRO.2013.06.120.

[61] H. Deng, S. Roussanaly, and G. Skaugen, “Techno-economic analyses of CO2 liquefaction: Impact of product pressure and impurities,” *International Journal of Refrigeration*, vol. 103, pp. 301–315, Jul. 2019, doi: 10.1016/J.IJREFRIG.2019.04.011.

[62] C. Hammar, “Heat integration between CO2 Capture and Liquefaction and a CHP Plant: Impact on Electricity and District Heating Delivery at Renova’s CHP Plant in Sävenäs,” *Master Thesis Chalmers University of Technology*, 2022, Accessed: May 17, 2023. [Online]. Available: https://odr.chalmers.se/handle/20.500.12380/304511

[63] W. Gong, E. Remiezowicz, P. L. Fosbøl, and N. von Solms, “Design and analysis of novel CO2 conditioning process in Ship-Based CCS,” *Energies (Basel)*, vol. 15, Aug. 2022, doi: 10.3390/EN15165928.

[64] A. Lyngfelt, K. Andersson, and L. R. Pettersson, “Design of circulation system and downstream gas treatment of a full-scale boiler for Chemical-Looping Combustion,” *SSRN Electronic Journal*, Nov. 2022, doi: 10.2139/SSRN.4286370.

[65] J. Kemper, L. Sutherland, J. Watt, and S. Santos, “Evaluation and Analysis of the Performance of Dehydration Units for CO2 Capture,” *Energy Procedia*, vol. 63, pp. 7568–7584, Jan. 2014, doi: 10.1016/J.EGYPRO.2014.11.792.

[66] J. Kemper, L. Sutherland, J. Watt, and S. Santos, “Evaluation and Analysis of the Performance of Dehydration Units for CO2 Capture,” *Energy Procedia*, vol. 63, pp. 7568–7584, Jan. 2014, doi: 10.1016/J.EGYPRO.2014.11.792.

[67] NiGen, “TEG Dehydration Process | Gas Dehydration System,” *NiGen*, Apr. 29, 2021. https://nigen.com/teg-dehydration-process-gas-dehydration-system/ (accessed Mar. 20, 2023).

[68] S. Chen *et al.*, “Feasibility analysis and process simulation of CO2 dehydration using triethylene glycol for CO2 pipeline transportation,” *Chin J Chem Eng*, vol. 40, pp. 179–186, Dec. 2021, doi: 10.1016/J.CJCHE.2020.12.025.

[69] N. Wildgust *et al.*, “Pre-feasibility study of CCS in western Nebraska,” *International Journal of Greenhouse Gas Control*, vol. 84, pp. 1–12, May 2019, doi: 10.1016/J.IJGGC.2019.03.002.

[70] F. Magli, M. Spinelli, M. Fantini, M. C. Romano, and M. Gatti, “Techno-economic optimization and off-design analysis of CO2 purification units for cement plants with oxyfuel-based CO2 capture,” *International Journal of Greenhouse Gas Control*, vol. 115, Mar. 2022, doi: 10.1016/J.IJGGC.2022.103591.

[71] Aspentech, “Aspen Plus®,” 2023. https://www.aspentech.com/en/products/engineering/aspen-plus (accessed Feb. 24, 2023).

[72] AspenTech, “Aspen Energy Analyzer,” 2023. https://www.aspentech.com/en/products/pages/aspen-energy-analyzer (accessed May 14, 2023).

[73] Skövde Värmevek AB, “Biomass conditions - data sheet.” SBL4-Kontract MW, Sweden, 2014.

[74] Z. Cheng, L. Qin, J. A. Fan, and L. S. Fan, “New Insight into the Development of Oxygen Carrier Materials for Chemical Looping Systems,” *Engineering*, vol. 4, no. 3, pp. 343–351, Jun. 2018, doi: 10.1016/J.ENG.2018.05.002.

[75] Skövde Värmeverk AB, “Turbine-generator set - data sheet.” 2014.

[76] Inc. Aspen Technology, “Aspen Physical Property System: physical property methods and models v11.1,” Sep. 2001. Accessed: Apr. 18, 2023. [Online]. Available: http://web.ist.utl.pt/~ist11061/de/ASPEN/Physical_Property_Methods_and_Models.pdf

[77] M. N. Saeed, M. Shahrivar, G. D. Surywanshi, T. R. Kumar, T. Mattisson, and A. H. Soleimanisalim, “Production of aviation fuel with negative emissions via chemical looping gasification of biogenic residues: Full chain process modelling and techno-economic analysis,” *Fuel Processing Technology*, vol. 241, p. 107585, Mar. 2023, doi: 10.1016/J.FUPROC.2022.107585.

[78] W. Wagner *et al.*, “The IAPWS industrial formulation 1997 for the thermodynamic properties of water and steam,” *J Eng Gas Turbine Power*, vol. 122, no. 1, pp. 150–180, Jan. 2000, doi: 10.1115/1.483186.

[79] The Engineering ToolBox, “Oxygen - Thermophysical properties,” *The Engineering ToolBox*, 2008. https://www.engineeringtoolbox.com/oxygen-d_1422.html (accessed May 09, 2023).

[80] H. Farajollahi and S. Hossainpour, “Macroscopic model-based design and techno-economic assessment of a 300 MWth in-situ gasification chemical looping combustion plant for power generation and CO2 capture,” *Fuel Processing Technology*, vol. 231, p. 107244, Jun. 2022, doi: 10.1016/J.FUPROC.2022.107244.

[81] H. Deng, S. Roussanaly, and G. Skaugen, “X Techno-economic analyses of CO2 liquefaction: Impact of product pressure and impurities,” *International Journal of Refrigeration*, vol. 103, pp. 301–315, Jul. 2019, doi: 10.1016/J.IJREFRIG.2019.04.011.

[82] L. Sutherland and J. Watt, “Technical Reports: Evaluation and analysis of the performance of dehydration units for CO2 capture,” Stoke Orchard, Cheltenham, UK, Apr. 2014.

[83] I. Kemp, “Robin Smith, Chemical Process Design and Integration , John Wiley & Sons Ltd (2005) 687 pp, Hardback: ISBN 0 471 48680 9, Paperback: ISBN 0 471 48681 7,” *Chemical Engineering Research & Design - CHEM ENG RES DES*, vol. 83, pp. 1155–1156, Sep. 2005, doi: 10.1205/cherd.br.0509.

[84] L. Brandels, “SP4: Chemical Looping Combustion 1,” *ENCAP CO2 Project*, 2009, Accessed: May 09, 2023. [Online]. Available: http://www.cgseurope.net/Sections.aspx?section=491.492.504

[85] G. Towler and R. Sinnott, “Chapter 14 - Design of pressure vessels,” in *Chemical Engineering Design (Third Edition)*, G. Towler and R. Sinnott, Eds., Butterworth-Heinemann, 2022, pp. 441–495. doi: https://doi.org/10.1016/B978-0-12-821179-3.00014-5.

[86] BASF, “3Å Molecular Sieve,” 2015 [Online]. Available: www.catalysts.basf.com/adsorbents

[87] G. Cinti *et al.*, “CO2 capture from cement production: D4.4 Cost of critical components in CO2 capture processes,” 2015.

[88] A. Kohl and R. Nielsen, *Gas purification handbook*, 5th edition. Gulf Publishing Company, 1997.

[89] G. Towler and R. Sinnott, “Chapter 6 - Materials of construction,” in *Chemical Engineering Design (Third Edition)*, G. Towler and R. Sinnott, Eds., Butterworth-Heinemann, 2022, pp. 217–238. doi: https://doi.org/10.1016/B978-0-12-821179-3.00006-6.

[90] Charles Maxwell, “Cost Indices - Chemical Engineering Plant Cost Index (CEPCI),” *Towering Skills*, 2023. https://toweringskills.com/financial-analysis/cost-indices/ (accessed Apr. 12, 2023).

[91] P. Bartocci, A. Abad, A. C. Flores, and M. de las Obras Loscertales, “Ilmenite: A promising oxygen carrier for the scale-up of chemical looping,” *Fuel*, vol. 337, p. 126644, Apr. 2023, doi: 10.1016/J.FUEL.2022.126644.

[92] M. Yousaf, A. Mahmood, A. Elkamel, M. Rizwan, and M. Zaman, “Techno-economic analysis of integrated hydrogen and methanol production process by CO2 hydrogenation,” *International Journal of Greenhouse Gas Control*, vol. 115, p. 103615, Mar. 2022, doi: 10.1016/J.IJGGC.2022.103615.

[93] Nord Pool, “Market data,” *Nord Pool*, 2023. https://www.nordpoolgroup.com/en/Market-data1/Dayahead/Area-Prices/SE/Yearly/?view=table (accessed May 04, 2023).

[94] C. Linderholm, M. Schmitz, P. Knutsson, and A. Lyngfelt, “Chemical-looping combustion in a 100-kW unit using a mixture of ilmenite and manganese ore as oxygen carrier,” *Fuel*, vol. 166, pp. 533–542, Feb. 2016, doi: 10.1016/J.FUEL.2015.11.015.

[95] Susanne Åkerfeldt and Karl-Anders Stigzelius, “Sweden’s carbon tax,” *Regeringskansliet*, 2018, Accessed: May 08, 2023. [Online]. Available: https://www.government.se/government-policy/swedens-carbon-tax/swedens-carbon-tax/

[96] Trading Economics, “EU Carbon Permits, Historical data 2005-2022 and Forecast 2024,” 2023. https://tradingeconomics.com/commodity/carbon (accessed May 31, 2023).

[97] N. Meunier, R. Chauvy, S. Mouhoubi, D. Thomas, and G. De Weireld, “Alternative production of methanol from industrial CO2,” *Renew Energy*, vol. 146, pp. 1192–1203, Feb. 2020, doi: 10.1016/J.RENENE.2019.07.010.

[98] D. Bellotti, M. DIerks, F. Moellenbruck, L. Magistri, K. Görner, and G. Oeljeklaus, “Thermodynamic and economic analysis of a plant for the CO2 hydrogenation for methanol production,” *E3S Web of Conferences*, vol. 113, p. 01013, Aug. 2019, doi: 10.1051/E3SCONF/201911301013.

[99] E. Störner, F. Lind, and F. Rydén, “Oxygen Carrier Aided Combustion in Fluidized Bed Boilers in Sweden-Review and Future Outlook with Respect to,” *Affordable Bed Materials. Applied Sciences*, vol. 2021, no. 17, p. 7935, 2021, doi: 10.3390/app11177935.

[100] D. Kearns, H. Liu, and C. Consoli, “TECHNOLOGY READINESS AND COSTS OF CCS,” 2021. Accessed: Jun. 06, 2023. [Online]. Available: https://www.globalccsinstitute.com/wp-content/uploads/2021/04/CCS-Tech-and-Costs.pdf

[101] J. C. Abanades *et al.*, “Emerging CO2 capture systems,” *International Journal of Greenhouse Gas Control*, vol. 40, pp. 126–166, Sep. 2015, doi: 10.1016/J.IJGGC.2015.04.018.

A. Molecular sieve sizing

In this chapter, the procedure followed to size the dehydration adsorber (molecular sieve) is shown. The calculations have been performed thanks to the steps shown by CEMCAP together with Kohl & Nielsen [87], [88].

In order to calculate the direct cost of the molecular sieve technology, the absorber, and desorbed dimensions are needed. For this, the steps reported in the CEMCAP 2015 are followed [87]. It is important to note that the cost of a dehydration unit, such as molecular sieve, to achieve the specifications of the Northern Lights project have been disregarded by different CO_2 compression and liquefaction reports. An example would be Deng et al 2019, where the paper has a direct cost for the technology based on the amount of water separated.

The cost of the molecular sieve mentioned by CEMCAP is calculated through the following equation [87]:

$$CC_{mol.sieve}(€) = 2 \cdot CC_{adsorber} + 3600 \frac{€_{2015}}{ton} \cdot m_{adsorbent} \qquad (A.1)$$

The capital cost of the two adsorber columns are calculated by estimating its size and then, using the Chemical Engineering Design book in order to evaluate the cost.

As explained in the main text, Sizing the dehydration unit Technoeconomic analysis, the adsorbent material is selected to be a molecular sieve with a capacity of 16.8 kg water per 100 kg adsorbent and a bulk density of 720 kg/m^3. An example of molecular sieve supplier can be BASF which produces a type A zeolite structure with a pore size of 3Å [86]. As the costs for the BASF molecular sieve are not public, the assumed capacity, bulk density, and the adsorbent price will be considered for this work, as it is mentioned in Table 3.5.

Assuming a pressure drop along the bed of 0.33 psi/ft, the superficial gas velocity can be calculated through a modification of the Ergun equation for molecular sieve adsorbents.

$$\frac{\Delta P}{L} = B\mu v + C\rho v^2 \qquad (A.2)$$

Where ΔP is the pressure drop across the bed (psi), L is the bed length (ft), μ is the gas viscosity (cP), v is the superficial gas velocity (ft/min), and ρ the gas density (lb/ft^3).

In order to calculate the velocity, the constants B and C need to be assumed, which depend on the particle type and are shown in Table A.1.

Table A.1. Values for B and C for equation A.2 for different particle types.

Particle type	B	C
1/8 in. Bead	0.056	0.0000869
1/8 in. Extrudate	0.0722	0.000124
1/16 in. Bead	0.152	0.000136
1/16 in. Extrudate	0.238	0.0021

The size used in this work is the most similar to the molecular sieve supplier which is 1/8 in. bead (3 mm). With the superficial gas velocity and the volumetric gas flow rate going into the

molecular sieve technology, the cross-sectional area of the bed can be calculated. From the cross-sectional area, the diameter of the column can be calculated.

$$A_{c.s.} = v\,V \tag{A.3}$$

Where A is the cross-sectional area (ft^2), v is the superficial gas velocity (ft/min) and V is the gas volumetric flow rate in (ft^3/min).

The total length of the bed is the sum of the length of the equilibrium Section (LES) and the length of the unused bed (LUB).

The LES can be calculated with the following formula:

$$LES = 100\ G/\rho_{bed}\left(\frac{\Delta Y}{\Delta X}\right)t \tag{A.4}$$

Where G is the gas feed rate (kmol/h m^2), ρ_{bed} is the adsorbent bulk density (kg/m^3), ΔX is equal to the sorbent design capacity (mole per 100 kg) and $\Delta Y = Ye - Yo$ are the concentrations of water in the gas feed and in the gas in equilibrium with the regenerated adsorbent (mole/mole) and t is the time from the start of adsorption (h). The time of adsorption, also known as the cycle time, is assumed to be around 4 hours.

LUB is assumed to be half of the MTZ (mass transfer zone of active adsorption), which can be calculated from the following equation:

$$MTZ = \left(\frac{v}{35}\right)^{0.3} Z \tag{A.5}$$

Where v is the superficial gas velocity (ft/min) and Z is a constant that depends on the particle type. Z is equal to 1.7 for 1/8 in. sieve and 0.85 for 1/16 in. sieve.

The total height of the column can be assumed to be the evaluated length of the adsorbent bed (LES+LUB) plus 2-3 meters to account for internals. In this work, 2 m is chosen.

All the data used and calculated in this chapter are summarized in Table A.2.

Table A.2. Data used and calculated to size the molecular sieve equipment (adsorber).

Variable	Value	Units
Gas volumetric flow rate into the molecular sieve	188.15	ft^3/min
Gas feed rate	457.38	kmol/h
Gas viscosity	0.016191	cP
Gas density	3.90753	lb/ft^3
Gas velocity	29.87	ft/min
Adsorbent capacity	16.4	kg water/100 kg of adsorbent
Adsorbent bulk density	720	kg/m^3
Pressure drop along the bed	0.075	bar/m
Cycle time (time of adsorption)	4	hours
Adsorbent capacity (ΔX)	16.8	kg water/100 kg adsorbent
Fraction of water removed (ΔY)	$3.252 \cdot 10^{-3}$	mol/mol
Cross-Sectional area	6.3	ft
Column diameter	0.86	m
LES	0.0015	m
LUB	0.2486	m
Thickness of the column	0.0148	m
Column shell mass	724.84	kg
Total high of the column	2.25	m
Mass of adsorbent in the column	104.73	kg

B. Heat integration

The methodology of heat integration is given in detail in this part of the Appendix. The process flow diagram is presented below in Figure B.1 with numbered streams to easier visualize the streams included in the heat integration and heat exchanger network design. The numbered streams are presented in Table B.1 and with stream descriptions in Table B.2. For more detailed flow diagrams of e.g., steam cycle and refrigeration cycle, see Figure 3.3 and Figure 3.6. Heat exchangers found in the flow diagram in Figure B.1 and those found within the steam cycle and refrigeration cycle are also included in the heat integration. All streams subject to temperature- or phase change except for two streams were included in the heat integration. The two streams not included were the ones associated with the CO_2 liquefaction stream of the refrigeration cycle to be cooled from 30 °C to -12.6 °C. The evaporator of the refrigeration cycle was thereby fixed and designed to specifically cool down that stream, to simplify the overall design of the refrigeration cycle. However, the condenser of the refrigeration cycle was included in the heat integration.

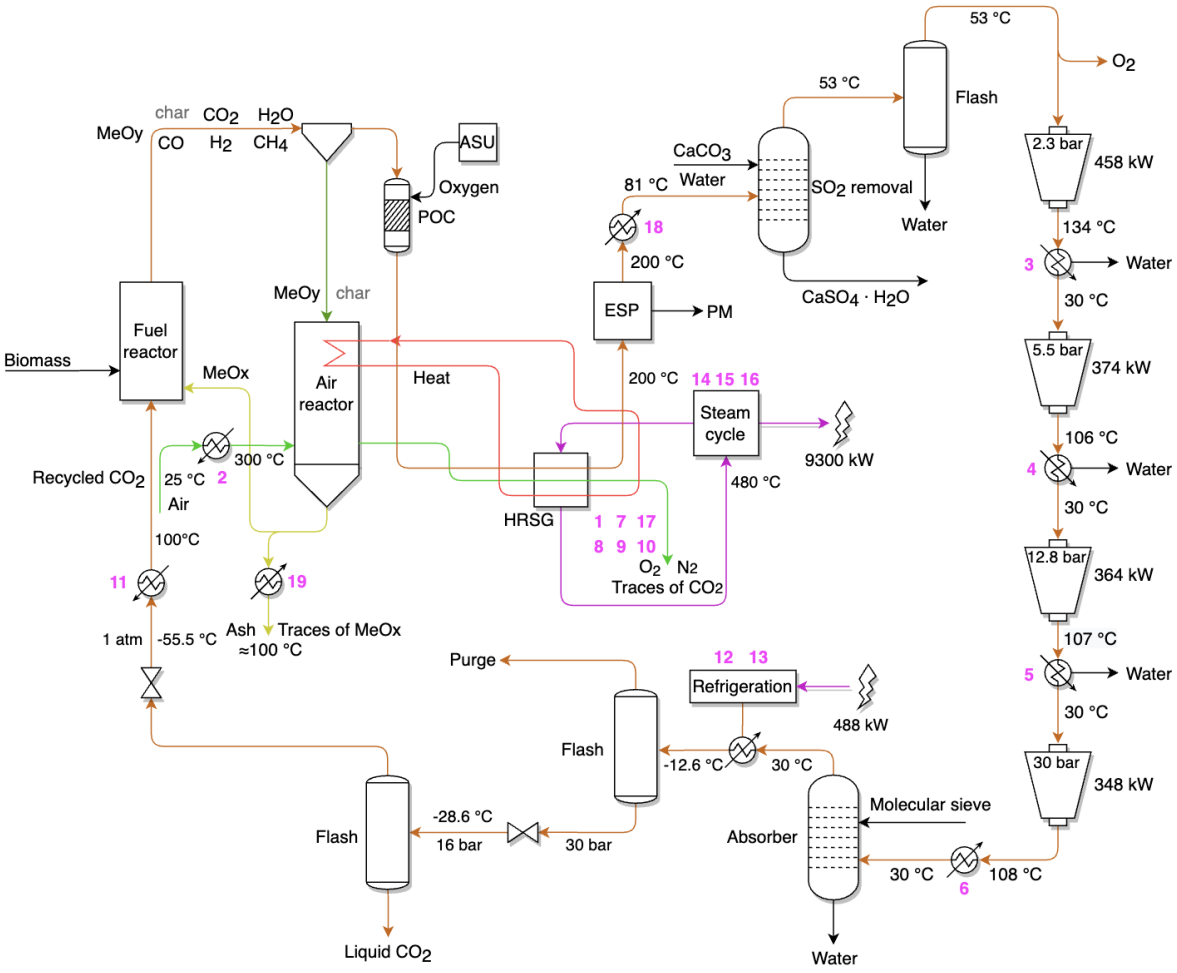

Figure B.1. Process flow diagram, numbered for stream characterization.

The following table, Table B.1, summarizes the streams included in the heat integration. The streams are numbered in Table B.1 and cross-referenced in Figure B.1 for easier location.

Table B.1. Streams included in the heat integration.

Stream name	Stream number	Inlet temperature (°C)	Outlet temperature (°C)	$\dot{m} \cdot c_p$ (kW/°C)	Heat duty (kW)
AIR-HR	1	1050	35	15.9	16,120
AIR-PH	2	25	300	18.1	4,976
CO2-MC1	3	133.7	30	13.1	1,354.9
CO2-MC2	4	105.9	30	5.82	442.1
CO2-MC3	5	106.6	30	5.55	425.5
CO2-MC4	6	108.3	30	5.77	452.1
FG-HR1	7	938.3	200	21.7	16,010
HRSG-H1	8	117.2	302.3	65.9	12,200
HRSG-H2	9	302.3	302.4	194,400	19,440
HRSG-H3	10	302.4	480	47.1	8367
R-CO2-H	11	-55.5	100	0.57	88.65
RC-1-C	12	137.7	25.1	3.42	385.2
RC-2-C	13	25.1	25	17,730	1,773
ST1-C	14	108	107.9	267,600	26,760
ST2-C	15	198.4	165.6	4.05	133
ST2-C2	16	165.6	165.5	35,910	3,591
AR	17	1050	1049.9	170,600	17,060
FG-HR2	18	200	81	45.48	5,412
ASH-C	19	938.3	100	0.85	712.2

The streams are also further described in Table B.2 below.

Table B.2. Stream descriptions.

Stream name	Stream number
AIR-HR	AR hot exhaust air
AIR-PH	Air preheater into the AR
CO2-MC1	Multicompressor intercooler 1
CO2-MC2	Multicompressor intercooler 2
CO2-MC3	Multicompressor intercooler 3
CO2-MC4	Post-multicompressor cooler 4
FG-HR1	Flue gas from FR and POC into the ESP
HRSG-H1	HRSG water heating from subcooled- to saturated liquid at 90 bar

HRSG-H2	HRSG water boiler from saturated liquid to saturated vapor
HRSG-H3	HRSG steam superheater from saturated vapor
R-CO2-H	CO_2 stream preheater into the FR
RC-1-C	Ammonia refrigeration cycle cooler from the compressor down to saturated vapor
RC-2-C	Ammonia refrigeration cycle total condenser
ST1-C	Turbine low pressure condenser
ST2-C	Turbine medium pressure (bleed stream) cooler down to saturated vapor
ST2-C2	Turbine medium pressure (bleed stream) total condenser
AR	AR isothermal integrated cooler
FG-HR2	Flue gas from the ESP cooled to enter SO_2 cleaning
ASH-C	Ash and a trace of oxygen carrier to be cooled before disposal

Given the streams presented in the tables above, a GCC of the streams included in the heat integration was constructed and is shown in Figure B.2 below.

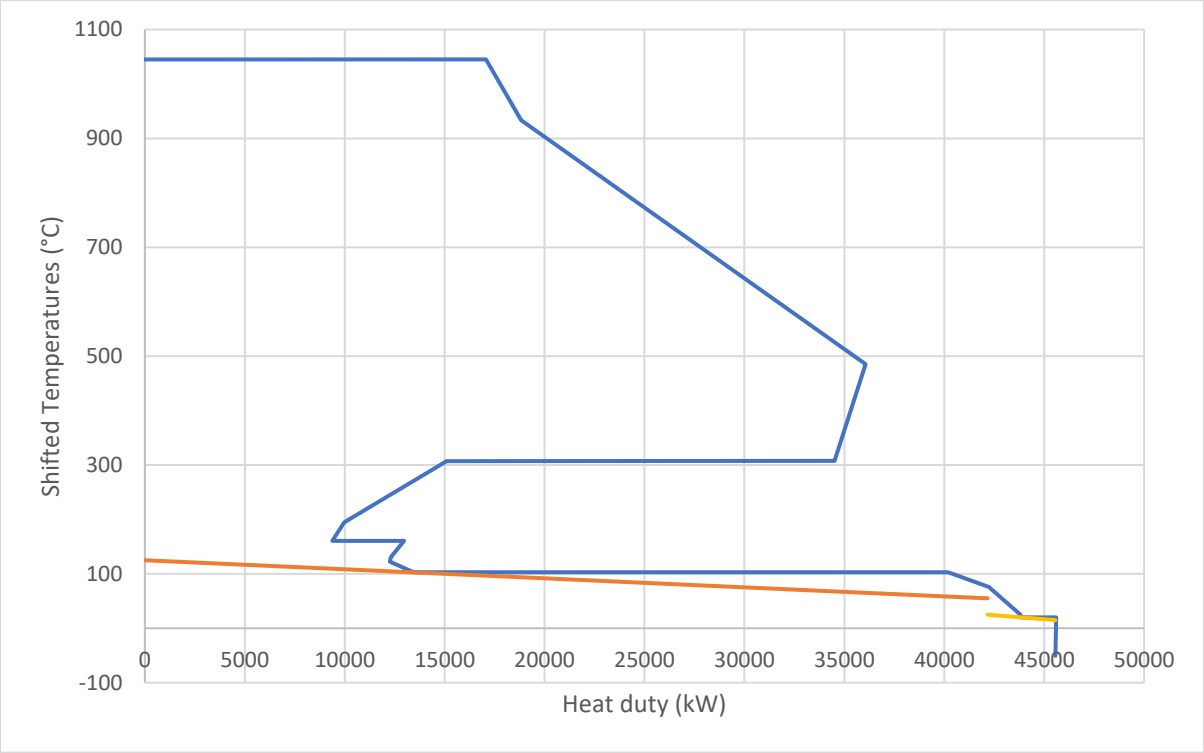

Figure B.2. GCC of the streams included in the heat integration.

The blue lines in Figure B.2 represent the process streams, the orange line the DH, and the yellow line the cooling water need.

Five streams needed heating which were prioritized at the beginning of the design to eliminate the need for other hot utilities. The hot flue gases from the AR and FR, as well as the cooling jacket associated with the AR were used for air preheating and HRSG. The CO_2 preheating for the FR was heated using the low energy content of the stream "ST2-C", which is associated with lowering the superheated temperature of the turbine bleed stream exhaust down to saturated vapor. The multicompressor intercoolers were the first heat exchangers used for DH production, followed by the refrigeration cycle ammonia cooling of the stream "RC-1-C" down to DH temperatures. The DH temperature has risen up to 53.3 °C at this point. The order of streams first cooled using DH were decided to be the hot streams with the lowest outlet temperatures to maximize the mean log temperature difference of the heat exchangers, with the exception of the stream "ST1-C" (turbine exhaust condenser at 108 °C).

The stream "ST1-C" had the highest amount of energy content and had to be prioritized relatively early in the DH production, in order to fully utilize all of its heat. The condenser associated with this stream contained a lot of energy, hence, raising the DH temperature by approximately 44 °C, from 62.2 °C to 105.9 °C. Since the stream itself was to be condensed at 108 °C, that implied that the minimum temperature difference of this condenser was only 2.1 °C, thereby leading to a high heat exchanger area. However, the placement of the condenser within the heat exchanger network was inevitable and could not have been arranged in any other manner, due to limitations in the ability of other hot streams to produce DH. Hence, if the associated condenser had been placed earlier in the DH production chain, some previous heat exchangers would not have been able to heat up the DH, thereby calling for the need to use cooling water instead. In the same way, if it had been placed later in the DH production chain, the condenser would not fully have been able to produce DH, and some DH energy would be lost to cooling water, thereby losing revenue. The added heat exchanger area of the condenser is justifiable due to the maximized DH revenue. The remaining streams are utilized to increase DH production to its fullest potential. In cases where DH production is not feasible, cooling water is employed instead. Figure B.3 below illustrates the heat exchanger network design.

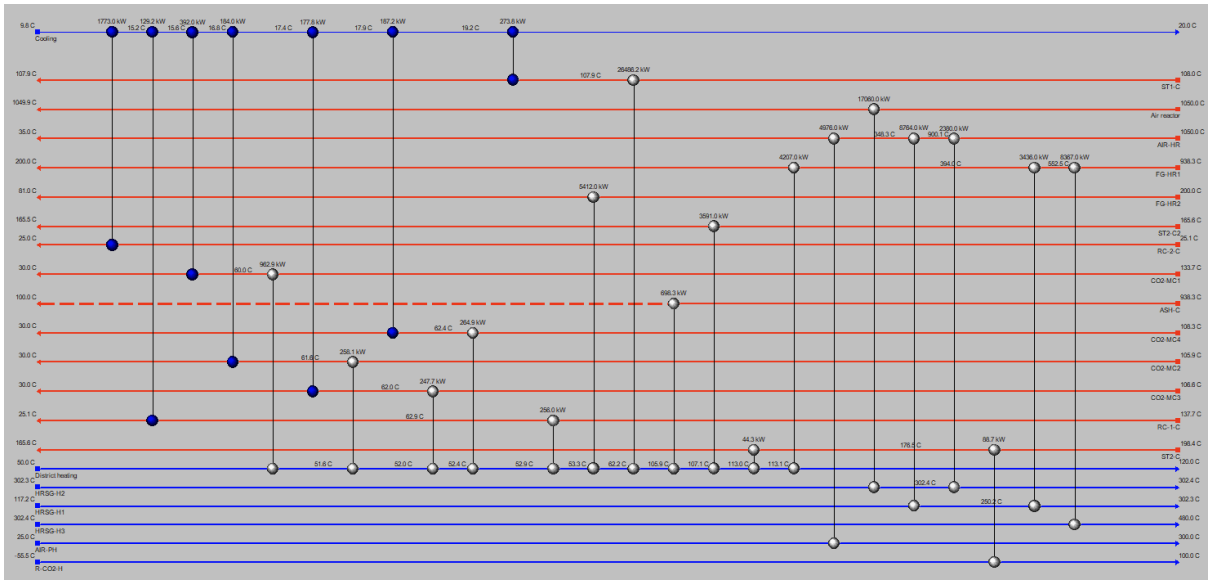

Figure B.3. Heat exchanger network design.

As can be seen from Figure B.3, the condenser connected between “ST1-C” and “District heating” is the most energy intensive stream in the heat exchanger network and raises the DH temperature by approximately 44 °C.

The ash cooling is associated with the stream “ASH-C” and is assumed to be performed similarly as the other fluid heat exchangers, even though that stream is a solid containing ash and traces of oxygen carrier, but the heat transfer coefficient of the solid is assumed to be lower than that of the fluids.

The stream “ST2-C” is cooled using two small heat exchangers. The first one is used to preheat the CO_2-stream that enters the FR as a fluidization agent. The second small heat exchanger is used for district heating. The heat exchanger associated with district heat production could probably have been eliminated, had the CO_2 preheat temperature increased from 100 °C to a higher temperature. This could maybe be done in future work with an optimized HEN design. However, the costs of HX as opposed to the costs of other parts of the CLC-process were almost negligible, and therefore optimizing the HEN design fully was deemed not necessary.

C. Steam temperature sensitivity analysis GCC

In this Appendix, the process GCC and cooling utilities are shown for the different sensitivity analysis cases presented which are done using Aspen Energy Analyzer.

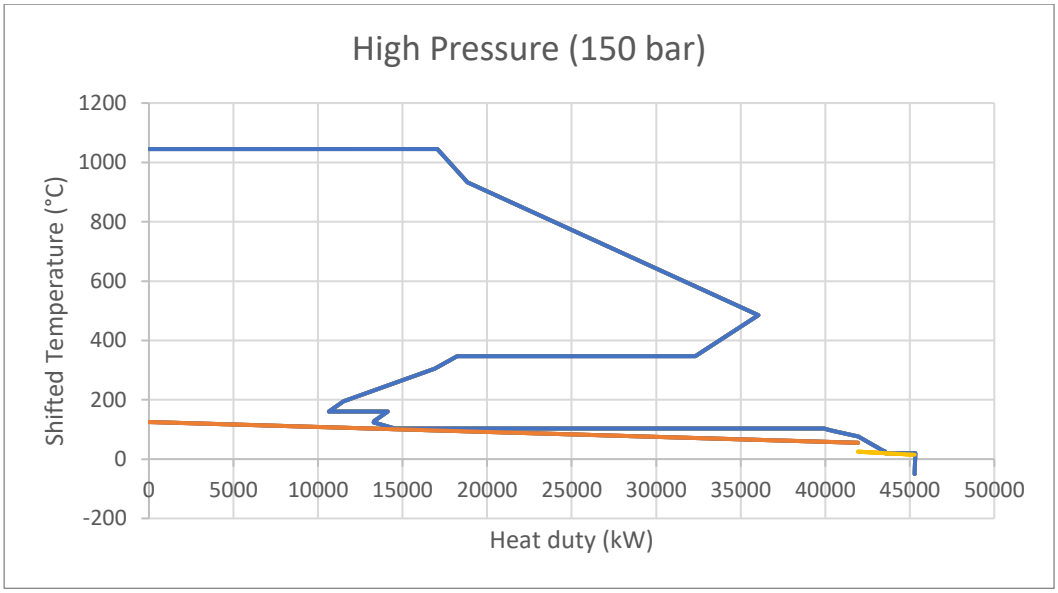

Figure C.1. Process GCC for the high-pressure case of 150 bar.

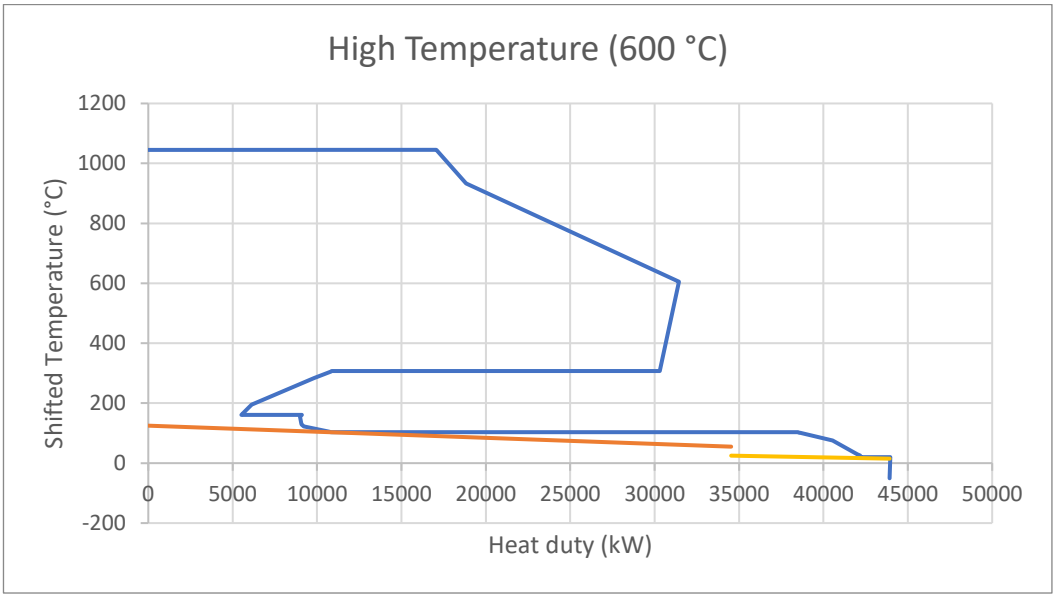

Figure C.2. Process GCC for the high-temperature case of 600 °C.

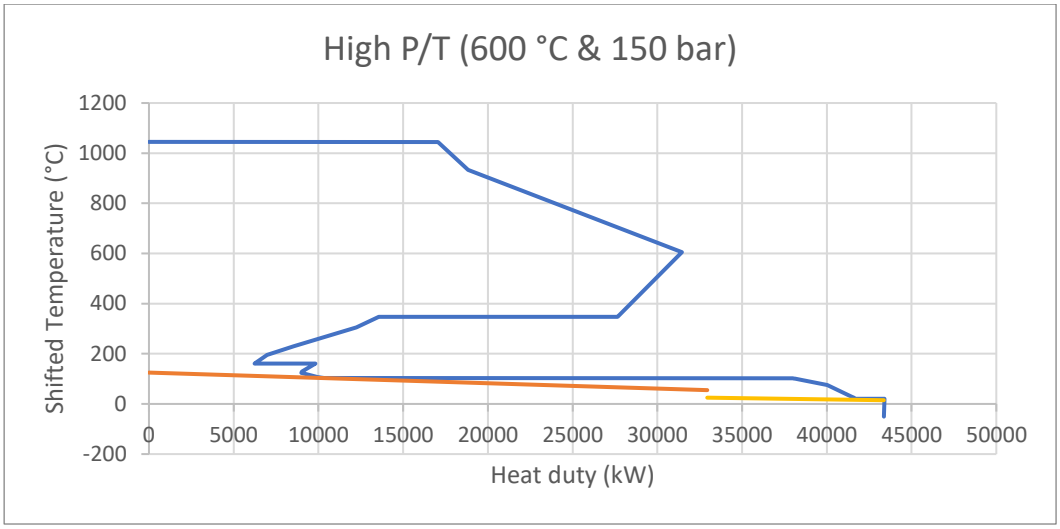

Figure C.3. Process GCC for the high temperature and pressure case of 600 °C and 150 bar.

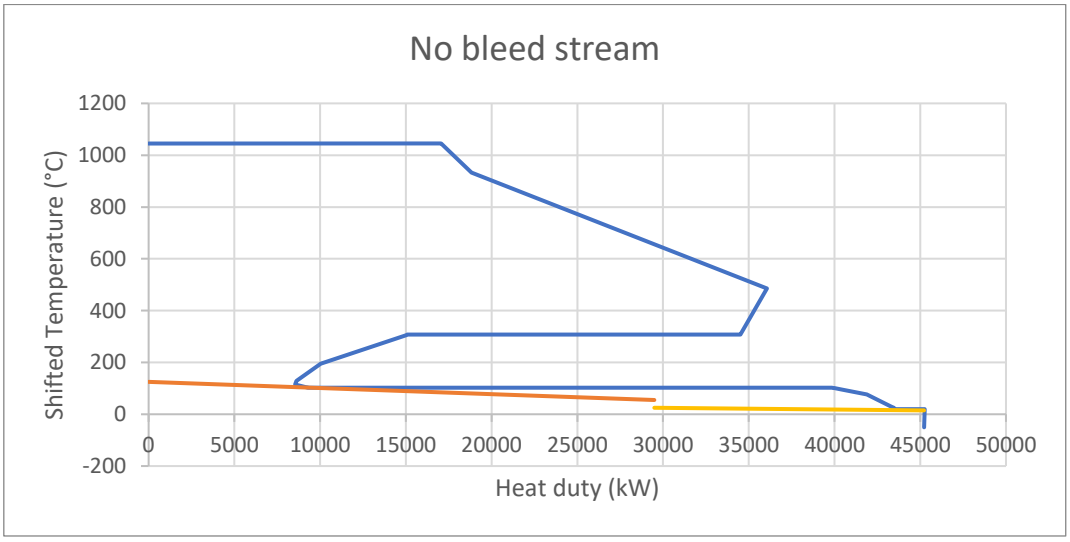

Figure C.4. Process GCC for the case of having no bleed stream exhaust from the turbine, focusing on electricity production.

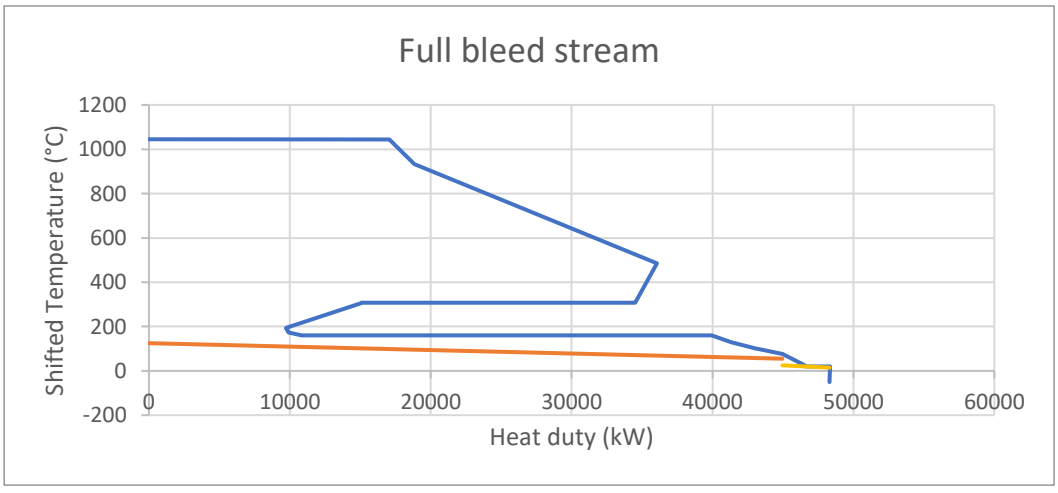

Figure C.5. Process GCC for the case of having a full bleed stream exhaust from the turbine, focusing on district heat production.

D. Flash sizing

The flashes used along the process have been sized as pressure vessels, as can be seen in Section 3.9.2. The position and flash naming can be seen in the following figure.

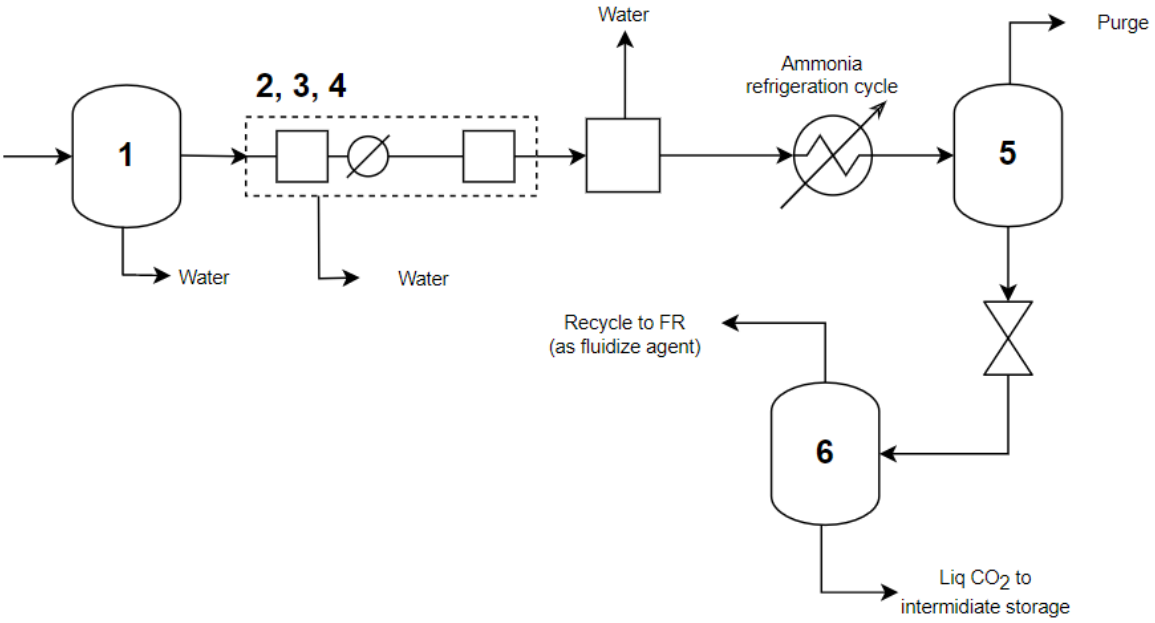

Figure D.1. Process diagram naming the flashes used.

The diameter and liquid volume have been extracted from the Aspen Process Economic Analyzer approximations. The height has been assumed to be equal to the diameter, except when the diameter value was below 1 m, which then a height of 1 m was assumed [85]. The results are shown in Table D.1.

Table D.1. Results of flash sizing. The naming of each flash corresponds to the names in the figure above.

	1	**2**	**3**	**4**	**5**	**6**	**Source**
Diameter (m)	1.37	1.22	0.91	0.91	1.37	1.22	Aspen Economics
Liquid volume (m3)	5.40	4.27	2.40	2.40	5.85	4.27	Aspen Economics
Height (m)	1.37	1.22	1.00	1.00	1.37	1.22	[85]
Designed pressure (bar)	1.03	2.43	9.82	13.00	32.43	16.71	Aspen Economics
Thickness (m)	1.00E-03	1.67E-03	5.08E-03	6.74E-03	2.56E-02	1.16E-02	Eq (3.9)
Shell mass (kg)	85.08	122.58	262.55	348.56	2322.56	852.30	Eq (3.10)